Preliminary Environmental Information Report

Volume III - Appendices

Appendix 9B: Coastal Modelling Report

The Infrastructure Planning (Environmental Impact Assessment) Regulations 2017 (as amended)

Prepared by: AECOM

Prepared for: Net Zero Teesside Power Ltd. & Net Zero North Sea Storage Ltd.

AECOM

Net Zero Teesside Project

Coastal modelling

March 2020

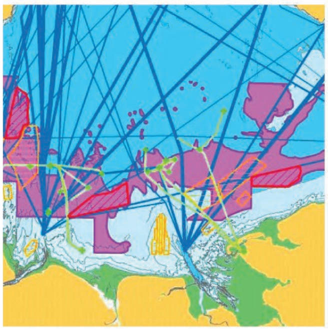

Innovative Thinking - Sustainable Solutions

Page intentionally left blank

Net Zero Teesside Project

Coastal modelling

March 2020

Document Information

Document History and Authorisation		
Title	Net Zero Teesside Project	
	Coastal modelling	
Commissioned by	AECOM	
Issue date	March 2020	
Document ref	R.3393	
Project no	R/4834/01	
Date	**Version**	**Revision Details**
16.03.2020	1	Issued for client review
27.03.2020	2	Issued for client use

Prepared (PM)	Approved (QM)	Authorised (PD)
Helen Godwin	Adam Fulford	Gordon Osborn

Suggested Citation

ABPmer, (2020). Net Zero Teesside Project, Coastal modelling, ABPmer Report No. R.3393.
A report produced by ABPmer for AECOM, March 2020.

Contributing Authors

Catherine Merrix

Notice

ABP Marine Environmental Research Ltd ("ABPmer") has prepared this document in accordance with the client's instructions, for the client's sole purpose and use. No third party may rely upon this document without the prior and express written agreement of ABPmer. ABPmer does not accept liability to any person other than the client. If the client discloses this document to a third party, it shall make them aware that ABPmer shall not be liable to them in relation to this document. The client shall indemnify ABPmer in the event that ABPmer suffers any loss or damage as a result of the client's failure to comply with this requirement.

Sections of this document may rely on information supplied by or drawn from third party sources. Unless otherwise expressly stated in this document, ABPmer has not independently checked or verified such information. ABPmer does not accept liability for any loss or damage suffered by any person, including the client, as a result of any error or inaccuracy in any third party information or for any conclusions drawn by ABPmer which are based on such information.

All content in this document should be considered provisional and should not be relied upon until a final version marked '*issued for client use*' is issued.

ABPmer
Quayside Suite, Medina Chambers, Town Quay, Southampton, Hampshire SO14 2AQ
T: +44 (0) 2380 711844 W: http://www.abpmer.co.uk/

Executive Summary

Numerical modelling has been undertaken to investigate potential impacts of temporary construction work associated with a new Carbon Capture, Utilisation and Storage (CCUS) project in the Tees Estuary, and the extent of thermal discharge resulting from an associated outfall.

This study presents the results of hydrodynamic modelling undertaken using the Delft3D flow modelling software. The model results indicate that the proposed cofferdam construction has the effect of locally reducing flows to the north and south of the construction, while slightly increasing flows to the west of the structure. The impact on flow speed is very limited, not tending to exceed 0.1 m/s in any of the vertical layers over a spring tide. In the surface layer impact on flows is restricted to within approximately 150 m of the structure when considering flow speed differences of >0.05 m/s.

Results of near-field thermal plume modelling undertaken using the CORMIX modelling software show that under spring conditions, the likely extent of a thermal plume (with a 15°C excess temperature at source) would be very localised: a 3°C temperature excess only extends approximately 45 m from the discharge point on the flood and 98 m on the ebb; for a 2°C temperature excess, the ebb extent of the plume increases to 140 m. Considering a further reduced excess temperature shows that a 0.1°C temperature excess is estimated to extend around 750 m from the origin on a spring flood tide, and 720 m on an ebb. In all cases tested, the mixing and plume dispersion appear to occur very rapidly from the origin with very little detectable change (>0.1°C) beyond ~800 m of the outfall location.

Contents

Tables

Figures

1 Introduction

AECOM Ltd. have commissioned ABPmer to undertake hydrodynamic and near-field thermal plume modelling of the Tees Estuary and surrounding region. Numerical modelling is required to provide a description of baseline conditions and investigate potential marine environmental impacts associated with the construction and operation of a new Carbon Capture, Utilisation and Storage (CCUS) project located on the south bank of the Tees Estuary (Figure 1).

The purpose of the numerical modelling is firstly to assess the potential impacts to the hydrodynamic regime of temporary works at a water intake location (shown in Figure 1); this is primarily the construction of a cofferdam structure and may also include some local dredging. Secondly, modelling is undertaken to assess the near-field impact of thermal discharge at the location of the planned outfall (Figure 1).

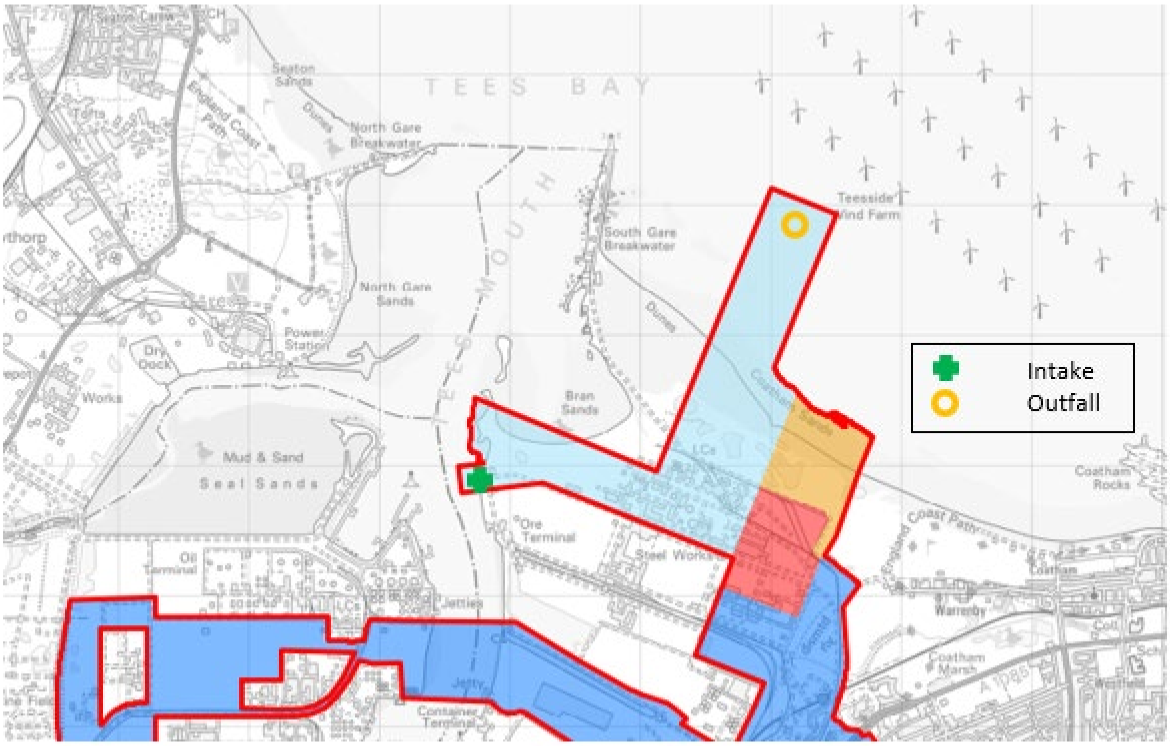

Source: AECOM ITT, 02/12/19

Figure 1. Study area showing existing intake and approximate outfall location

The approximate outfall location is illustrated above. The position is defined more accurately in Section 6,

Two stages of modelling have been undertaken for this phase of the work, which comprise the following:

- Hydrodynamic modelling; and
- Near-field thermal plume modelling.

1.1 Hydrodynamic modelling

The Deltares software package Delft3D has been used to construct a hydrodynamic model to establish baseline flow conditions within the Tees Estuary and extending approximately 10 km offshore and 30 km along the Hartlepool, Redcar and Cleveland coastline. The model design has been configured for the areas of particular interest at the proposed intake location and cofferdam site and the outfall location offshore of Redcar. The impact of cofferdam construction is assessed by defining the completed cofferdam within the model domain and assessing the impact on the hydrodynamic regime.

1.2 Near-field thermal plume modelling

The second stage of the work uses the baseline outfall conditions established from the hydrodynamic model to construct thermal plume simulations using the MixZon Inc. CORMIX modelling software. Sensitivity to a range of environmental variables has been considered in order to better assess and quantify the possibly extent of a plume from the outfall with particular thermal properties.

This report details the numerical modelling set up, calibration, and model results in the following report sections:

Section 2: Delft3D Model Setup: Details the model configuration and input conditions for the hydrodynamic modelling work.

Section 3: Delft3D Model Calibration: Demonstrates the model performance against available measured datasets.

Section 4: Hydrodynamic Conditions: Presents the baseline hydrodynamic conditions within the estuary based on the hydrodynamic modelling.

Section 5: Scheme Impact: Considers the impact of the cofferdam construction based on the modelling outputs.

Section 6: CORMIX Modelling: Provides details of the thermal plume model setup.

Section 7: Thermal Plume Modelling results: Presents the results of the thermal plume modelling and sensitivity tests.

2 Delft3D Model Setup

For the present study a three-dimensional hydrodynamic model has been run using the Delft3D software package developed by Deltares. The version of the software used for this study is version 4.03.01 The software is designed for complex applications within oceanographic, coastal and estuarine environments. The Delft3D-FLOW module has been used to simulate the tidal water variation and flows in the area of interest.

ABPmer holds an existing Delft3D model of the Tees Estuary, calibrated and validated against various datasets within the area (ABPmer 2003). This existing model forms the basis for the current study: The original model has been refined across the region of interest and updated with recent bathymetric data with high resolution coverage across key areas. The model performance has been cross checked against previous simulations and the calibration re-assessed against measured data available for this study. The setup of the Delft3D model is detailed in this section; the performance of the model is then demonstrated in the following Model Calibration chapter (Section 3) of this report.

2.1 Model grid

The Delft3D model uses a curvilinear computational grid, which allows a grid composed of various sizes to be used throughout a model domain. In addition to this, the original hydrodynamic model has been further refined using a 'domain decoupling' (dd) approach. This approach allows the creation of higher resolution grids which can be nested within the wider area domain, and dynamically coupled using defined dd boundaries. This is particularly useful for the present study where a relatively fine resolution is required at the intake site to adequately resolve the cofferdam structure, while the outer estuary and offshore region can be represented by a much coarser grid without any loss of accuracy in key areas. Two domains have been created in the Tees Estuary hydrodynamic model.

These are shown in Figure 2, with the outer grid shown in blue, and the nested (finer resolution) inner grid in black. A refinement factor of 1:3 was applied in the nested grid, in line with Deltares guidance, illustrated in Figure 3.

Beyond the Tees barrage the river section of the HD model does not align with the Tees River Channel. This part of the model was altered during the calibration phase of the previous modelling work (ABPmer 2003) to accurately represent the correct water volumes up to the tidal limit of the estuary when simulating pre-barrage conditions in the Tees. For the present study the barrage is in included in all simulations as a barrier which does not allow the movement of saline water upstream, and the flow across the barrage is represented as a time varying discharge (details of the of these are provided in Section 2.3.2). The upstream part of the Delft3D model is therefore effectively excluded from the hydrodynamic computations beyond the Tees Barrage.

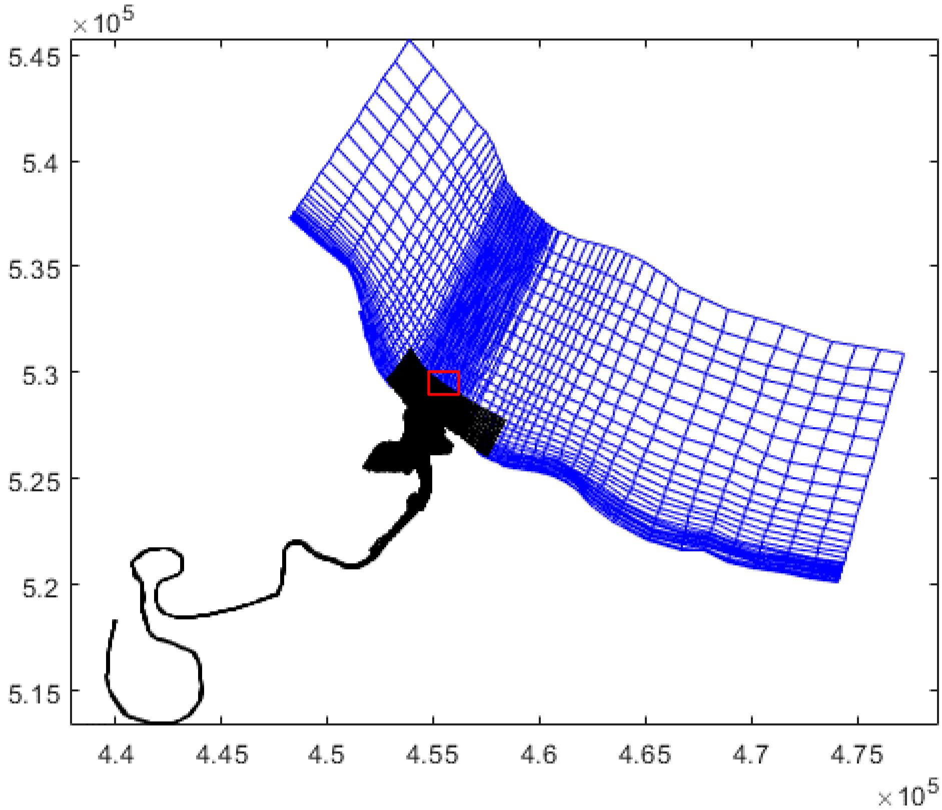

Red box shows extent of zoomed view (Figure 3)

Figure 2. Delft3D hydrodynamic model grid

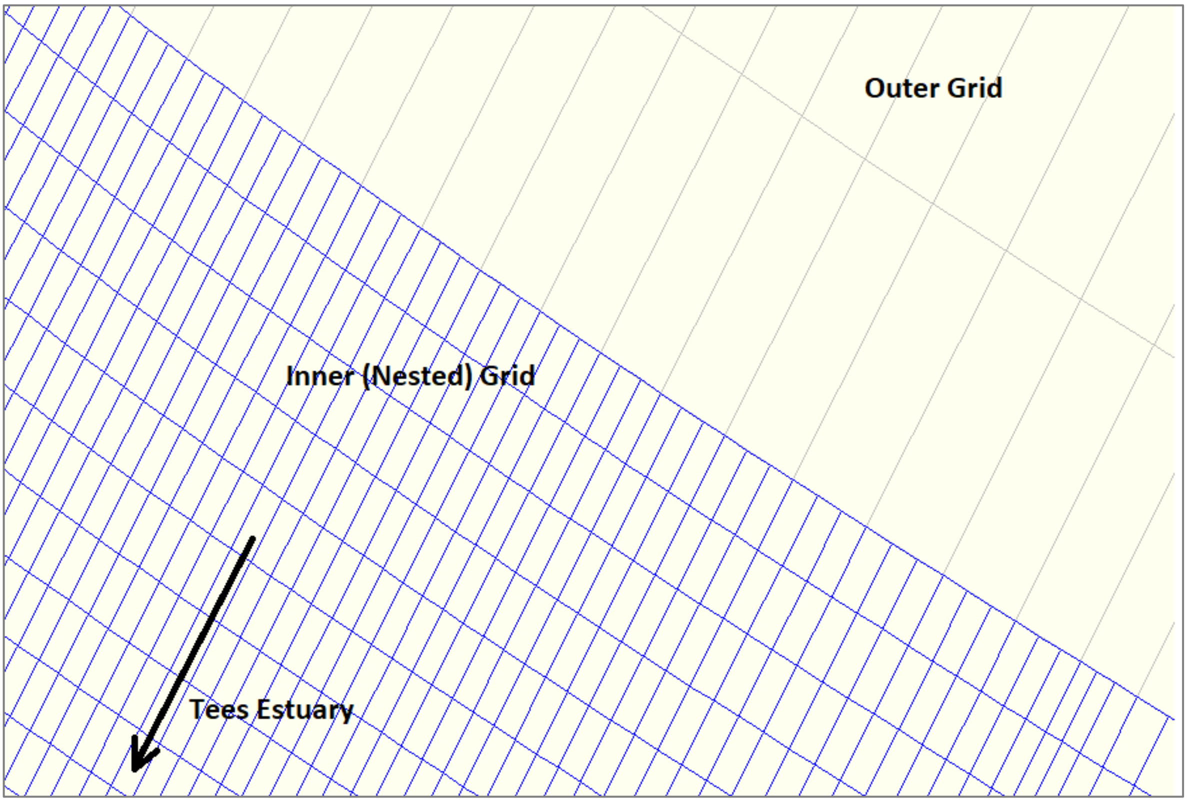

Figure 3. Delft3D hydrodynamic model grid – Refinement of nested grid

The finest resolution model grid covers the planned cofferdam location and has an approximate grid cell size of 17 m x 20 m, shown in Figure 4. The grid dimensions have been selected in order that the scheme can be adequately represented, and the implementation of the cofferdam in the hydrodynamic model is described in Section 5.1. Approximate grid cell resolutions for key areas in the model are listed in Table 1.

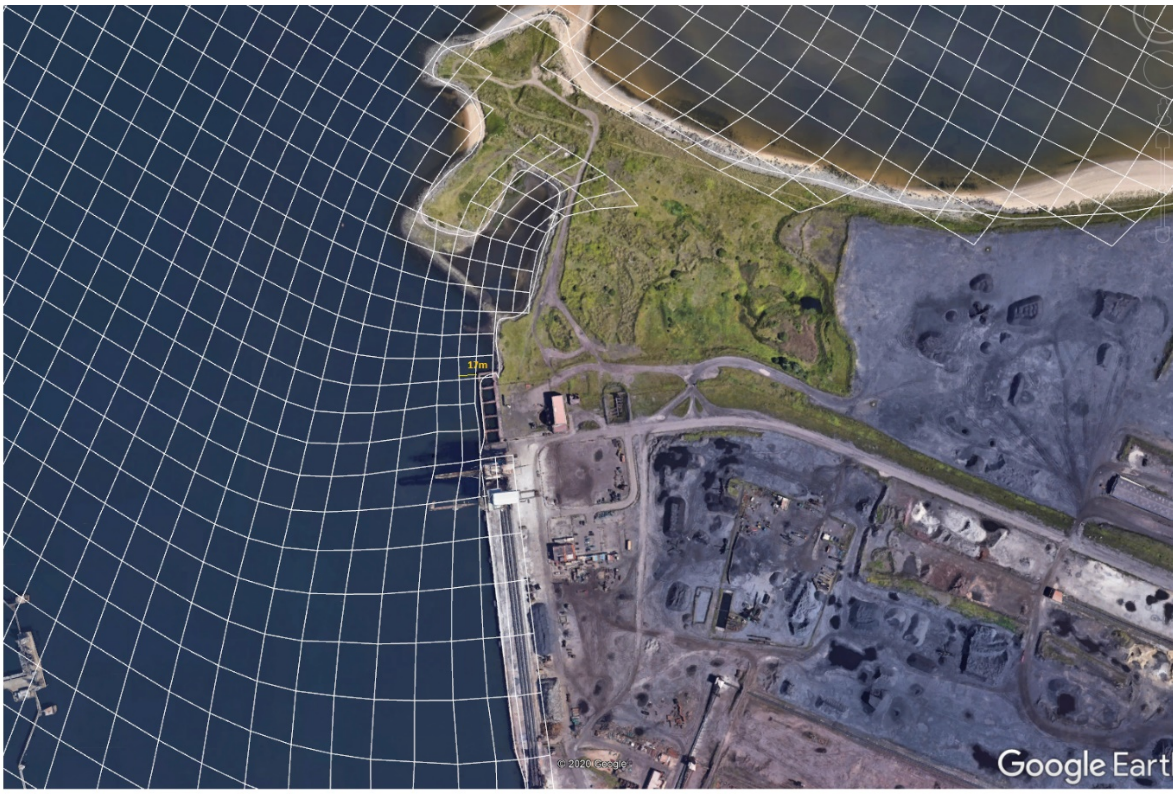

Note: dry cells not shown on grid, background image source: Google Earth, 2020

Figure 4. Model grid resolution across the cofferdam location

Table 1. Model grid resolution

Area	Average Dimensions (m)
Offshore boundary	1,000 x 1,000
Outfall location	160 x 80
Central Estuary	30 x 30
Cofferdam and intake location	20 x 17
Upper Tees	12 x 150

2.1.1 Vertical structure

The hydrodynamic model is three-dimensional (3D) with eight layers through the vertical representing 2, 3, 5, 7, 10, 15, 23 and 35% of the water column, respectively, from surface to bed. This configuration gives enhanced focus in the upper part of the water column, making the model suitable for any ongoing thermal plume or contamination modelling, which may be required in the future.

2.2 Bathymetry

The bathymetric data for the model grid construction has been compiled from the following sources:

PD Teesport Redcar Bulk Terminal Survey Data: Provided by AECOM as a digital .pdf drawing. This provides surveyed depths around the Redcar Bulk Terminal from soundings taken on 29/01/2020. Depths are provided to LAT.

PD Teesport Survey Data: xyz bathymetry data were provided by AECOM from PD Teesport surveys dating from 2019. Depth information has been provided relative to chart datum. These data cover the main channel to approximately 3.5 km beyond the estuary mouth and upstream to 2 km beyond the Tees Dock Tide Gauge.

LiDAR Contours: LiDAR data have been downloaded from the Defra survey download portal[1], to provide coverage of the intertidal areas within the Tees Estuary and outer coastline. Data have been downloaded from the available composite catalogue of the Tees area which means that sampling dates from the data may not be coincident across the spatial extent. However, the data is considered adequate for the purpose of model construction to achieve the correct volumes of water movement across the intertidal zones. The data have been cleaned to remove the water surface from the measurements and the data imported in 0.5 m depth contours up to the +3 m ODN level.

CMap: AECOM have provided bathymetry data for Tees Mouth and Tees Bay from the CMap database. Data were provided relative to chart datum and ODN. CMap is an electronic chart database managed by the Danish Hydraulic Institute (DHI) as part of their Mike software modelling provision. Spatial coverage provided by this database is adequate in the offshore region of the model but sparse within the estuary relative to the spatial resolution of the model grid.

Admiralty Charts: Admiralty charts of the Tees Estuary[2] have been used to inform the water depth in areas where alternative data were sparse. Chart depths were manually digitised for the areas of interest which included the Philips Inset Dock and dredged areas of the Tees river channel.

River Data: Beyond the region of the Teesport survey the depths in the Tees river have been extracted from previous ABPmer models of the Tees (ABPmer 2003). These originated from Tees and Hartlepool Port Authority surveys and Admiralty chart depths.

[1] https://environment.data.gov.uk/DefraDataDownload/?Mode=survey
[2] Admiralty Chart 2566 Tees and Hartlepool Bays

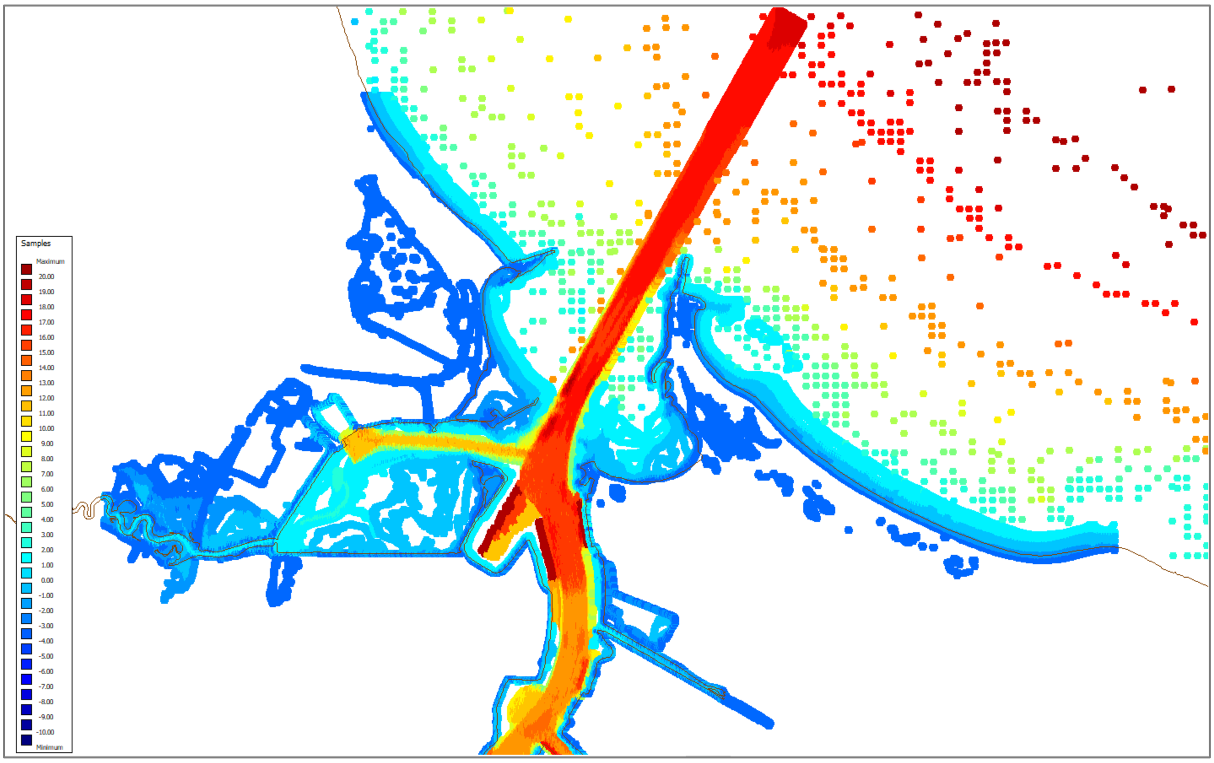

Figure 5. Scatter plot showing available bathymetry data

2.2.1 Bathymetry data processing

All bathymetry datasets were converted to Ordnance Datum Newlyn (ODN) using the values stated on the Admiralty Tide Tables for the Tees: ODN = CD +2.85 m. This relationship is consistent with the CMap conversions already supplied by AECOM.

Where bathymetry data from different sources overlapped, these datasets were cropped to consider only a single dataset for any spatial area and allow smooth interpolation of bathymetry through the model: prioritising the best quality datasets. In order of priority these were:

- PD Teesport Survey;
- LiDAR Contours;
- CMap;
- Admiralty Chart; and
- Previous model depths in the upper section for rivers.

The bathymetry interpolation across the model grid was visually assessed to ensure contours appeared smooth and consistent, particularly across the interface between the nested grids and in key areas of interest. Around the intake the interpolated values were checked against high resolution PD Teesport Redcar Bulk Terminal Survey Data to ensure the dredged depths were correctly represented around the cofferdam site.

2.3 Model Setup

2.3.1 Offshore tidal boundaries

The hydrodynamic model is defined by three offshore boundaries driven by tidal harmonics, shown in Figure 6.

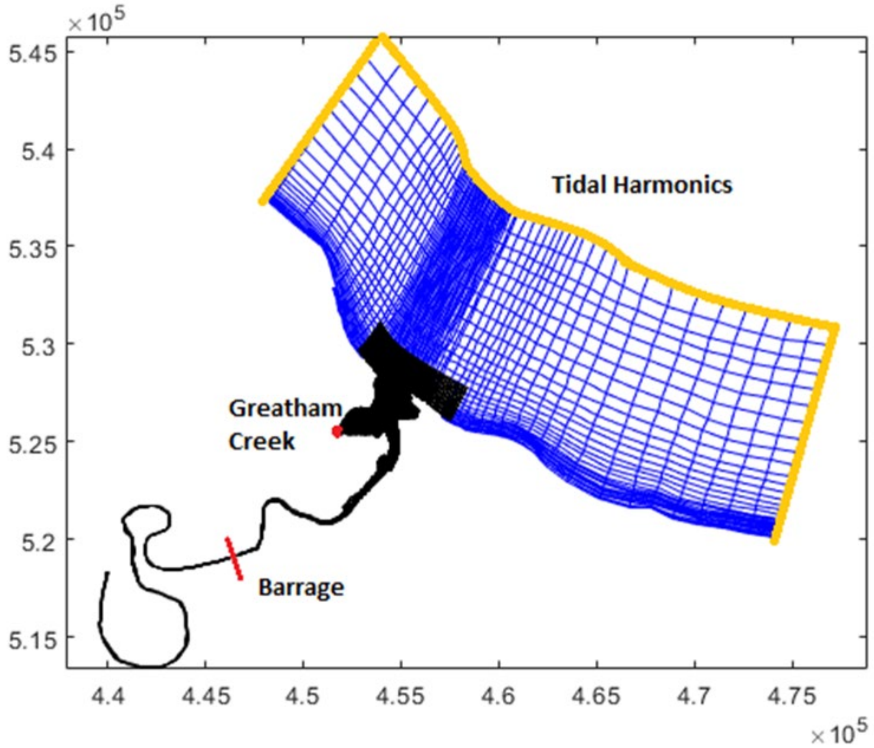

Figure 6. HD model domain and boundary positions (shown by yellow lines)

The harmonic constituents defined at these boundaries have been extracted from a wider area model (ABPmer 2003) previously constructed by ABPmer which has previously been calibrated and verified against three data sets. The tidal constituents included in each boundary are given in Table 2. The amplitude and phase of each constituent is defined along the model boundaries. Each boundary is described using more than one set of tidal harmonics to allow any gradient in surface elevation along the boundary to be replicated.

Table 2. Tidal constituents in the numerical model

Harmonic	Brief Description
A0	Initial constituent
M2	Main lunar semidiurnal constituent
S2	Main solar semi-diurnal constituent
N2	Lunar constituent due to monthly variation in the Moons distance
K2	Solar-lunar constituent due to changes in declination of the sun and the moon throughout their orbital cycle
O1	Main lunar diurnal constituent
K1	Solar-lunar constituent
L2	Elliptical lunar semi-diurnal constituent
Q1	Elliptical lunar diurnal constituent
P1	Main solar diurnal constituent
EPSILON2	Lunar semi-diurnal constituent
NU2	Lunar semi-diurnal constituent
LABDA2	Evectional semi-diurnal constituent
M4	Shallow water component
MS4	Shallow water component

2.3.2 Inclusion of the Tees Barrage

At the upstream boundary of the model the Tees barrage is included in the model as a 'thin dam' structure, which acts as a barrier to saline water to extend upstream of this point. In addition, a freshwater discharge was added at the section of the barrage. The setup of the discharge takes into consideration that the barrage acts as a barrier to the upstream movement of the tide. The freshwater release from the barrage is not continuous. Survey data available from previous studies indicates that the release of water typically occurs at mid-day, regardless of tidal state (Figure 7).

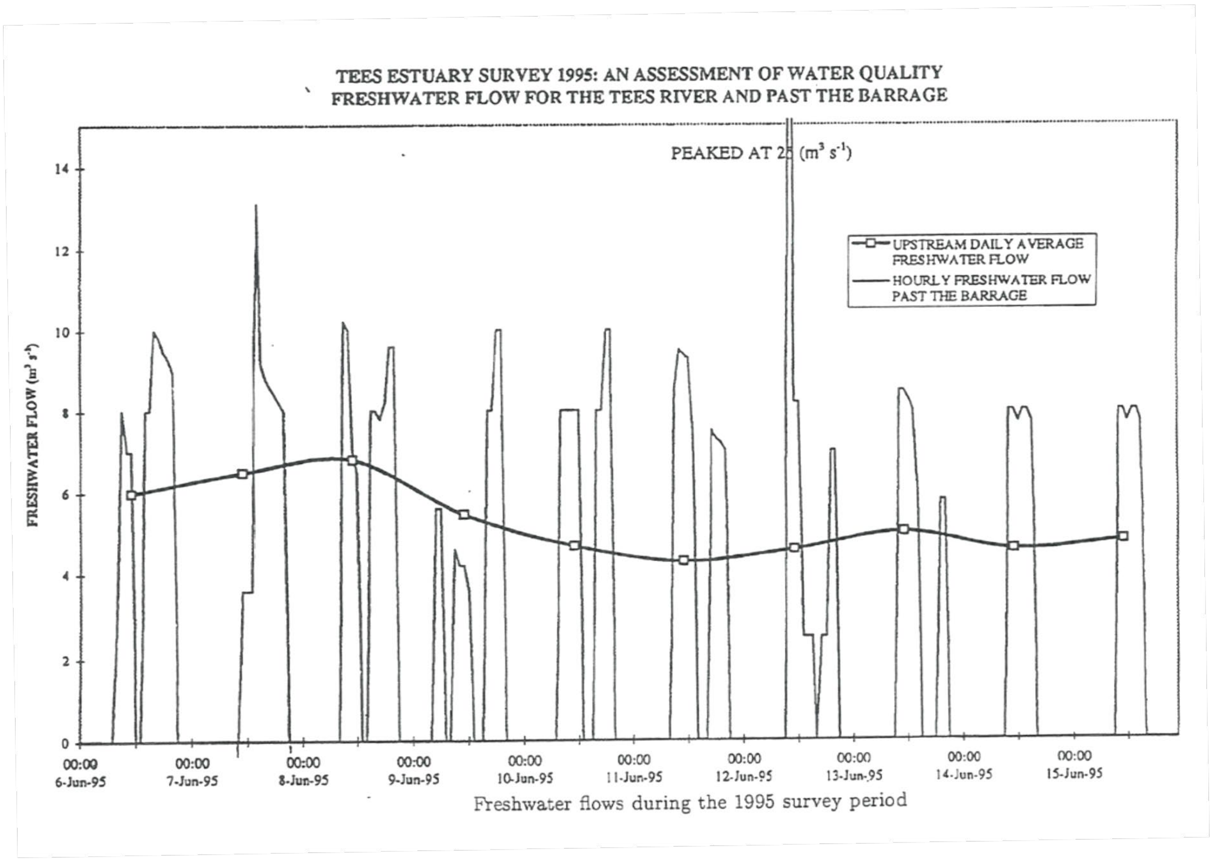

Extracted from:ABPmer 2003

Figure 7. Tees Estuary survey, 1995: Freshwater flow past the barrage

Freshwater discharges from the barrage have been calculated from flow data available from the National River Flow Archive (NRFA)[3]. Data from gauging stations at Leven Bridge and Low Moor have been assessed to derive the annual mean flow for the combined stations as well as the 5% and 95% exceedance values which have been extracted to represent the winter and summer conditions, respectively. Data from the measurement stations (Figure 8 are presented in Table 3, and the derived mean, summer and winter flows across the barrage in Table 4. The discharge from the barrage is defined in the model as a time varying input of fresh water, peaking at each mid-day in the simulation at the values calculated in Table 4.

[3] https://nrfa.ceh.ac.uk/data/search

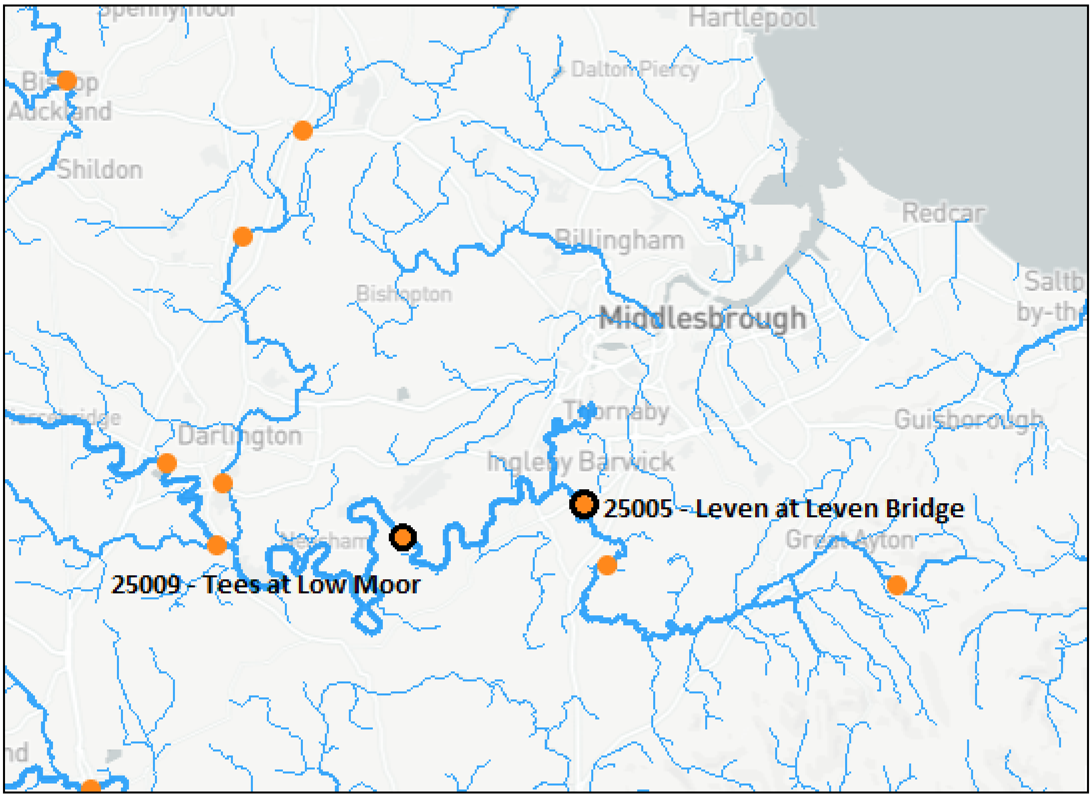

Figure 8. Flow data stations assessed for Tees Barrage discharge calculations

Table 3. Flow data from the Leven and Tees

	25005 - Leven at Leven Bridge	25009 - Tees at Low Moor
Period of Record:	1959 - 2008	1969 - 2018
Percent Complete:	>99 %	0.98
Base Flow Index:	0.42	0.39
Mean Flow:	**1.892 m^3/s**	**20.528 m^3/s**
95% Exceedance (Q95):	**0.249 m^3/s**	**3.07 m^3/s**
70% Exceedance (Q70):	0.517 m^3/s	6.15 m^3/s
50% Exceedance (Q50):	0.873 m^3/s	10.9 m^3/s
10% Exceedance (Q10):	4.248 m^3/s	46.5 m^3/s
5% Exceedance (Q5):	**6.78 m^3/s**	**67.7 m^3/s**

Source: National River Flow Archive, March 2020

Table 4. Peak discharge rates at the barrage for flow modelling

Parameter	Flow rate (m^3/s)
Mean Flow	22
Summer	3
Winter	74

2.3.3 Greatham Creek

A discharge has been defined in the model where freshwater enters the estuary at Greatham Creek. No local flow data has been forthcoming in the project, discharges have therefore been based on values adopted by JBA Consulting in previous modelling work (JBA, 2011) and set at a constant 1.8 m^3/s freshwater input for all modelled scenarios.

2.3.4 Salinity

Salinity was included in the hydrodynamic model because the Tees has both a vertical and lateral salinity distribution. The saline distribution has the potential to impact the quality of sediment transport modelling which may be required in the future.

Salinity values have been defined at all existing boundaries and discharge locations: The seaward boundary salinities were set to 35 ppt whilst at Greatham Creek and the Tees Barrage the discharges were defined as completely fresh (0 ppt).

An initial salinity value of 33.9 ppt was defined across the whole model domain based on values provided by AECOM from the Wood Draft Report (Wood, 2020) for seawater properties.

2.3.5 Wind speed

Wind speed data have been provided by AECOM to ABPmer from the location of the Durham Tees Valley airport anemometer. Data are available between 01/01/2015 and 31/12/2019 at hourly intervals, providing wind speed and direction. The wind speed and direction data have been analysed to calculate the monthly average wind speeds and direction across the five-year record (Table 5).

Table 5. Monthly average wind speeds (m/s) from Durham Tees Valley Airport

	Jan	Feb	Mar	Apr	May	Jun	Jul	Aug	Sep	Oct	Nov	Dec	Annual
Average WS	5.14	5.16	**5.32**	4.50	4.55	4.42	**4.08**	4.64	4.35	4.47	4.91	5.05	**4.72**
Average Dir	228	217	**236**	262	271	253	**234**	218	221	230	231	210	**227**

From these averages the highest and lowest average speeds were taken as the winter and summer peak values and the annual average used for the mean condition runs. The direction was sufficiently consistent that a value of 230 °N was selected for all model runs.

The measurement height of the records is 10 m above ground level and therefore require no further adjustment before being applied in the model.

The wind field was applied as a constant speed and direction across the model domain throughout each model simulation.

2.3.6 Bed roughness

The sediment type in the Tees Estuary varies between silt and gravel in the upper estuary, to sands at the estuary mouth. The majority of material moving at the bed is sand sized (ABPmer, 2003), and the bed roughness in the Delft3D HD model has, therefore, been set to a constant value throughout the model. The roughness formulation has been changed from Chezy to Manning (n) as the latter is designed for use in an environment where depths are shallow. A constant value of 0.025 ($m^{-1/3}s$) has been defined in both the U and V direction.

2.4 Model run period

The Delft3D hydrodynamic model was run for three simulation periods, described in the following paragraphs. The model takes approximately 24 hours of simulated time to 'warm up': where the flows and water levels stabilise to allow the hydrodynamic processes in the estuary to be simulated in a realistic way.

Calibration period: 20/04/2005 to 01/05/2005: The model was run for a 12-day period, including one day of warm up time, to coincide with the ADCP and CTD data available from PD Teesport (see Section 3). The model duration is centred on a spring tide, with a maximum tidal range of 4.80 m (mid estuary). This is slightly larger than the mean spring range of 4.6 m for the River Tees Entrance reported in the Admiralty tide tables (UKHO, 2020).

Validation period: 13/10/2001 to 27/10/2001: This model period was selected to duplicate the run period of the previous hydrodynamic model (ABPmer 2003). This 14-day run period includes a period of mean spring and mean neap range. The tidal range also reaches a 5.5 m at the peak of the spring tide. Repeating this model run time also allows flow speed and direction comparisons to be made against the previous project model runs and measured data available from the previous project.

2019 Seasonal Runs: 23/06/2019 to 08/07/2019: Following calibration and validation the model was simulated for a period in 2019 to generate outputs for summer, winter and average conditions, described in the model setup paragraphs in Section 2.3. These model runs were used to extract flow conditions for the CORMIX thermal plume modelling (Section 6) and the impact assessment of the Cofferdam construction (Section 5). The model was run for a 14-day simulation period, which was selected to ensure that mean spring and mean neap tidal conditions were captured within the model run time.

3 Delft3D Model Calibration

A calibration and validation exercise are required to provide a measure of confidence in the numerical model performance. Model data from the three run periods (Section 2.4) were used to undertake calibration and validation of the model, selected to coincide with the available calibration datasets, details of which are provided in the following sections.

3.1 Flow model calibration

3.1.1 Water levels

Measured water level data are available from two tide gauges in the Tees Estuary; Tees Dock and Riverside RORO, detailed in Table 6. All water level measurements were transformed to mODN using the 2.85 m adjustment sourced from the Admiralty tide tables for the Tees.

Table 6. Tide gauge data summary

Name	Dates	Location (OSGB)	Description
Riverside RoRo	20/11/2018 to 21/01/2020	454922 524424	Water level measurements relative to Chart Datum
Tees Dock	08/06/2009 to 14/08/2019	454311 523508	Water Level measurements relative to Ordnance Datum

Time series data of water levels were extracted from the numerical models for the nearest appropriate model grid cell to the measured locations (shown in Figure 9). Time series comparisons of the measured and modelled datasets are shown in Figure 10 and Figure 11. It can be seen that there is good agreement in the phasing and amplitude between the two datasets at both locations. It is worth noting that the measured gauge data will also include any residual water variations driven by meteorological forcing at the time of measurements, while the modelled data represent only the tidal component of water level.

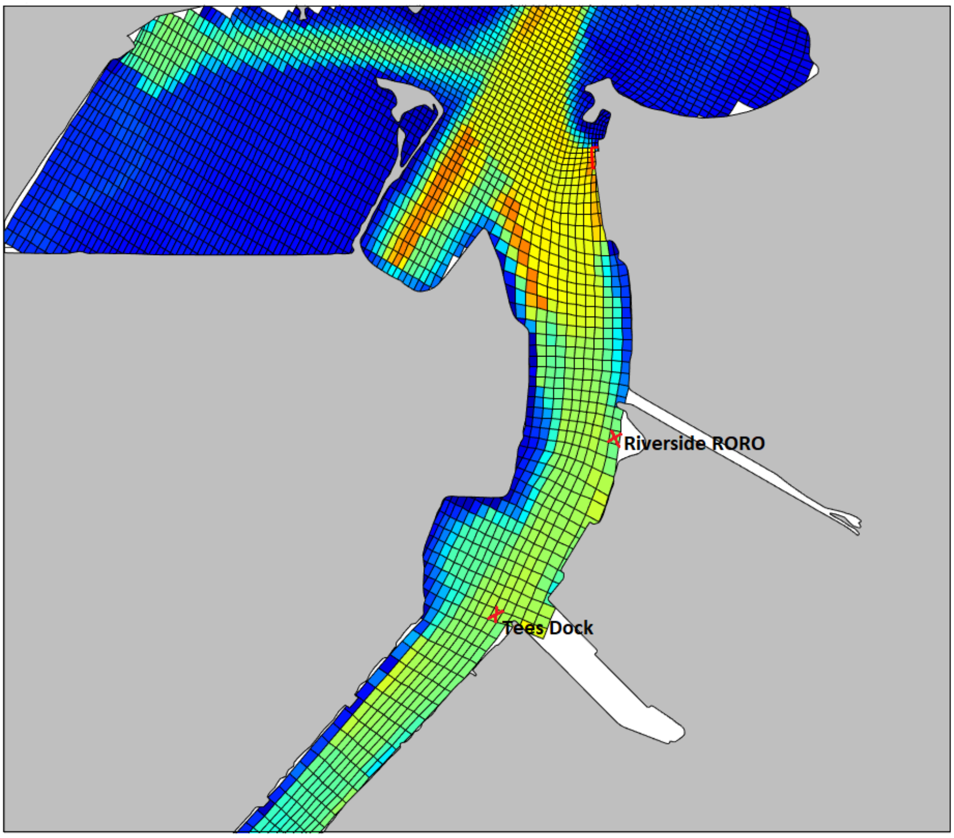

Figure 9. Location of model extraction points for tide gauge calibration

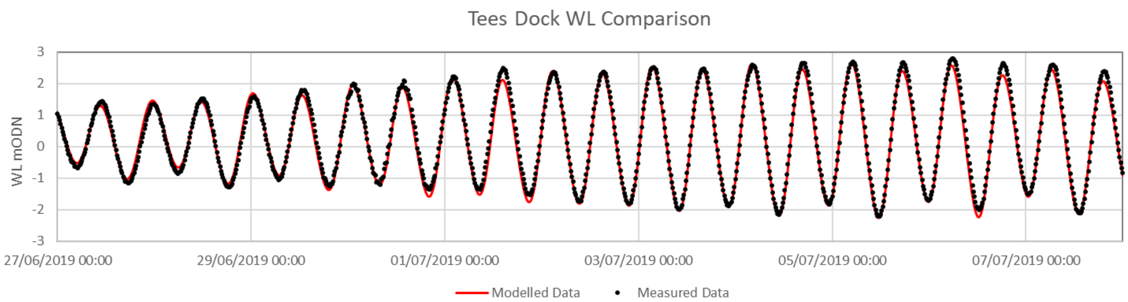

Figure 10. Water level comparison: Model vs measured data (Tees Dock)

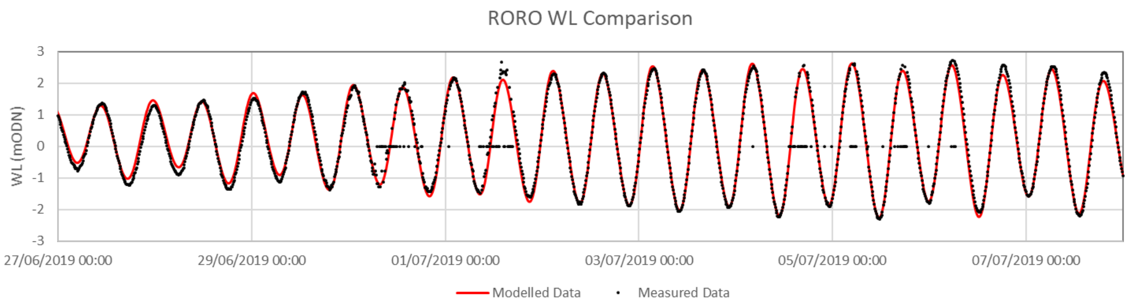

Figure 11. Water level comparison: Model vs measured data (Riverside RORO)

3.1.2 Flow speeds and direction

ADCP flow data 2005

ADCP survey data has been provided by AECOM from PD Teesport. These consist of field data and plots from a measurement campaign undertaken between 21/04/2005 and 20/04/2005. Flow data have been measured across 11 transects between the entrance to Philips Inset Dock and the bend in the Tees at Middlesbrough. For the purposes of model assessment, visual comparisons have been made between the transect plots provided by AECOM in the data files, and flow cross section data extracted from the model presented in a similar way for comparison. These comparisons are shown in Figure 12 to Figure 40. The following points should be considered when viewing these comparisons:

- Colour maps of speed and direction in the modelled outputs have been matched, visually, as closely as possible to the PD Teesport plots, however some small variation may exist between the two.
- The horizontal axis of the modelled transects represent model grid cells. These are plotted as being of equal width across the channel. This is a reasonable approximation across the transects considered – however it does mean that the X axis of the plots are not directly comparable and transect start and end points may not exactly align with the model cells.
- The vertical structure in the model is split into 8 layers, each representing a fixed percentage of the water column (see Section 2.1.1). The absolute depth of each of these layers will vary with position in the estuary (depending on water depth) as well as through time as the water level rises and falls. The model data layers have been plotted to visualise this variation.
- Modelled flow data across the transects are exported from the model at hourly intervals. When comparing against available measurements the nearest hourly record has been identified and plotted. The tidal state relative to high water has also been checked against the notes in the ADCP data files.
- Flow data comparisons have been presented for two transects at different stages of the tide to provide a selection of visual assessments within this report.

Throughout the comparison of flow speeds and direction in Figure 12 to Figure 40. there appears to be good visual agreement between the measured ADCP transects and the modelled outputs. The variation in surface flows and the main water column at various stages of the tide appears to be well simulated in the model and in agreement with the measured data. Variations in flow direction with depth also appear to correlate between the measurements and modelled data which lends confidence in the model's ability to simulate the flow through the vertical water structure.

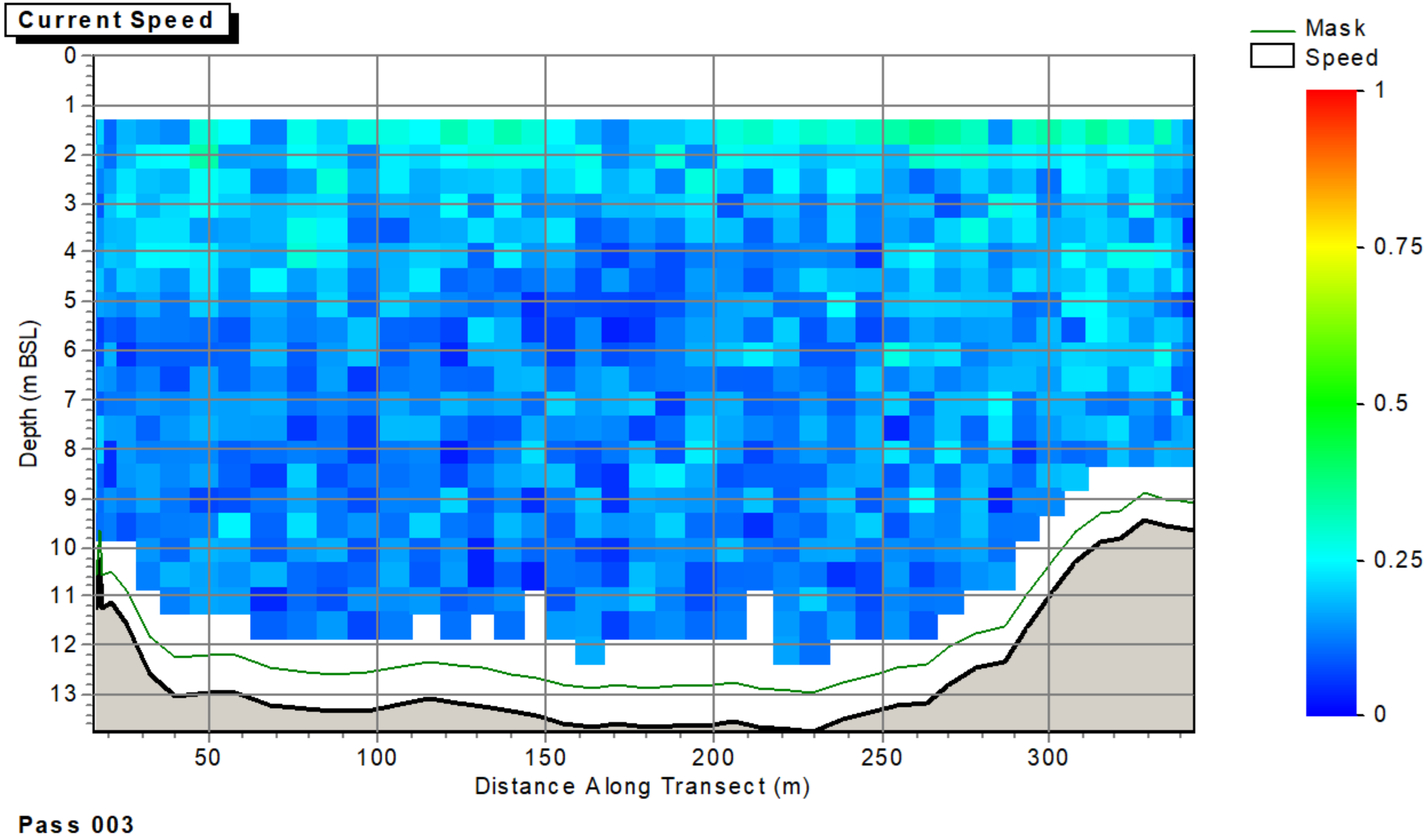

Figure provided by PD Teesport

Figure 12. Measured flow speeds, Transect 1, Pass 3: Ebb tide, cross section of speed with depth shown from west (left) to east (right)

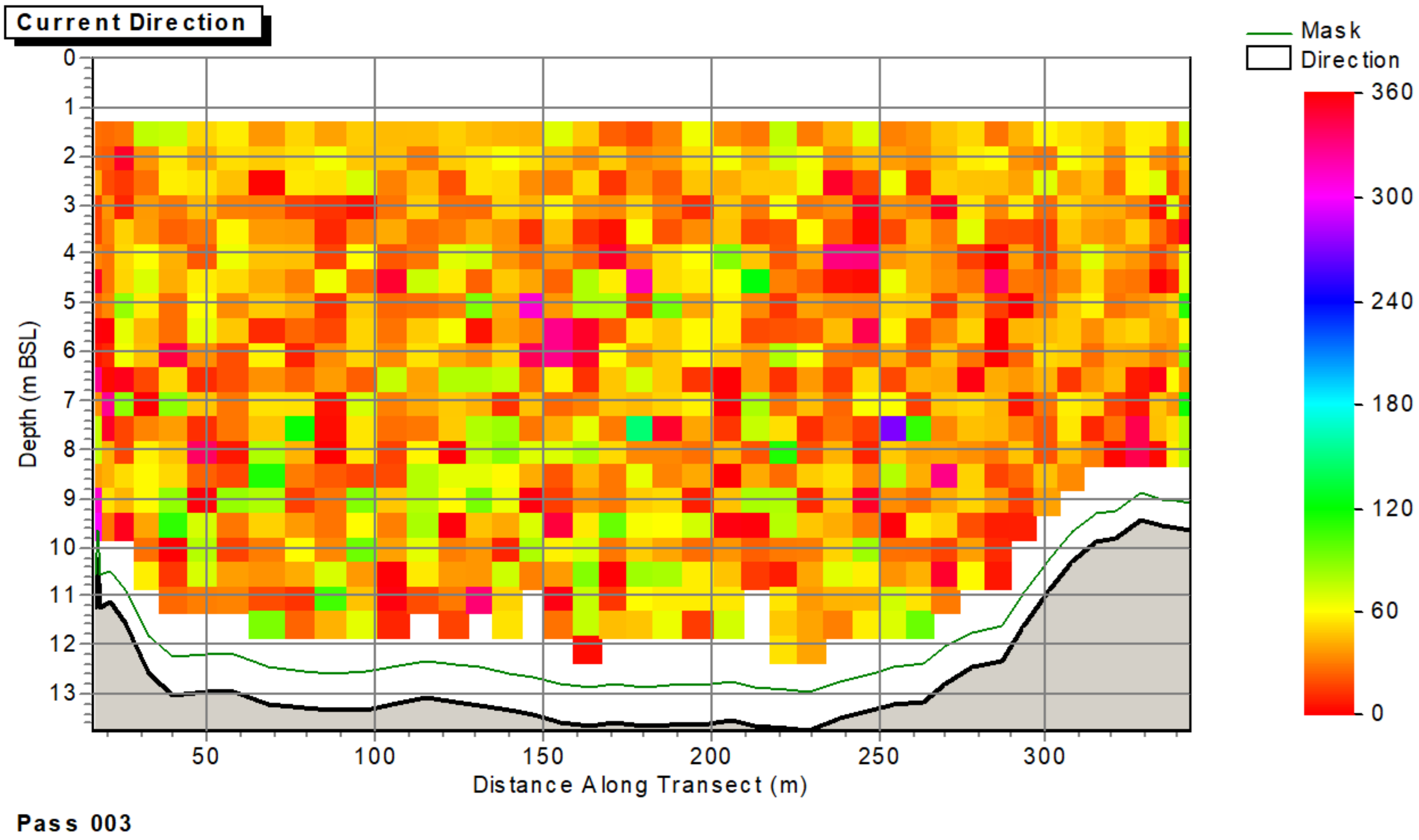

Figure provided by PD Teesport

Figure 13. Measured flow direction, Transect 1, Pass 3: Ebb tide, cross section of speed with depth shown from west (left) to east (right)

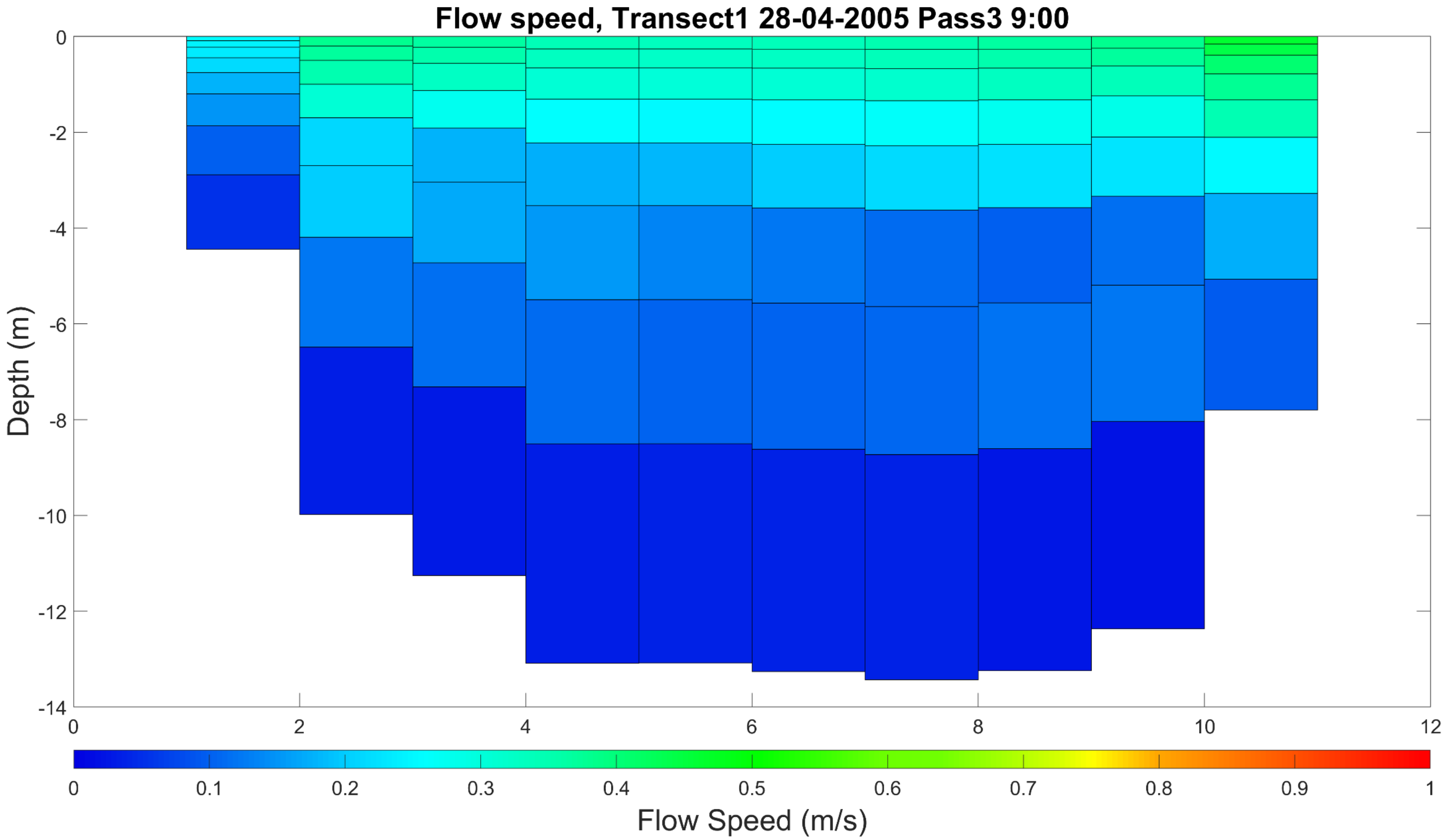

Figure 14. Modelled flow speed, Transect 1: Ebb tide, cross section of speed with depth shown from west (left) to east (right)

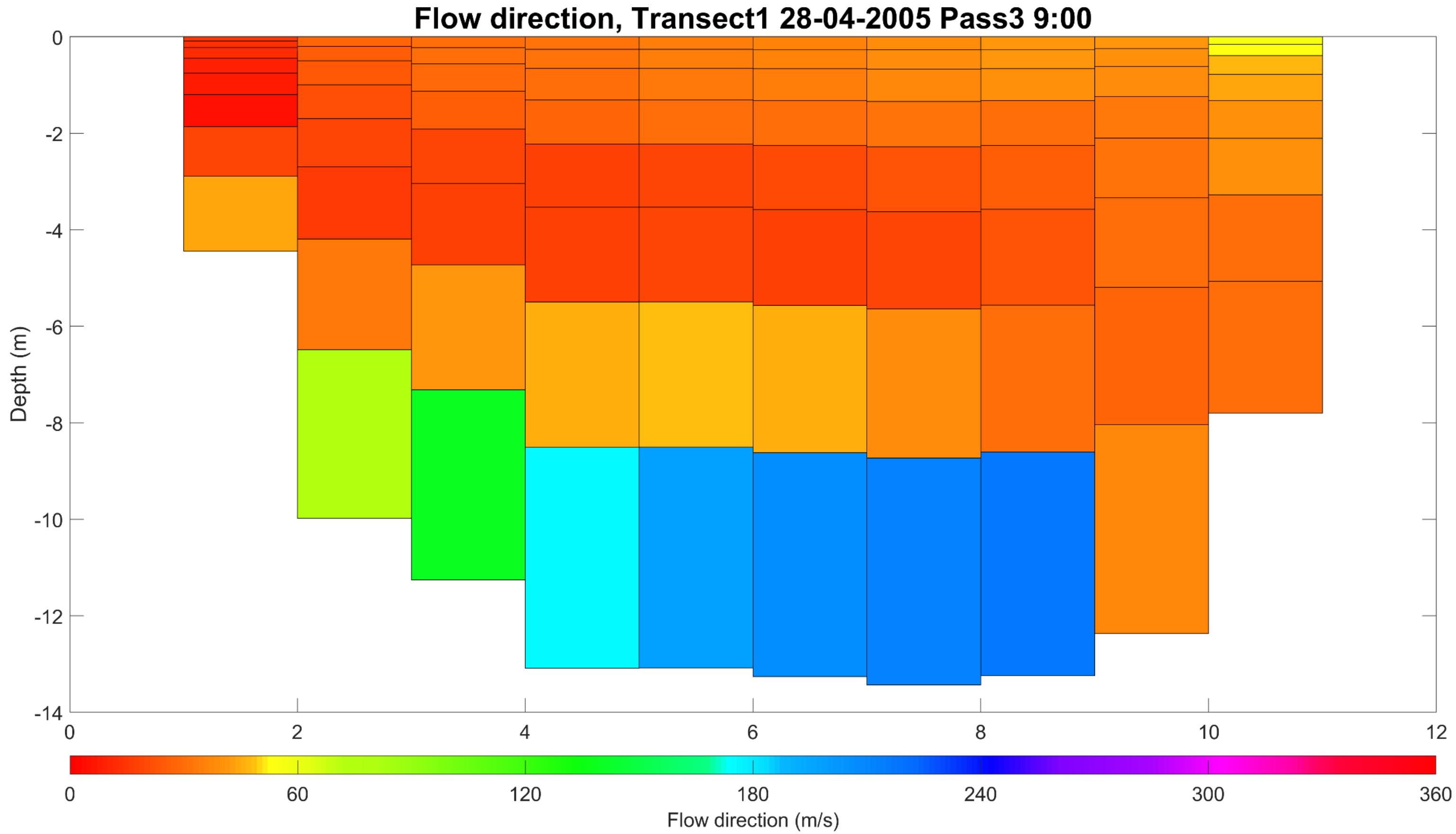

Figure 15. Modelled flow direction, Transect 1: Ebb tide, cross section of direction with depth shown from west (left) to east (right)

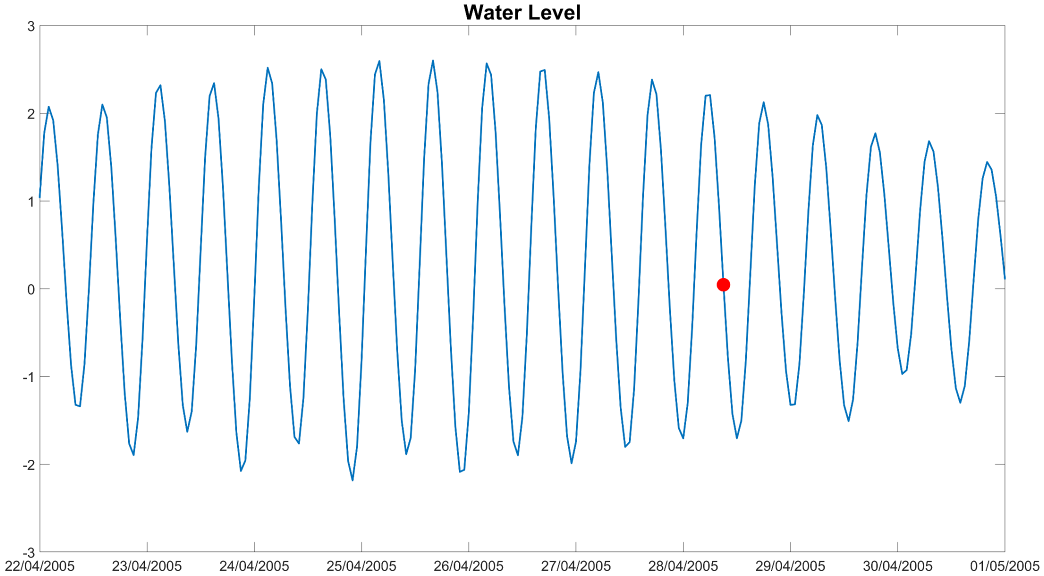

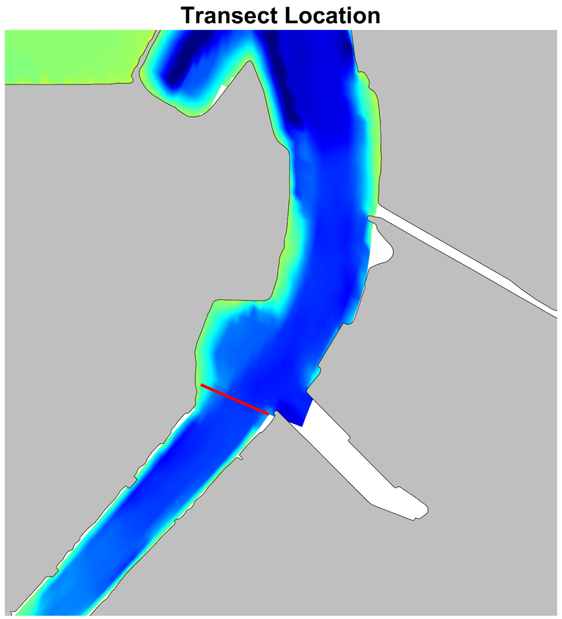

Figure 16. Tidal state and transect location extracted from the model for Transect 1 Pass 03: 28/04/2005

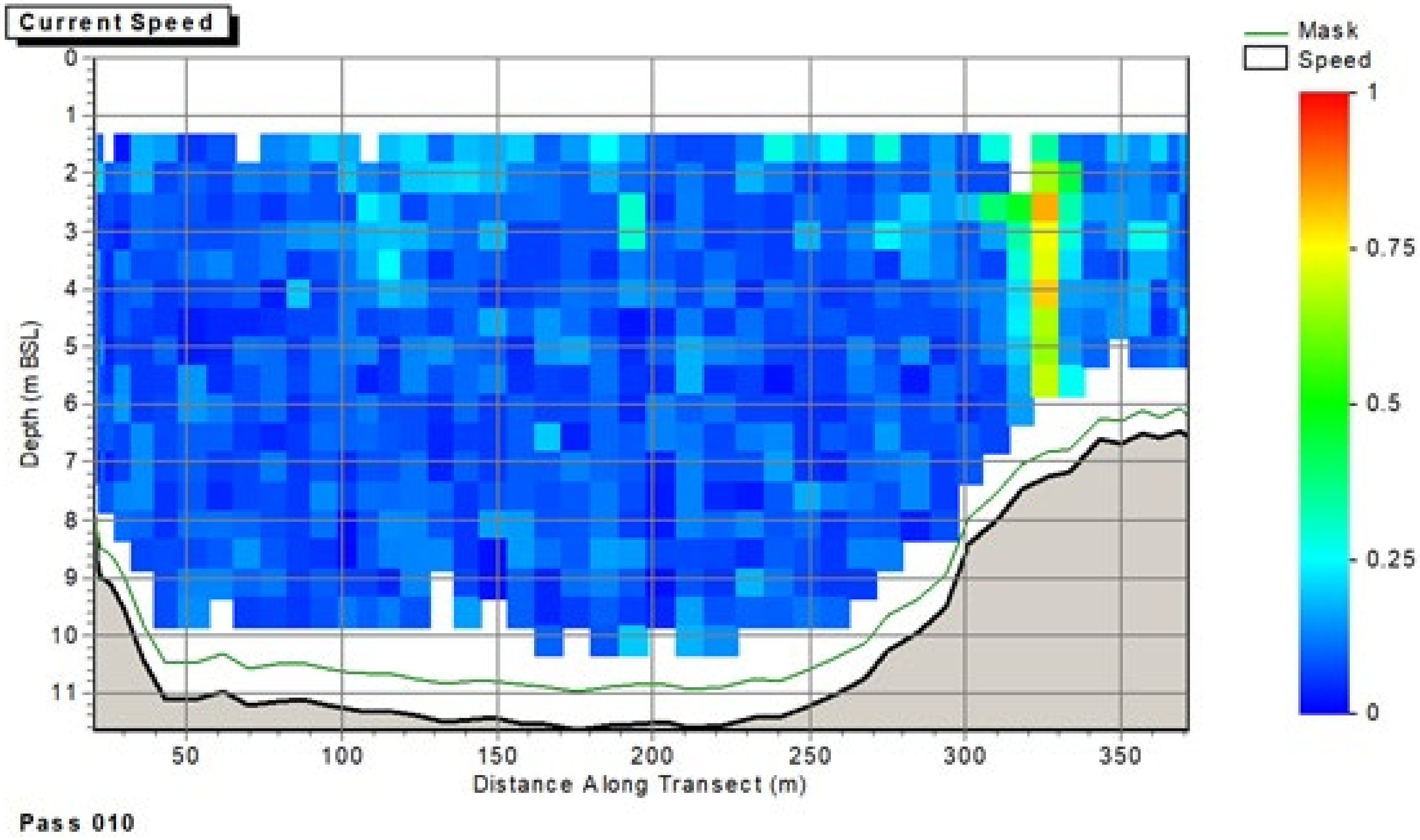

Figure provided by PD Teesport

Figure 17. Measured flow speeds, Transect 1, Pass 1: Low water, cross section of speed with depth shown from west (left) to east (right)

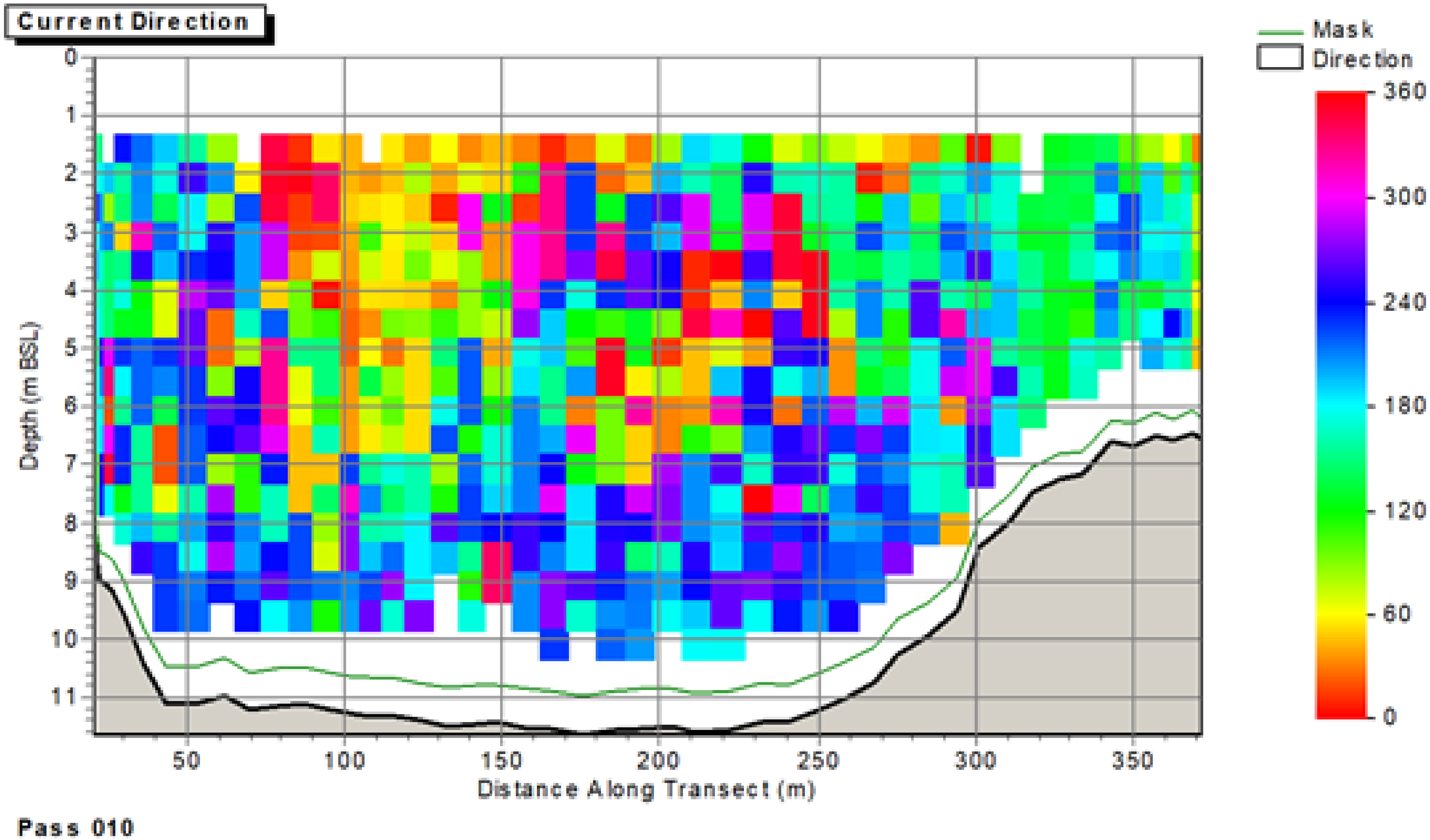

Figure provided by PD Teesport

Figure 18. Measured flow directions, Transect 1, Pass 1: Low water, cross section of speed with depth shown from west (left) to east (right)

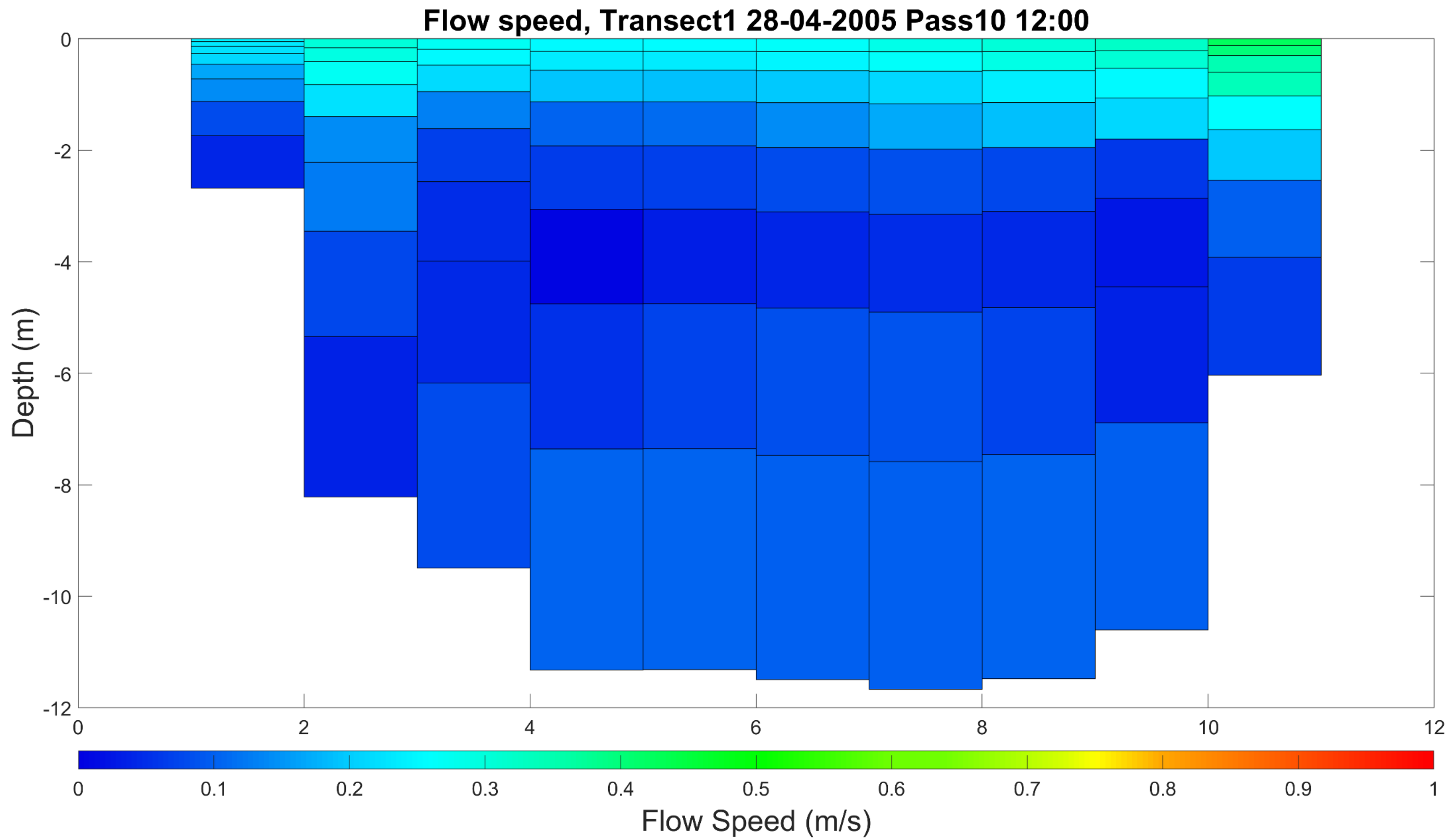

Figure 19. **Modelled flow speed, Transect 1: Low tide, cross section of speed with depth shown from west (left) to east (right)**

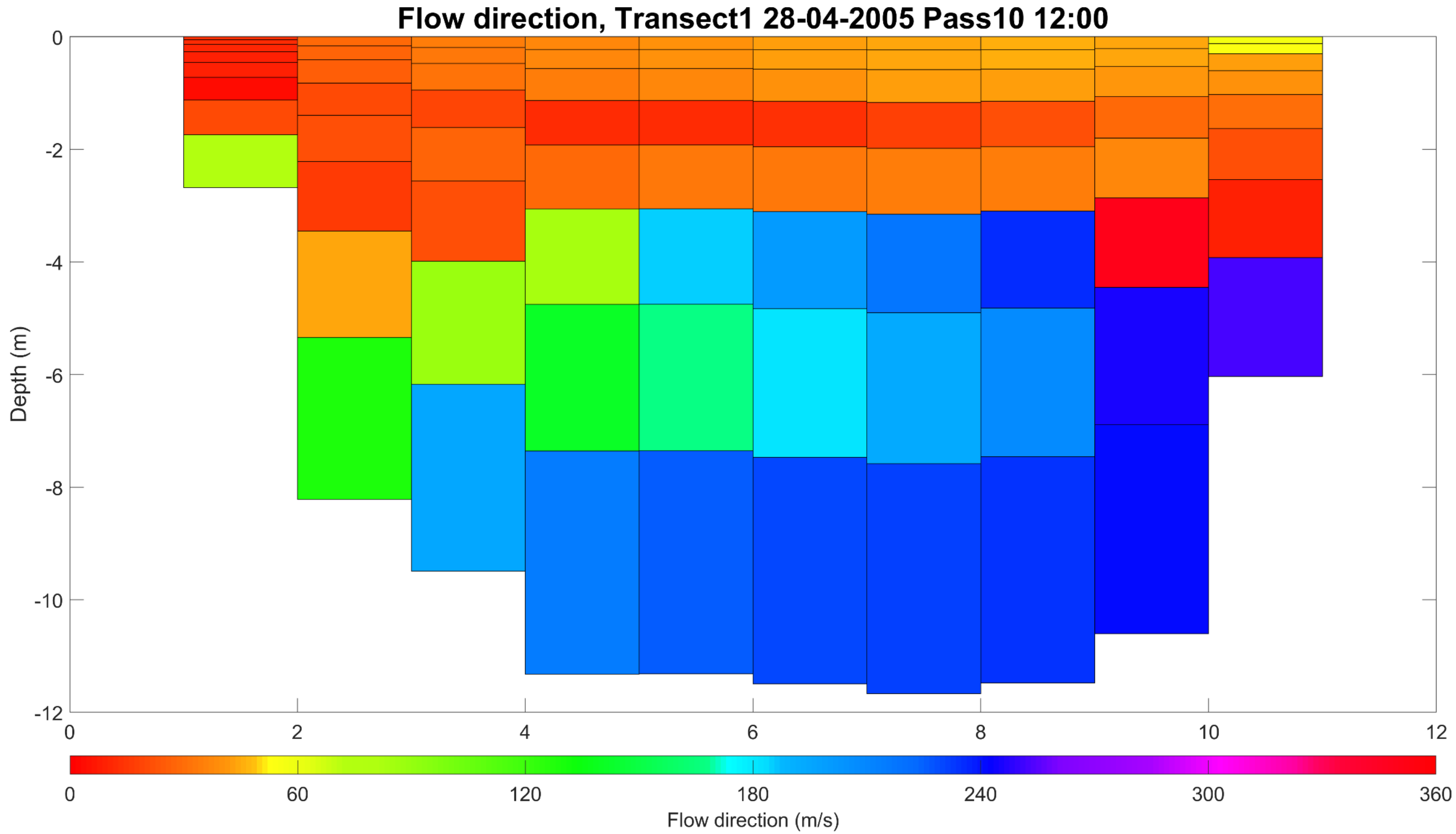

Figure 20. Modelled flow direction, Transect 1: Low tide, cross section of direction with depth shown from west (left) to east (right)

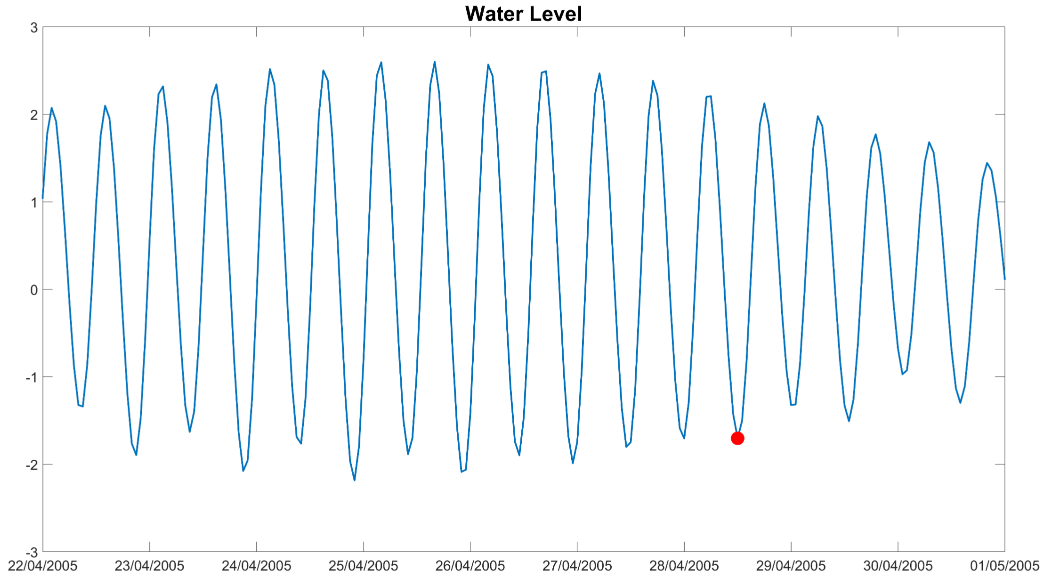

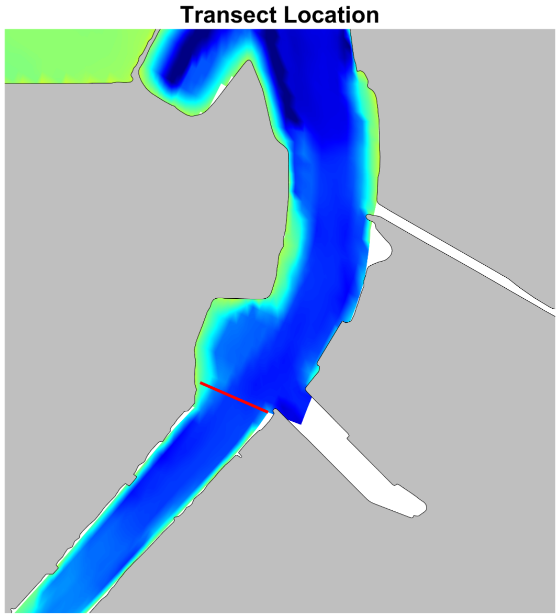

Figure 21. Tidal state and transect location extracted from the model for Transect 1 Pass 01: 28/04/2005

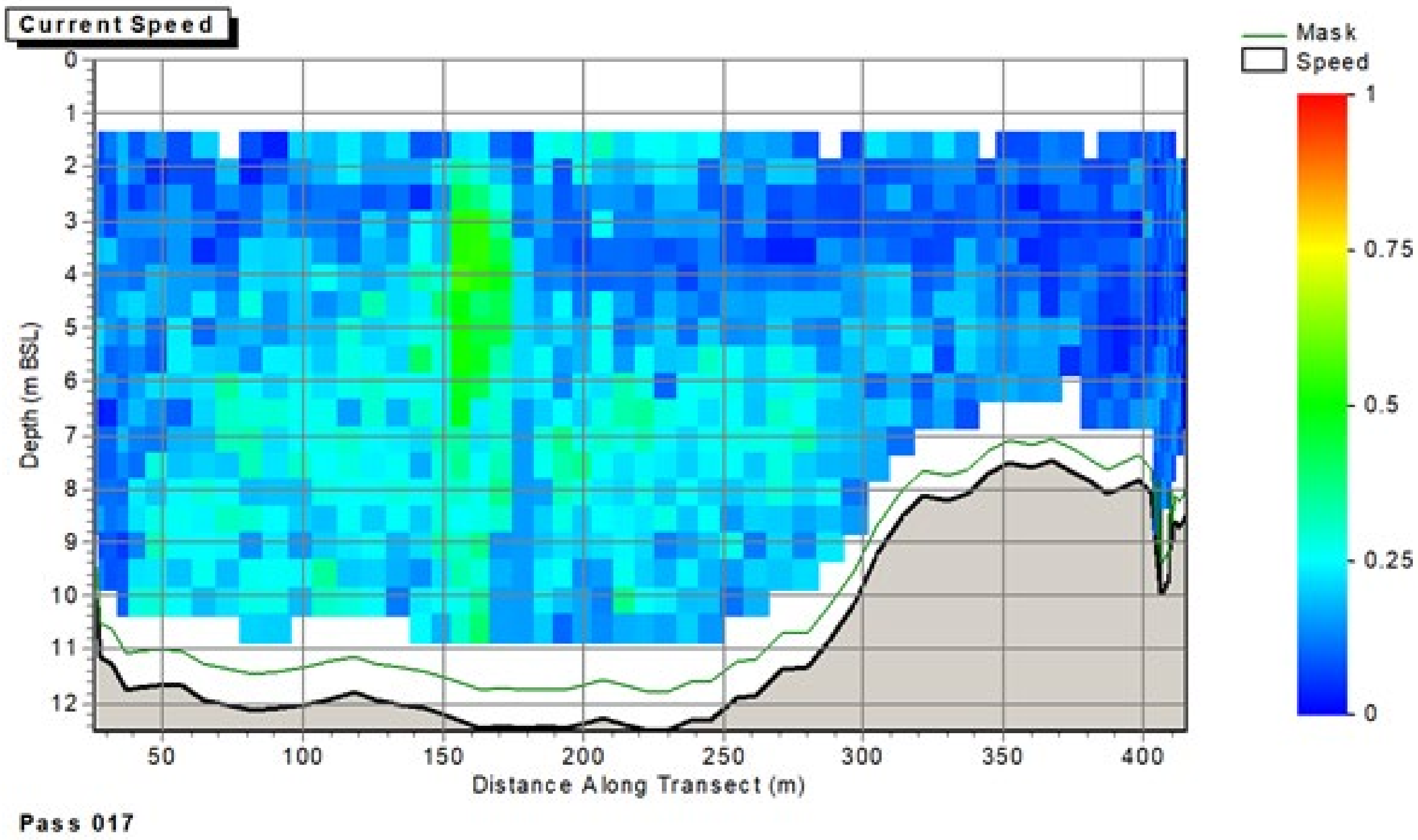

Figure provided by PD Teesport

Figure 22. Measured flow speeds, Transect 1, Pass 17: Flood tide, cross section of speed with depth shown from west (left) to east (right)

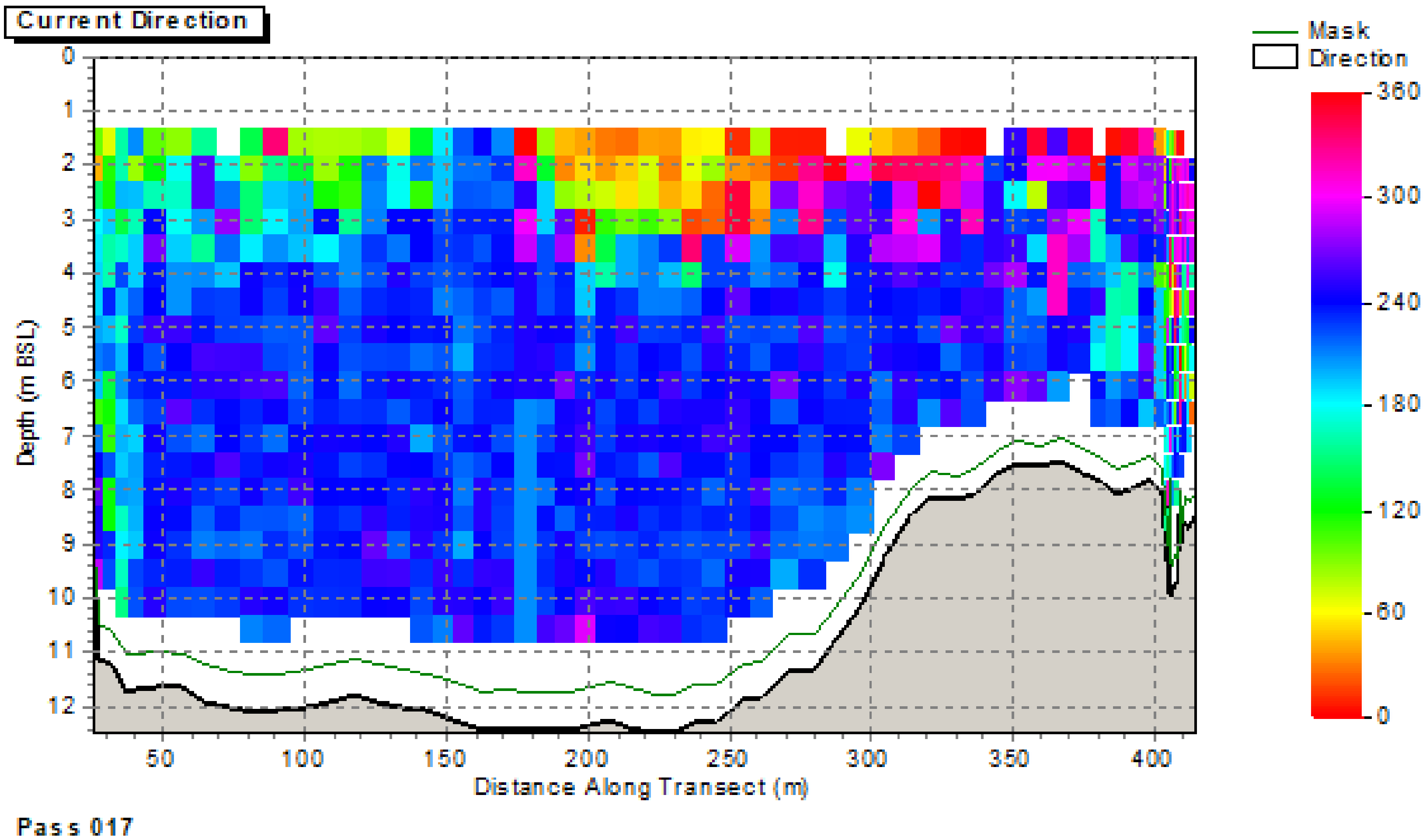

Figure provided by PD Teesport

Figure 23. Measured flow directions, Transect 1, Pass 17: Flood tide, cross section of speed with depth shown from west (left) to east (right)

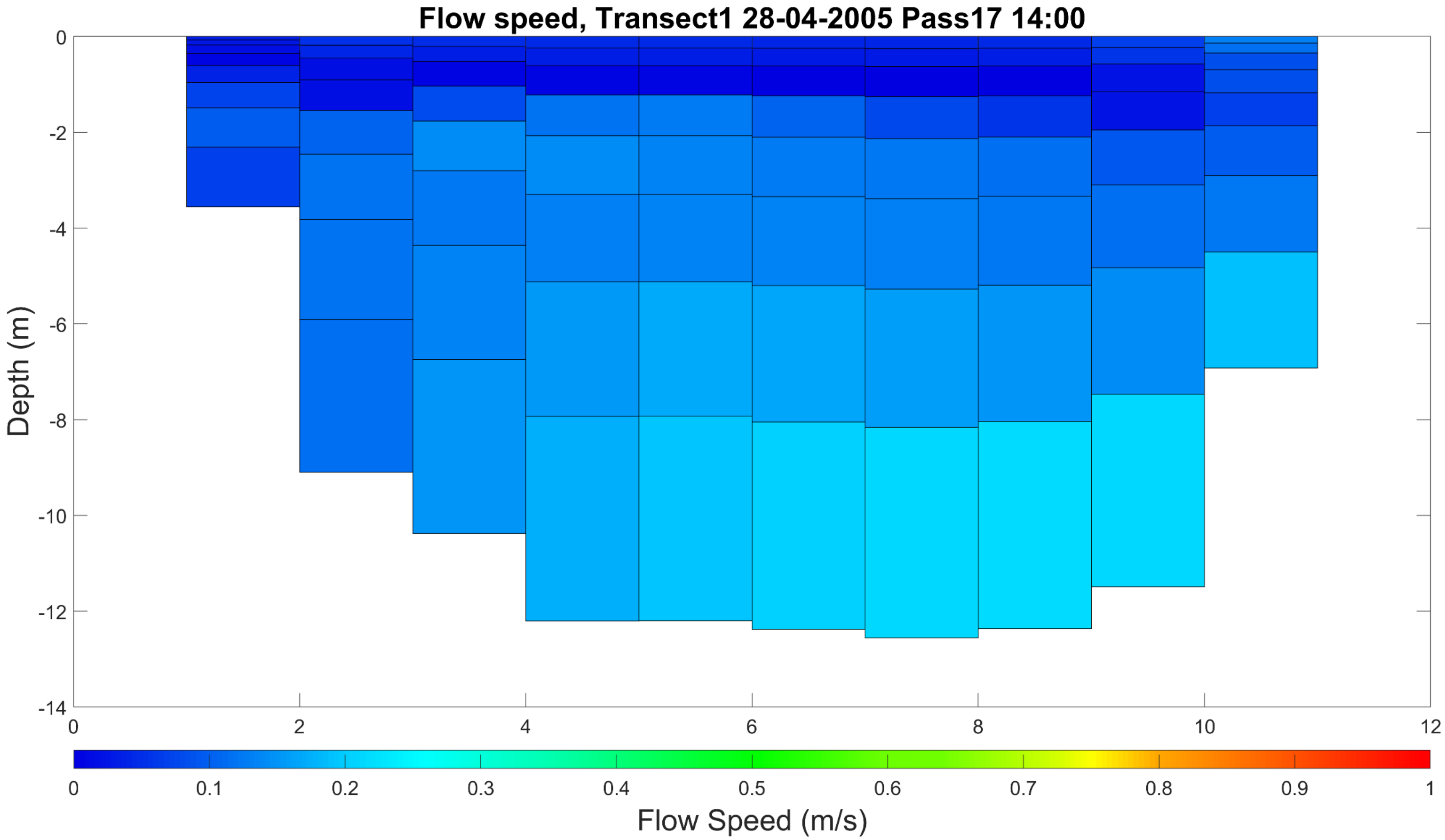

Figure 24. Modelled flow speed, Transect 1: Flood tide, cross section of speed with depth shown from west (left) to east (right)

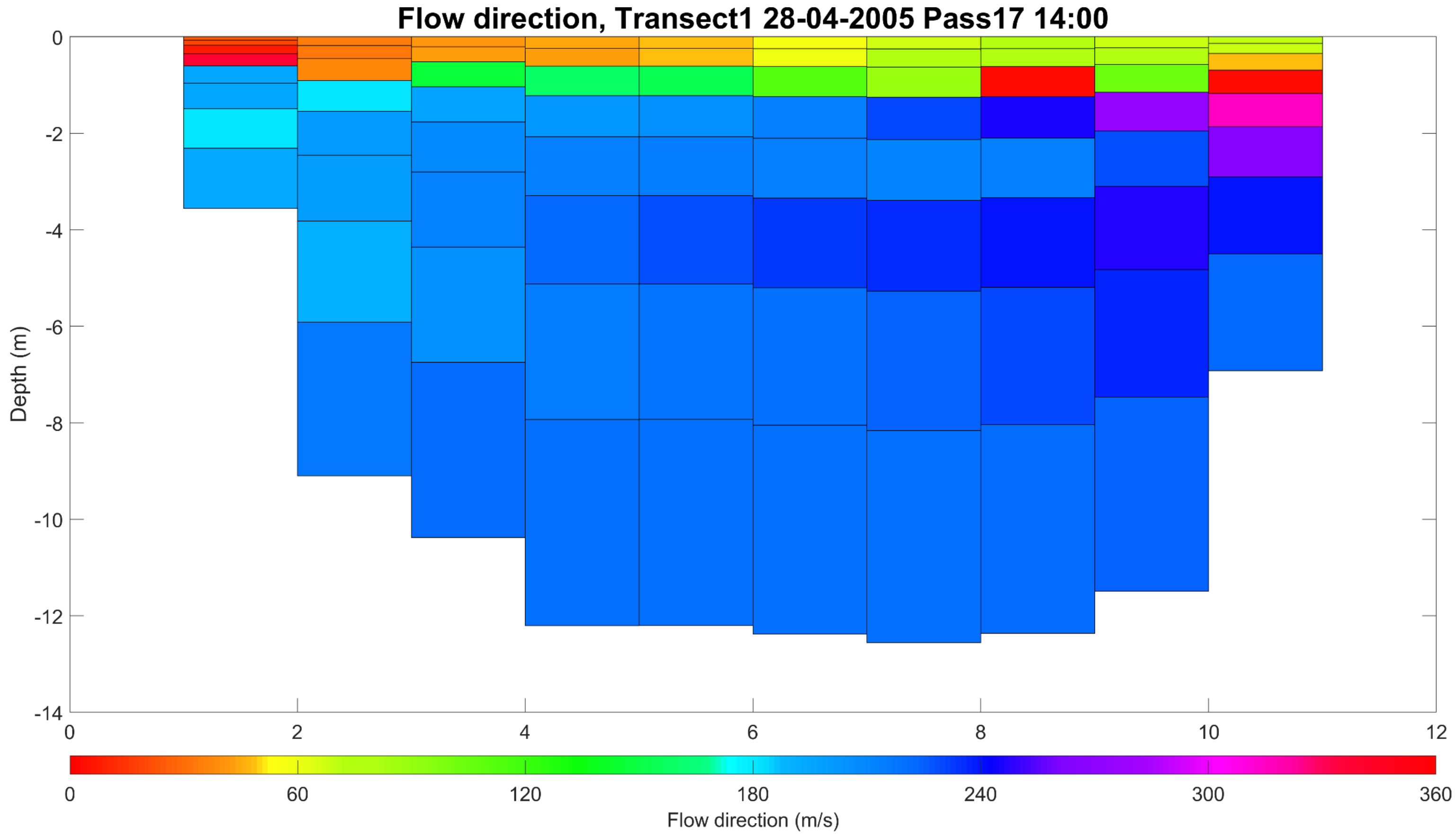

Figure 25. **Modelled flow direction, Transect 1: Flood tide, cross section of direction with depth shown from west (left) to east (right)**

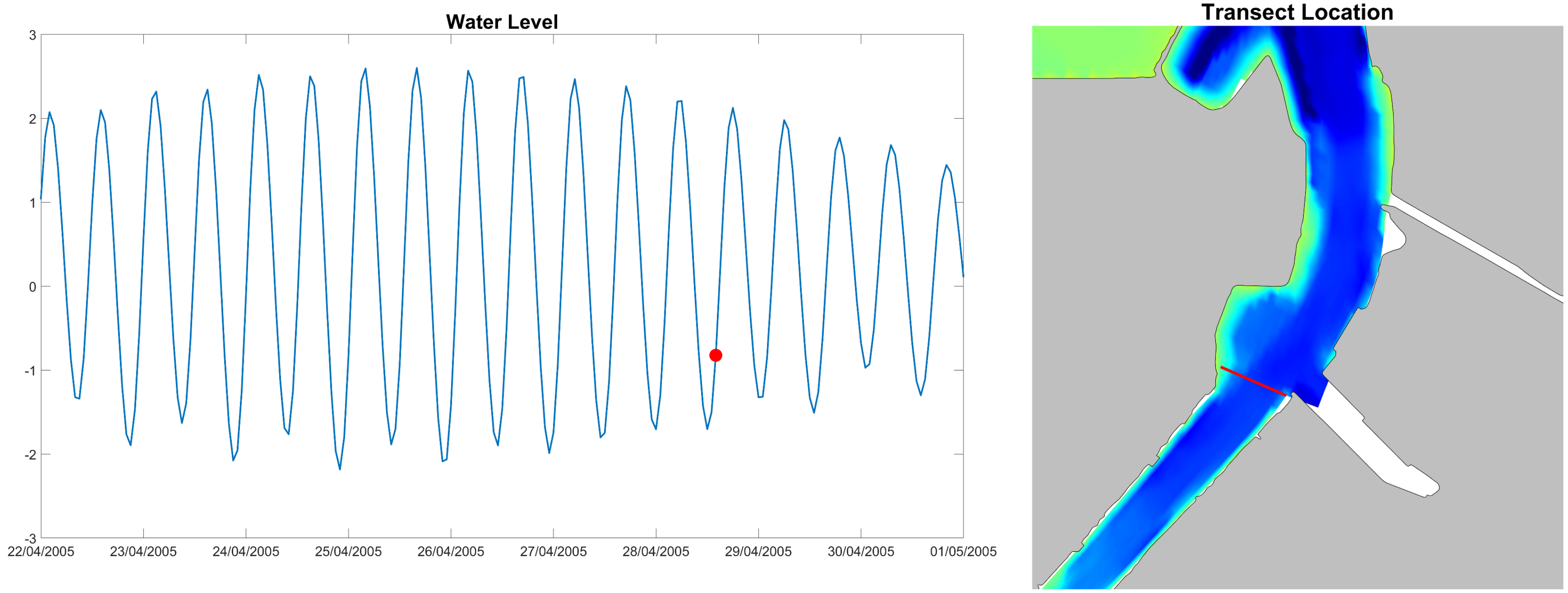

Figure 26. Tidal state and transect location extracted from the model for Transect 1 Pass 17: 28/04/2005

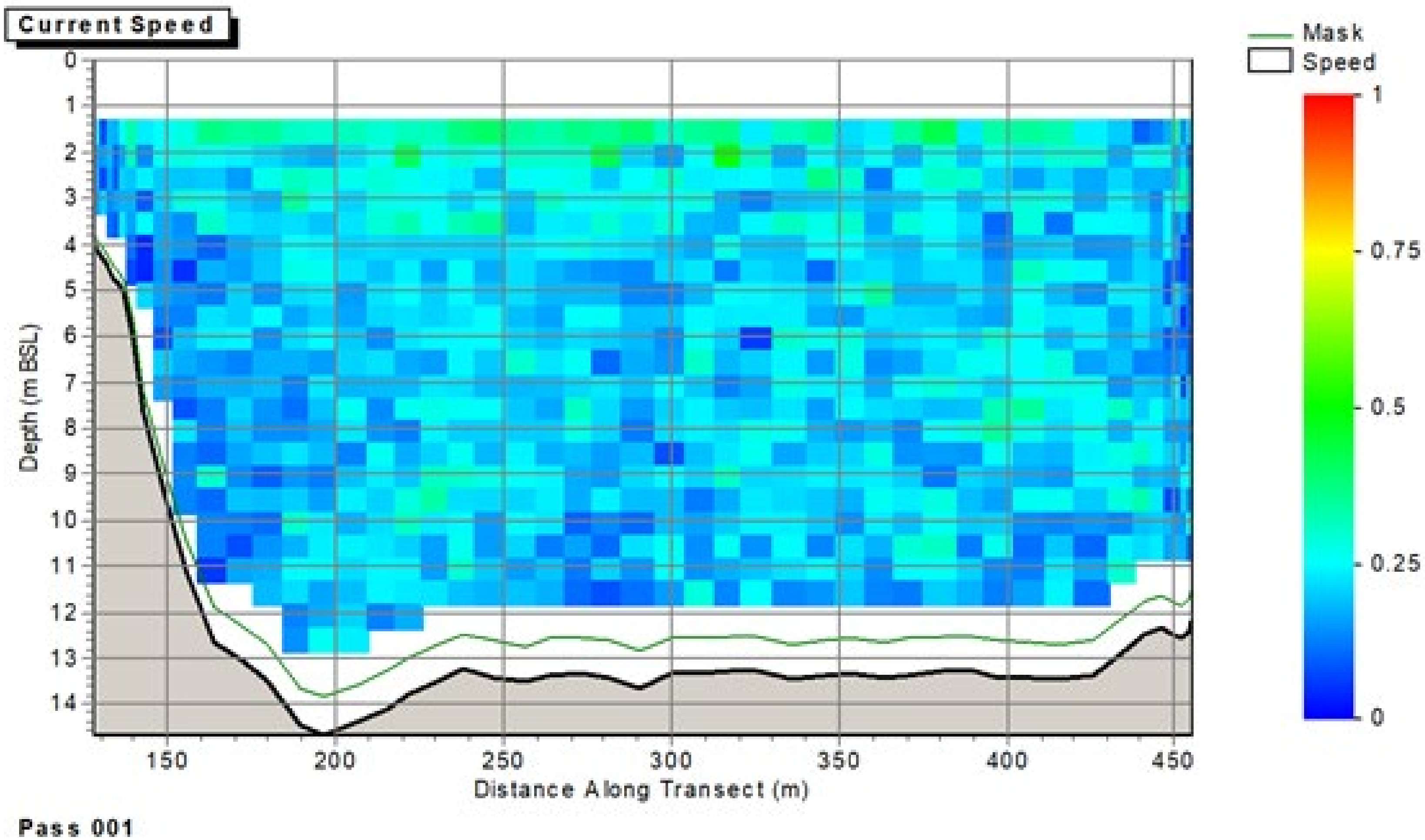

Figure provided by PD Teesport

Figure 27. Measured flow speed, Transect 7, Pass 1: Ebb tide, cross section of speed with depth shown from west (left) to east (right)

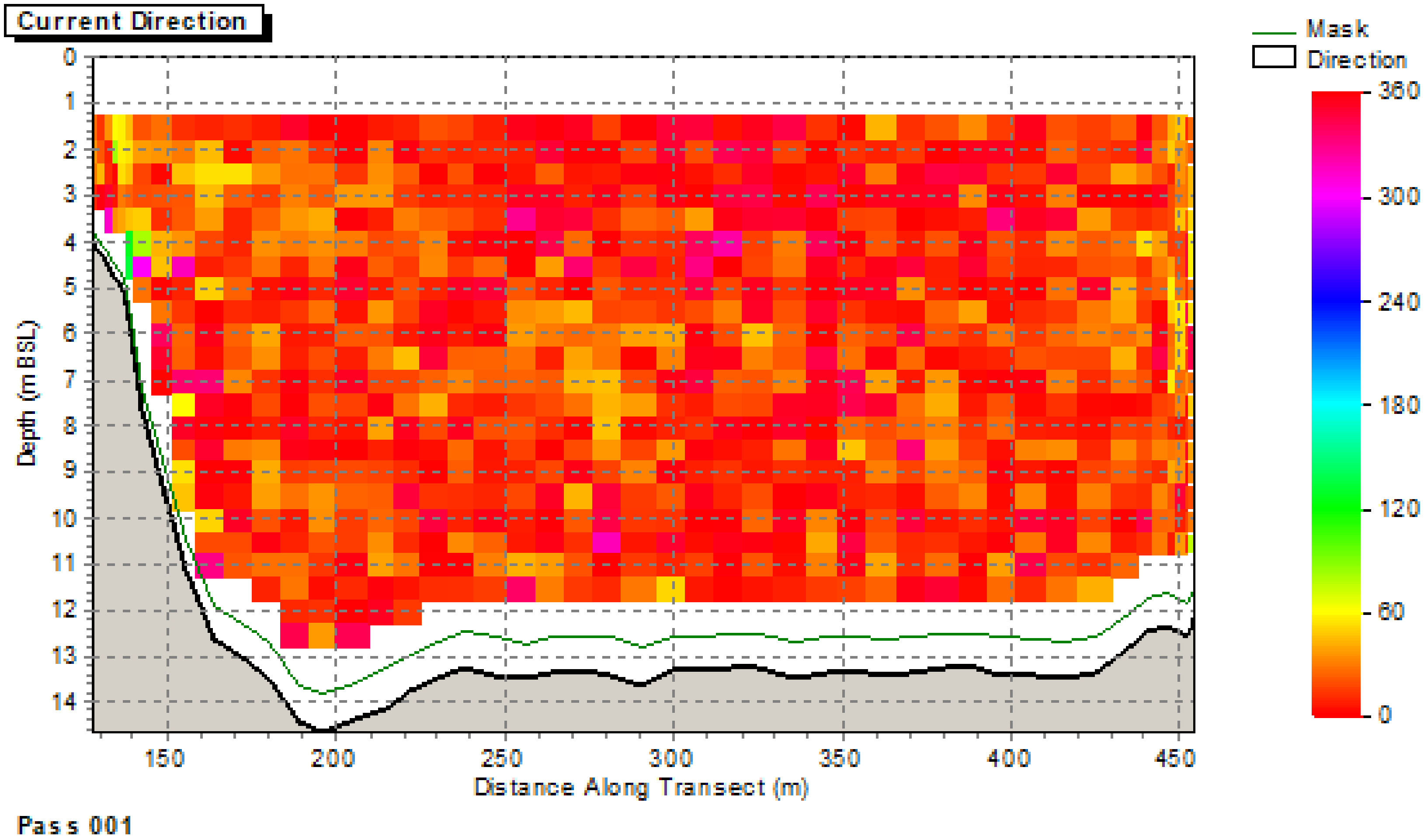

Figure provided by PD Teesport

Figure 28. Measured flow direction, Transect 7, Pass 1: Ebb tide, cross section of direction with depth shown from west (left) to east (right)

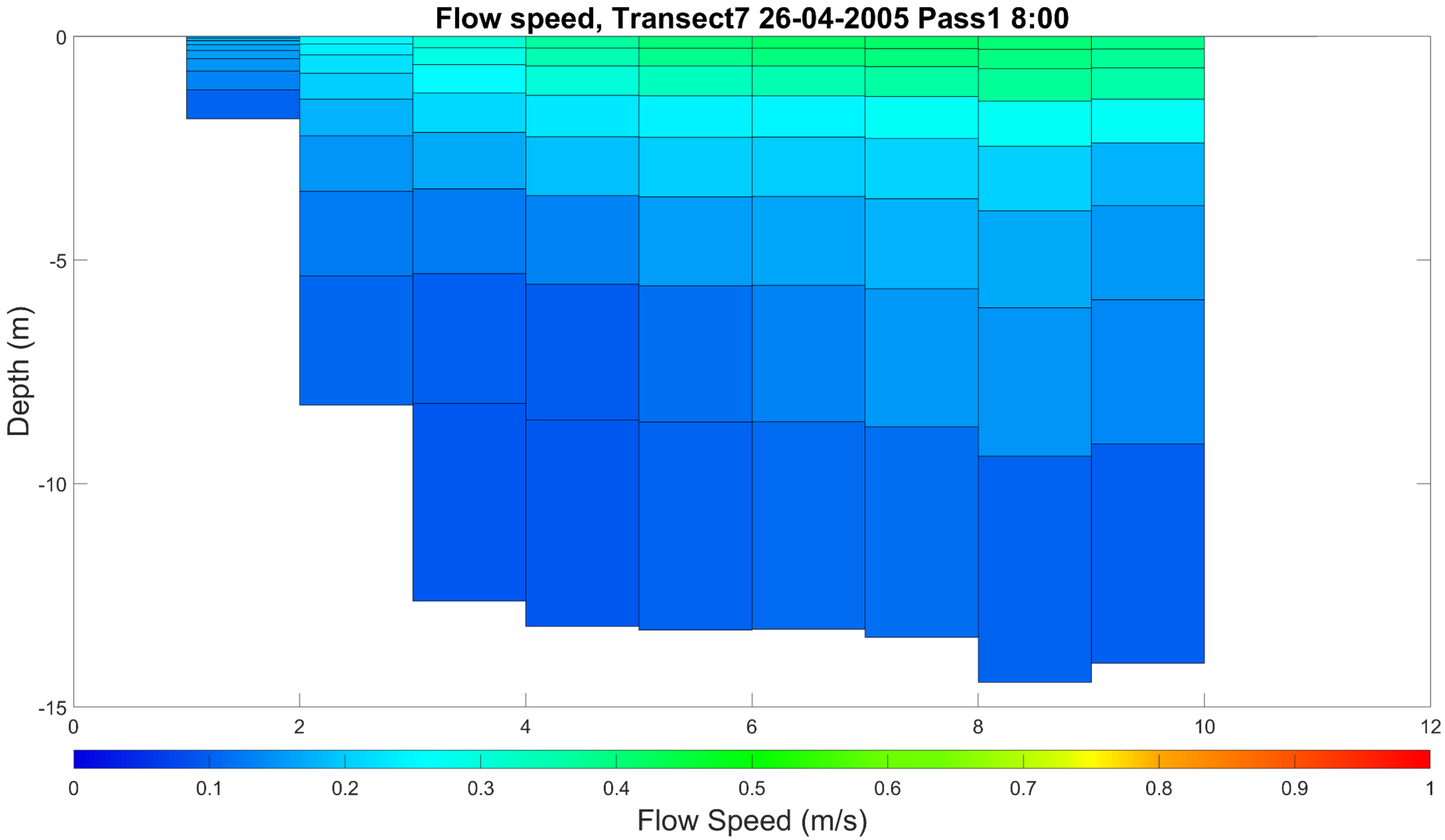

Figure 29. Modelled flow speed, Transect 7: Ebb tide, cross section of speed with depth shown from west (left) to east (right)

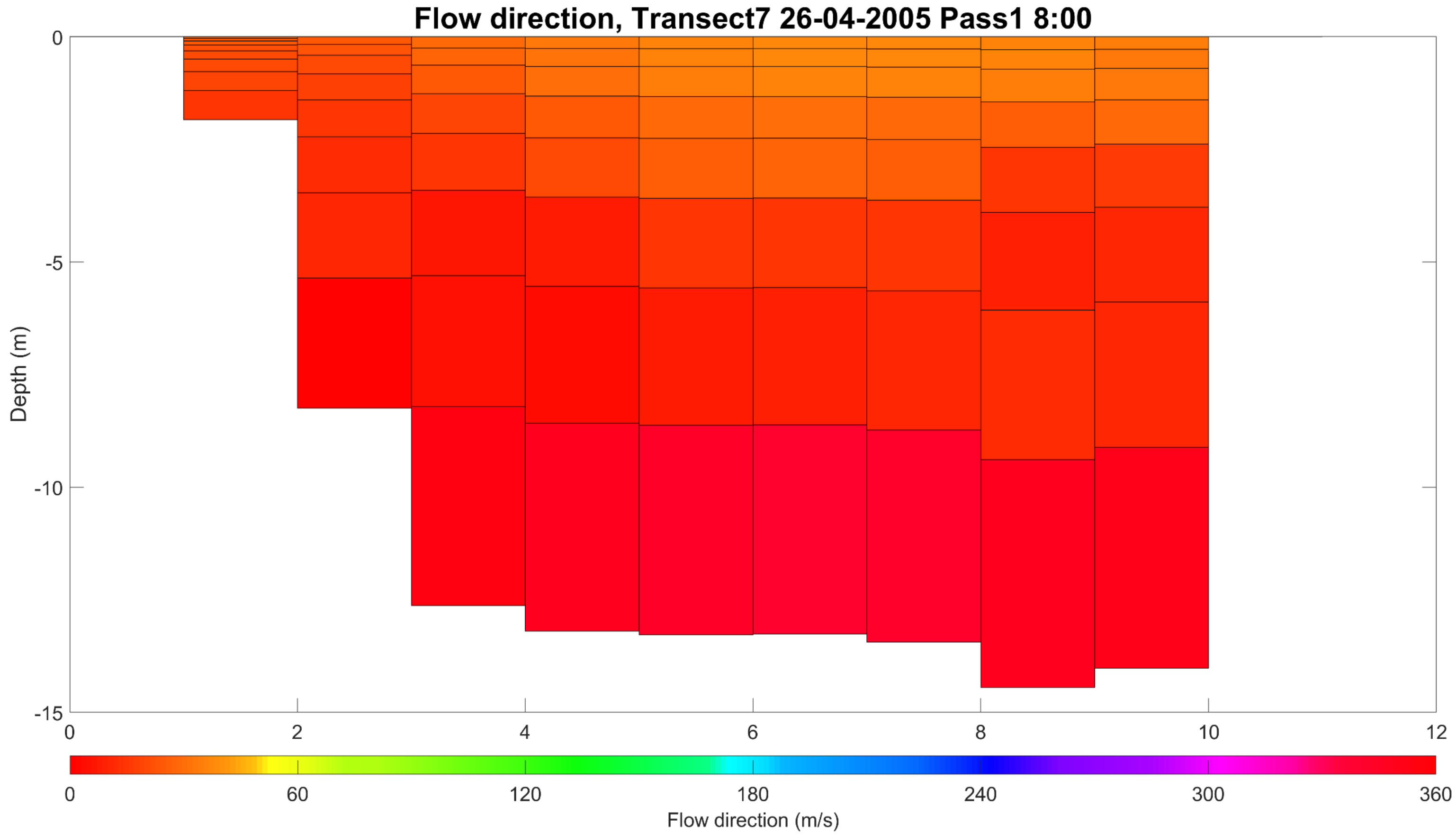

Figure 30. Modelled flow direction, Transect 7: Ebb tide, cross section of direction with depth shown from west (left) to east (right)

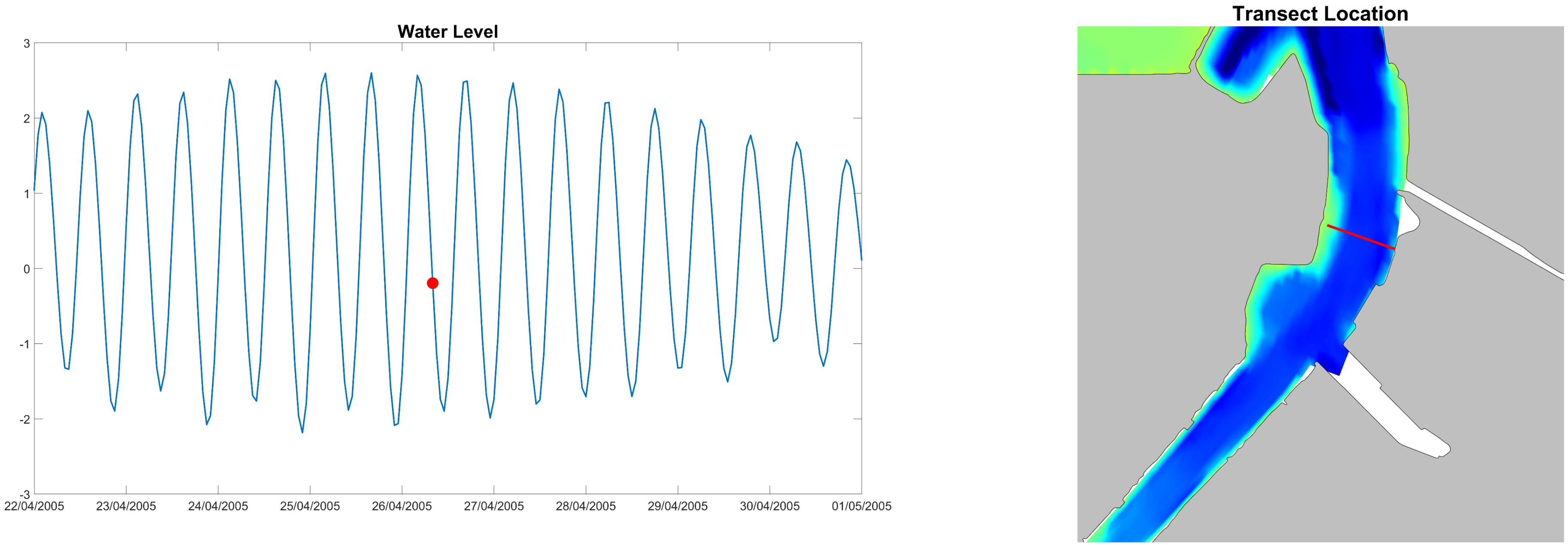

Figure 31. Tidal state and transect location extracted from the model for Transect 7 Pass 1: 26/04/2005

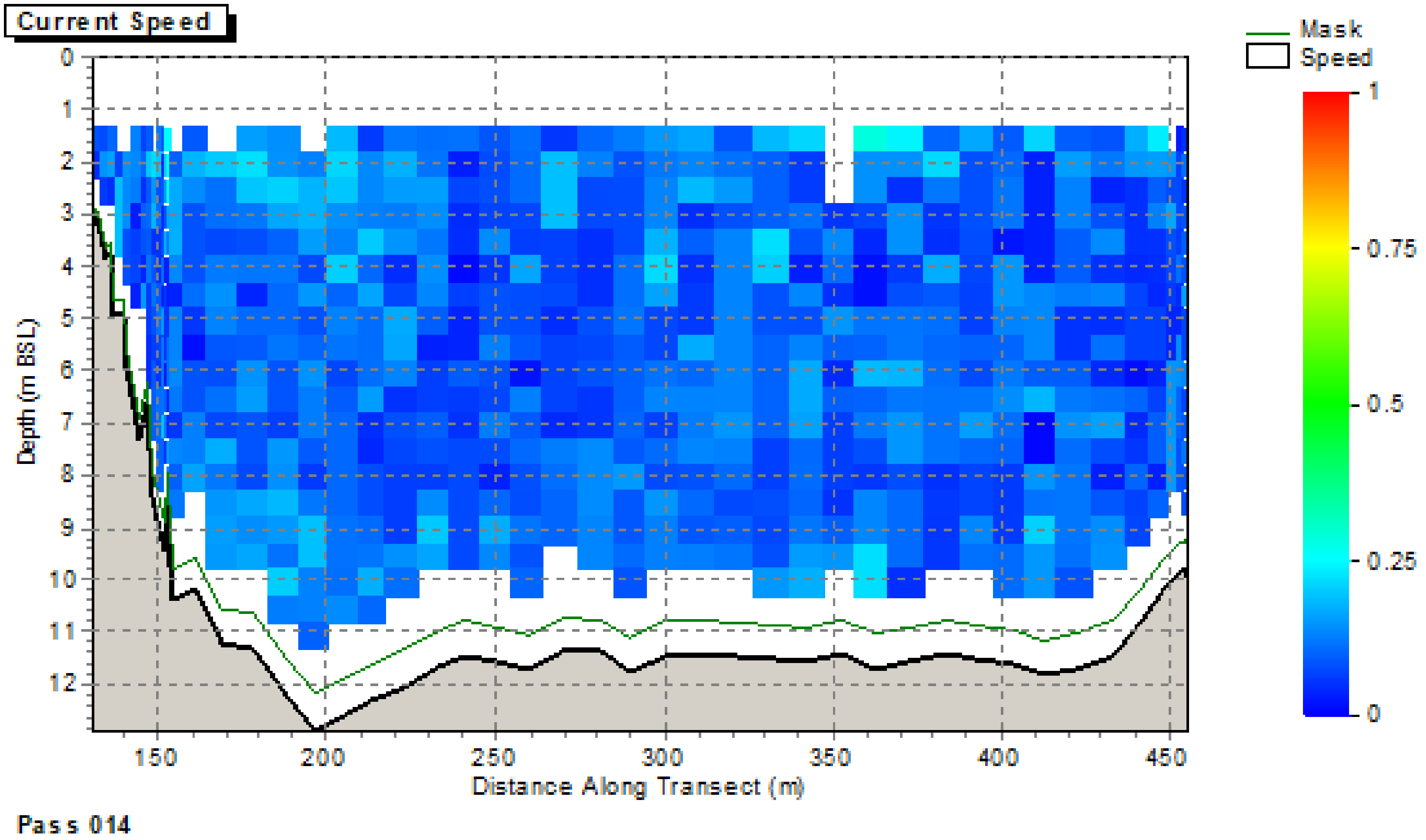

Figure provided by PD Teesport

Figure 32. Measured flow speed, Transect 7, Pass 14: Low water, cross section of speed with depth shown from west (left) to east (right)

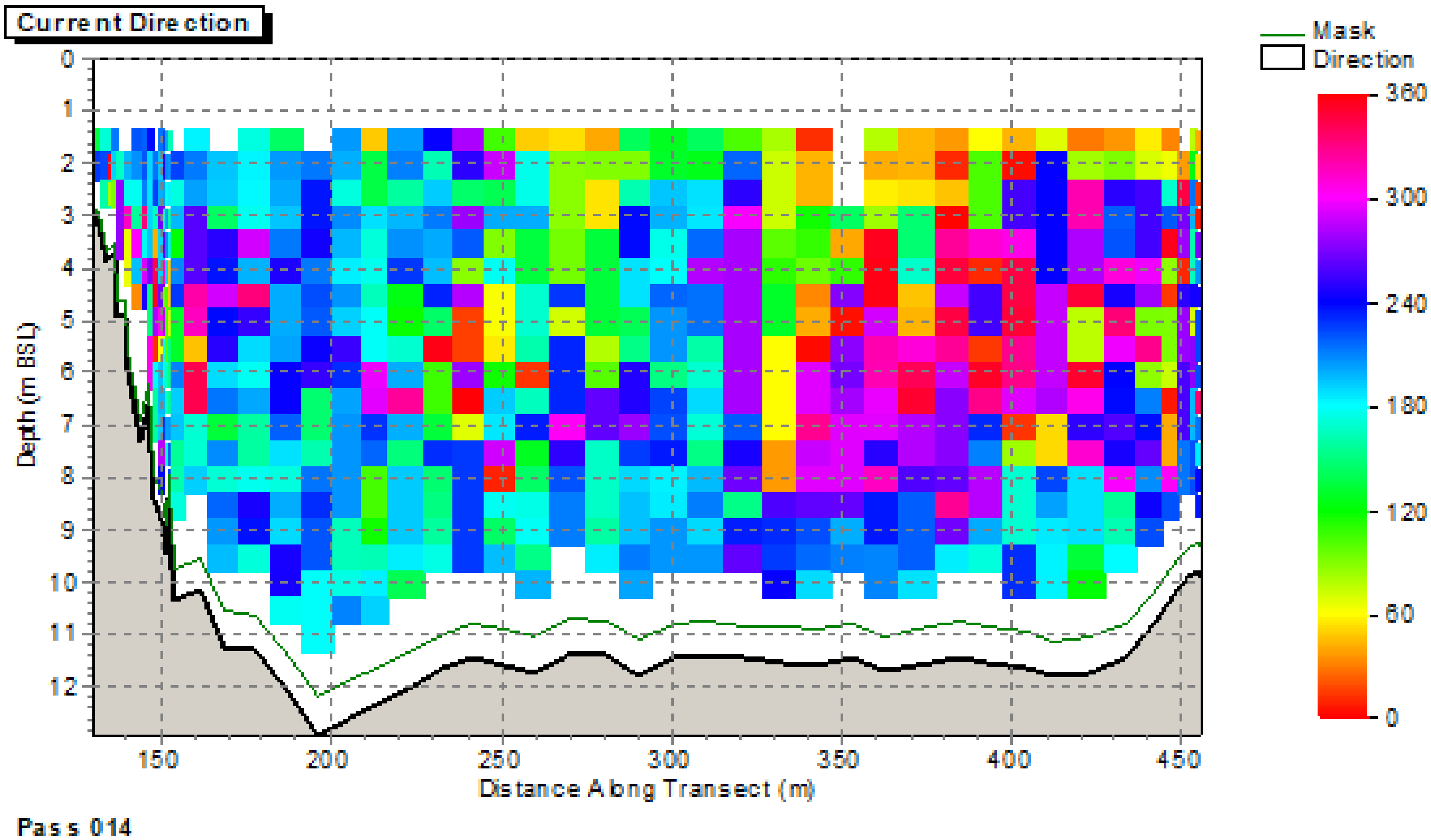

Figure provided by PD Teesport

Figure 33. Measured flow direction, Transect 7, Pass 14: Low water, cross section of direction with depth shown from west (left) to east (right)

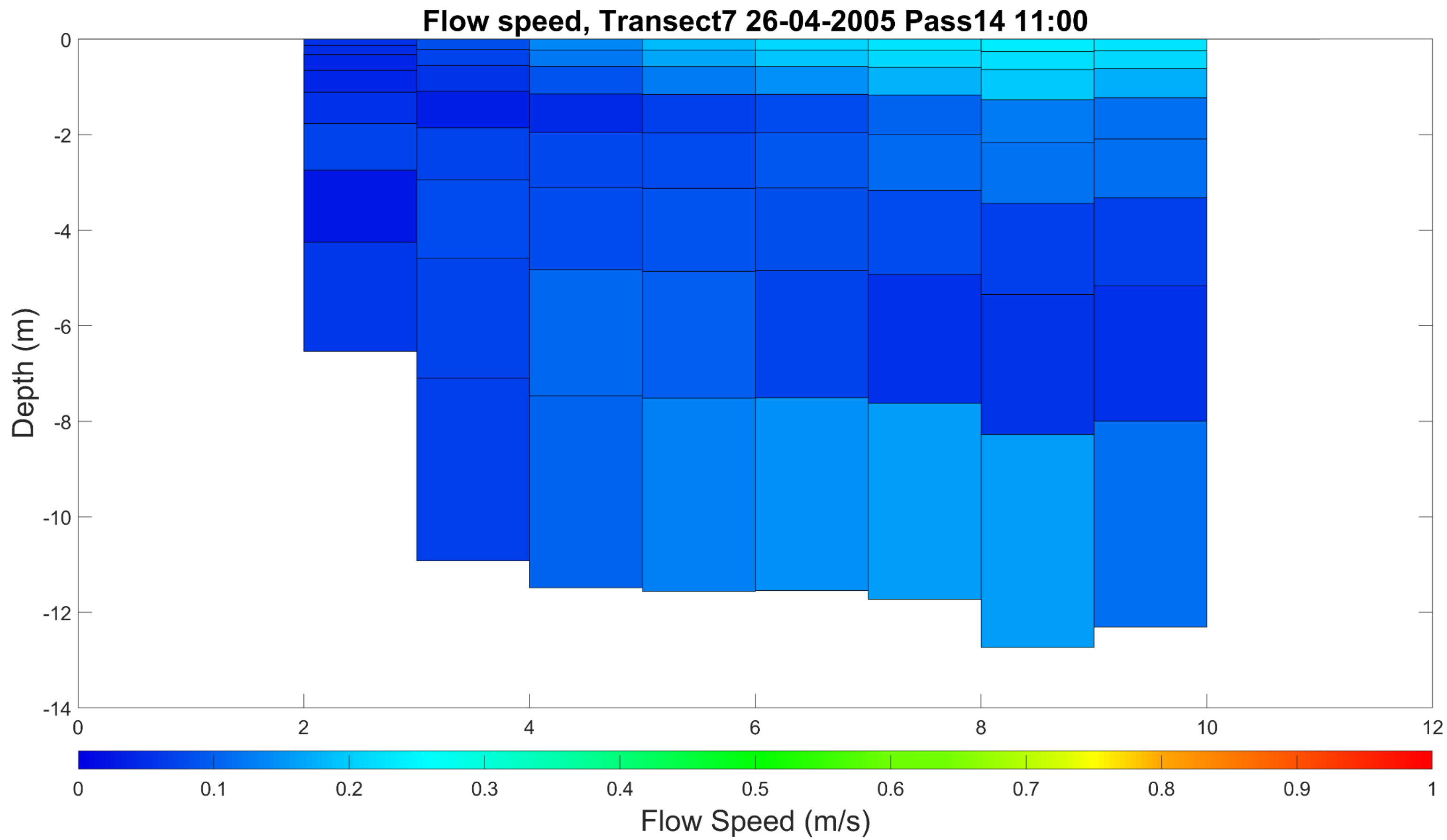

Figure 34. Modelled flow speed, Transect 7: Low water, cross section of speed with depth shown from west (left) to east (right)

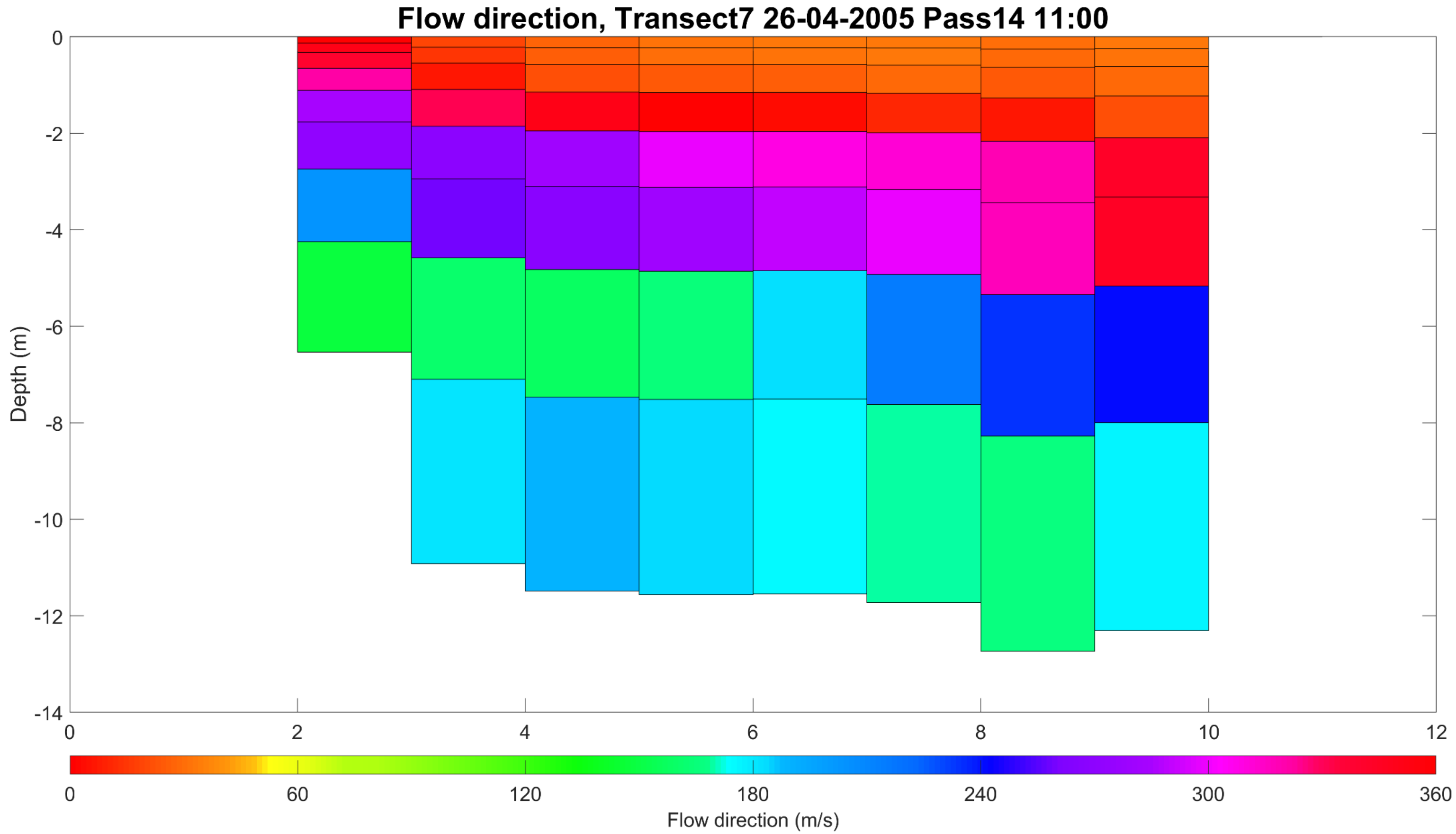

Figure 35. **Modelled flow direction, Transect 7: Low water, cross section of direction with depth shown from west (left) to east (right)**

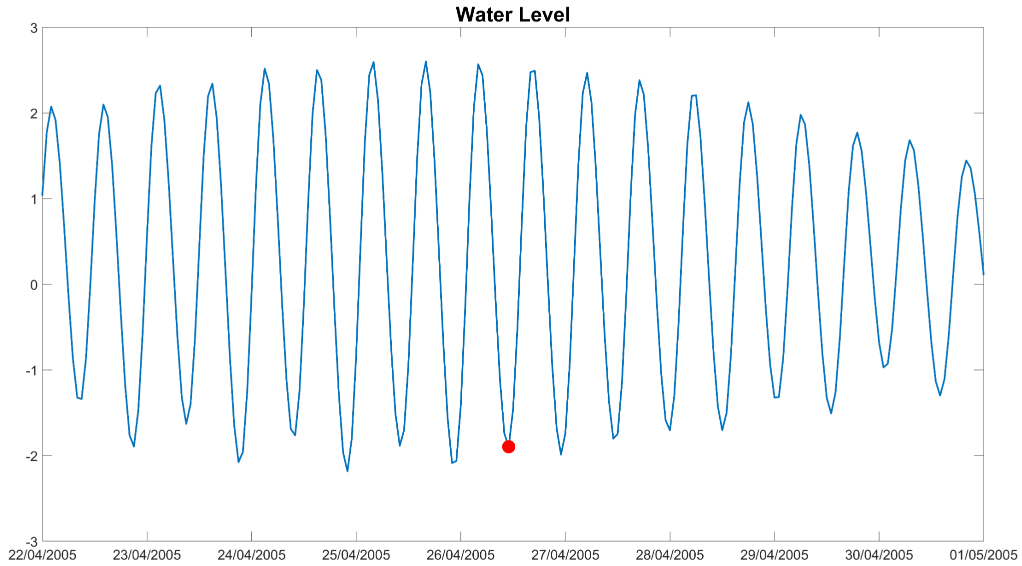

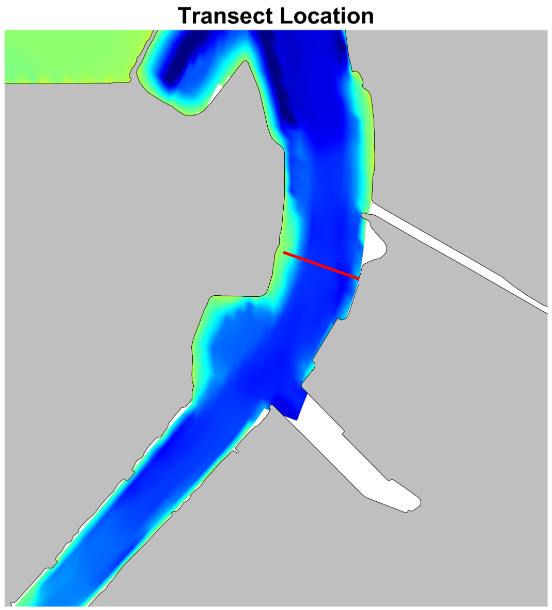

Figure 36. Tidal state and transect location extracted from the model for Transect 7 Pass 14: 26/04/2005

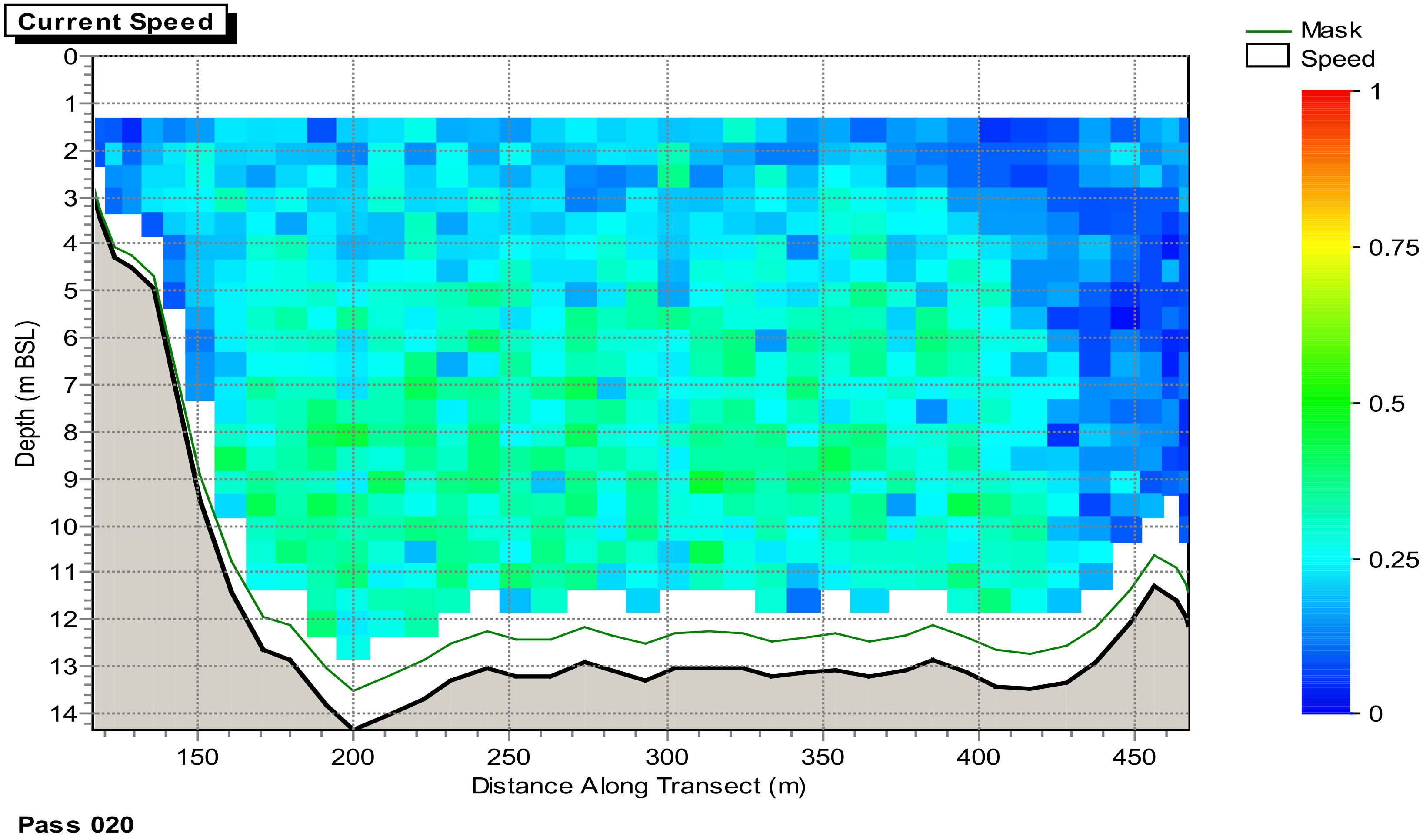

Figure provided by PD Teesport

Figure 37. Measured flow speed, Transect 7, Pass 20: Flood tide, cross section of speed with depth shown from west (left) to east (right)

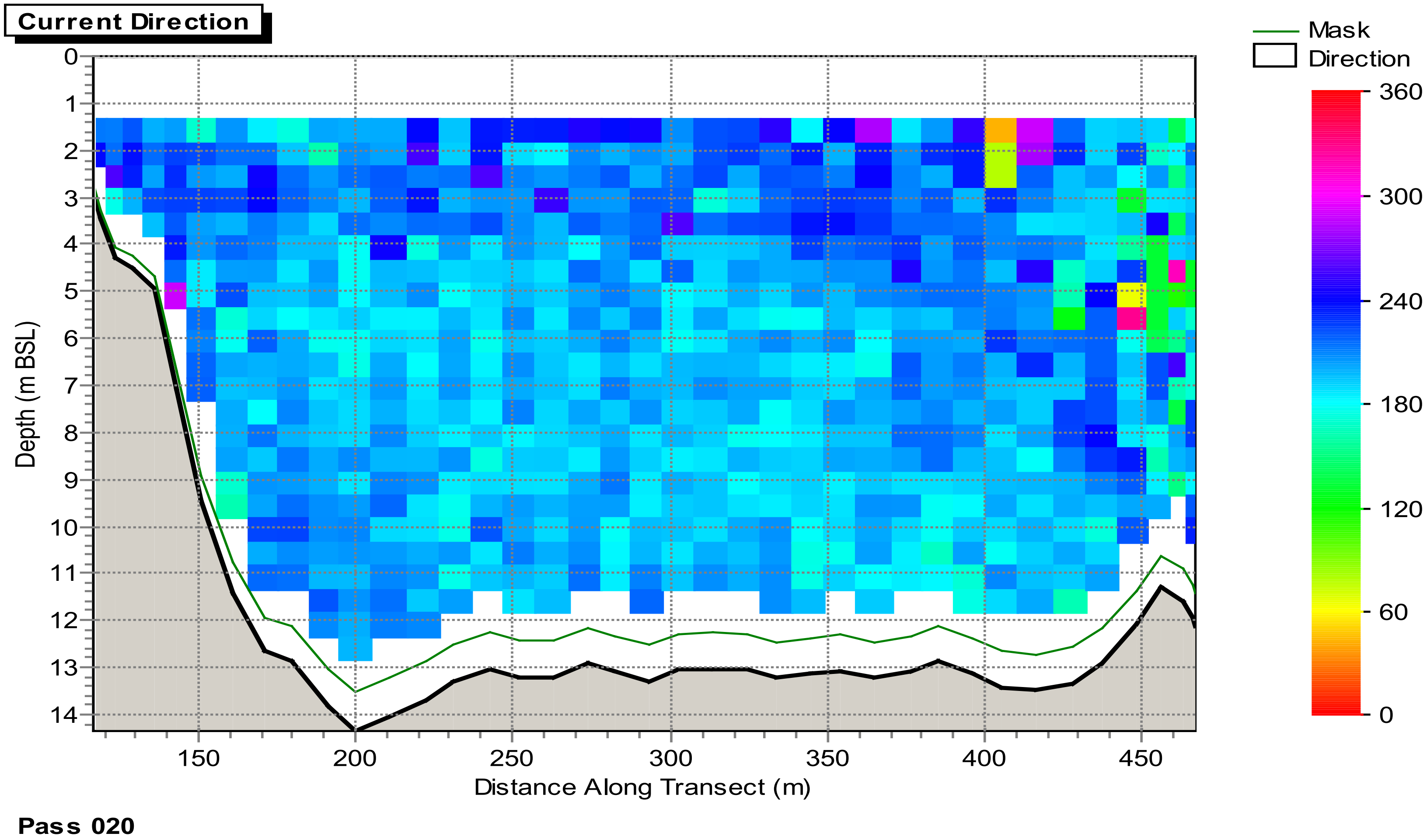

Figure provided by PD Teesport

Figure 38. Measured flow direction, Transect 7, Pass 20: Flood tide, cross section of direction with depth shown from west (left) to east (right)

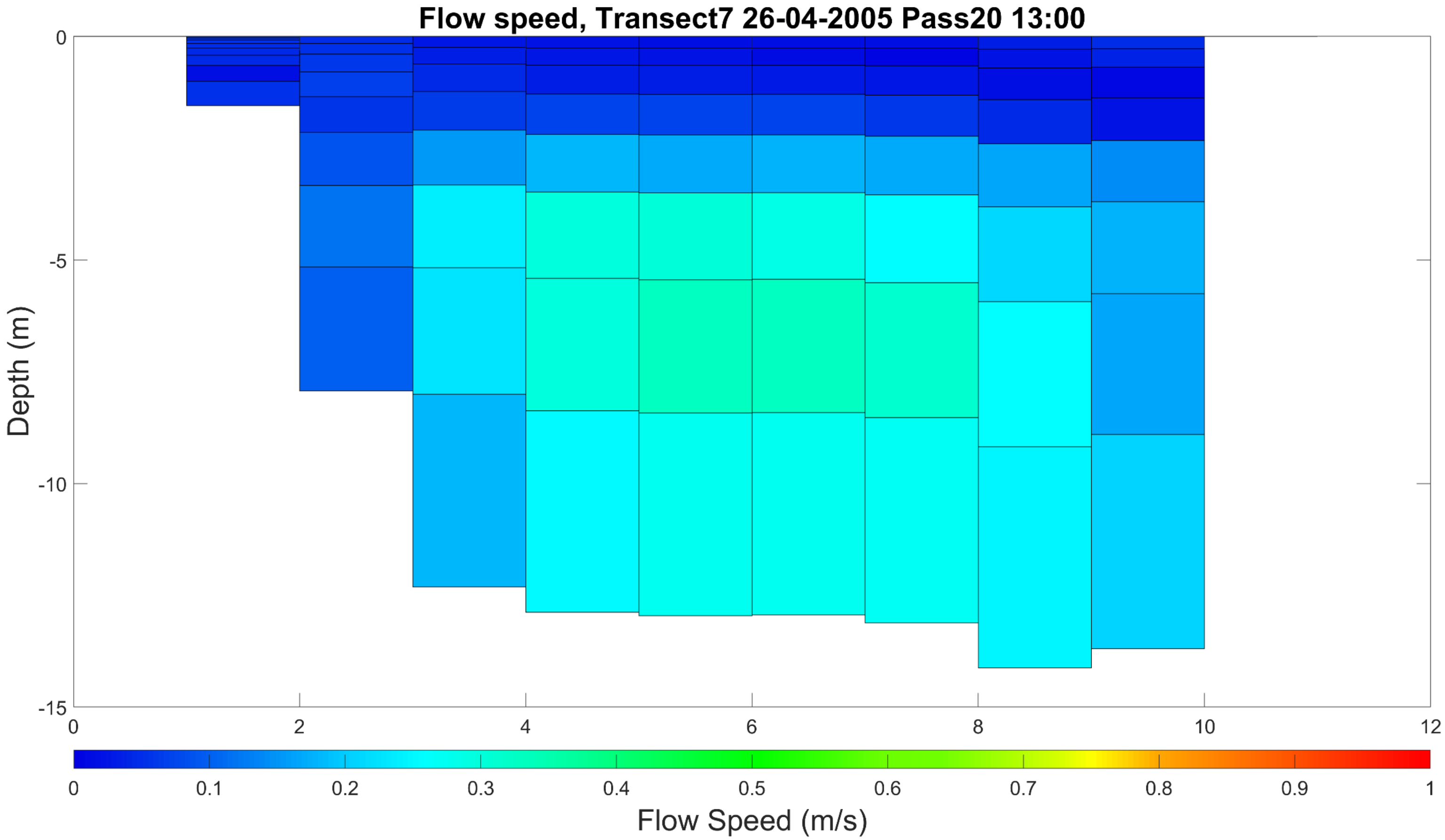

Figure 39. Modelled flow speed, Transect 7: Flood tide, cross section of speed with depth shown from west (left) to east (right)

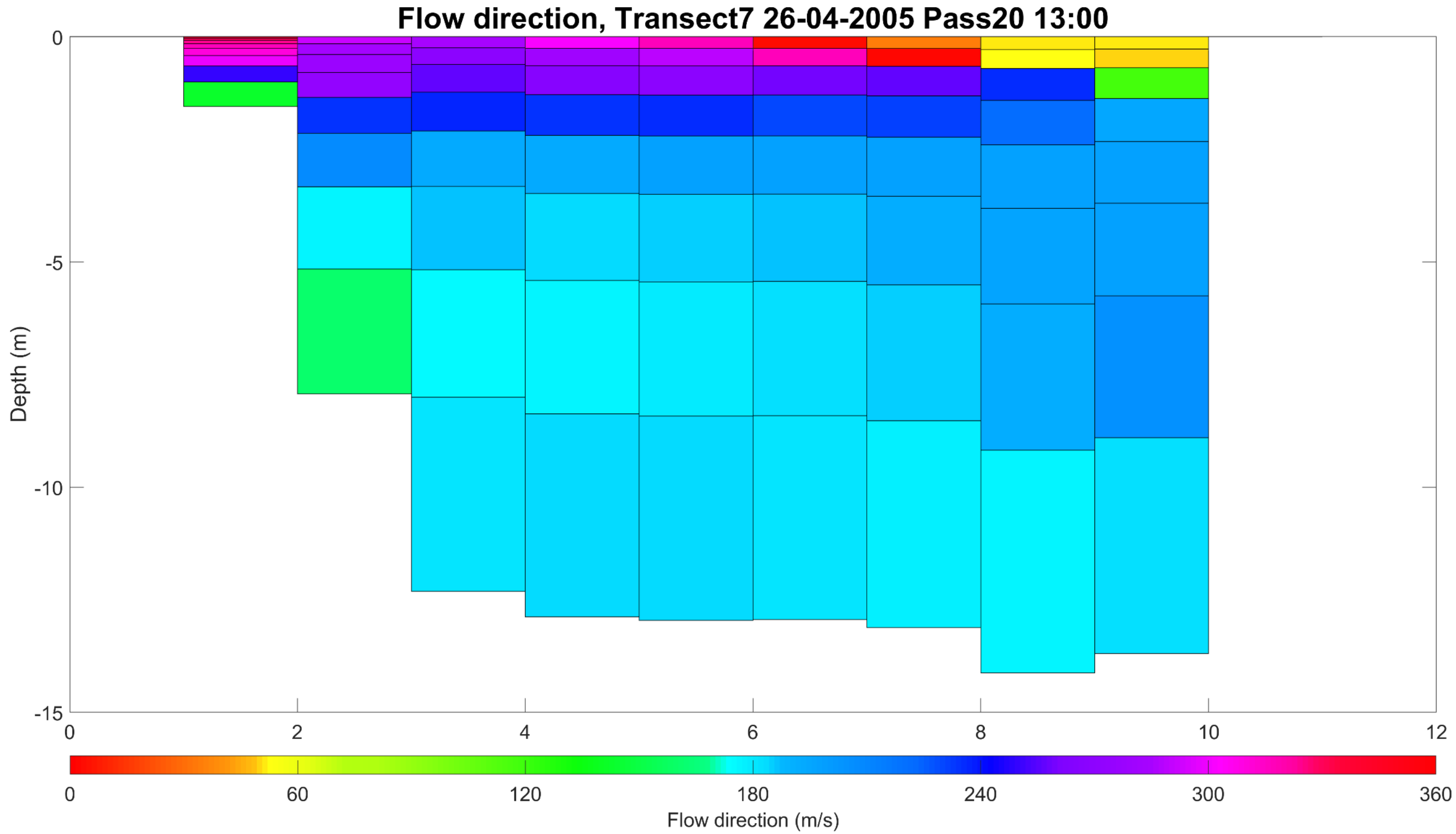

Figure 40. Modelled flow direction, Transect 7: Flood tide, cross section of direction with depth shown from west (left) to east (right)

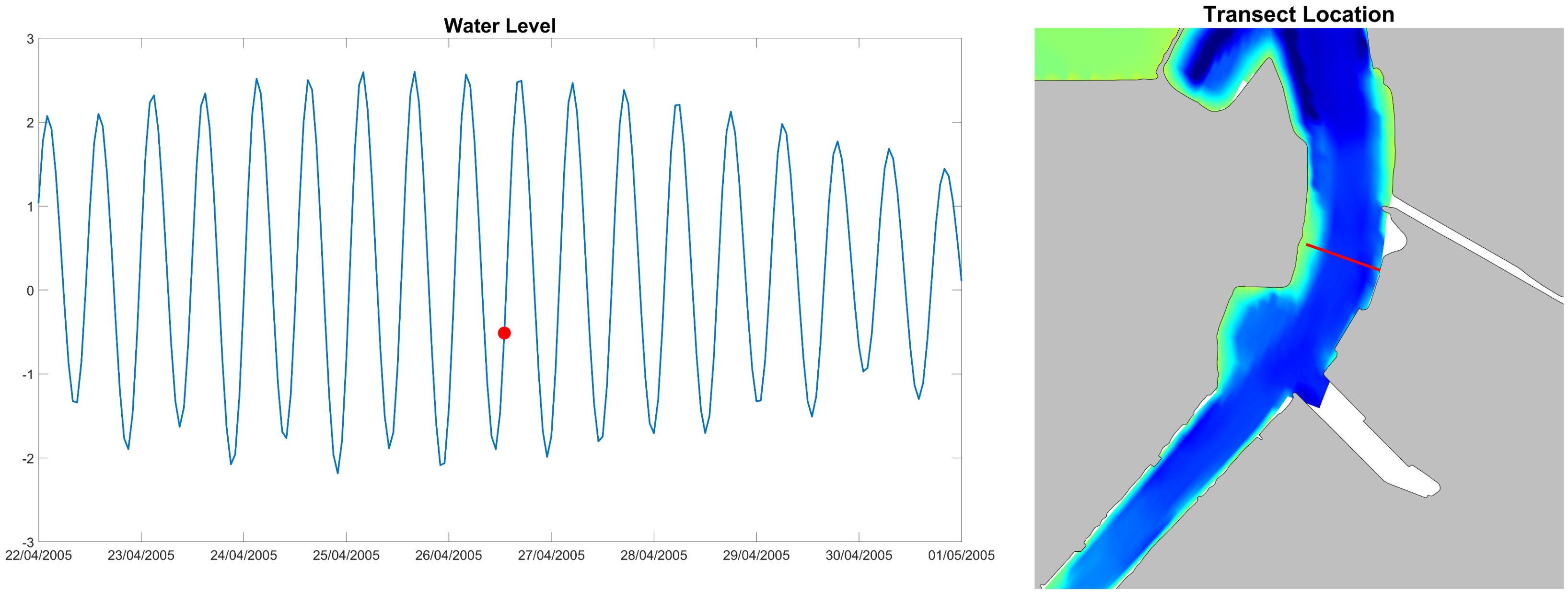

Figure 41. Tidal state and transect location extracted from the model for Transect 7 Pass 20: 26/04/2005

Timeseries flow data

Tees and Hartlepool Port Authority (THPA) previously provided measured flow speed and direction data from fixed current meter observations at a central location in the Tees Estuary. The location of the fixed current meter is data is shown in Figure 42 with the label Buoy 10. These data were processed in the previous study and assessed to identify spring and neap data periods of comparable magnitude to the model run period. The processed data for selected spring and neap tidal periods, have been utilised in this study to produce an equivalent comparison of measured and modelled data using the new modelled outputs. As an initial sense check, the modelled data were also compared against the previous modelled results.

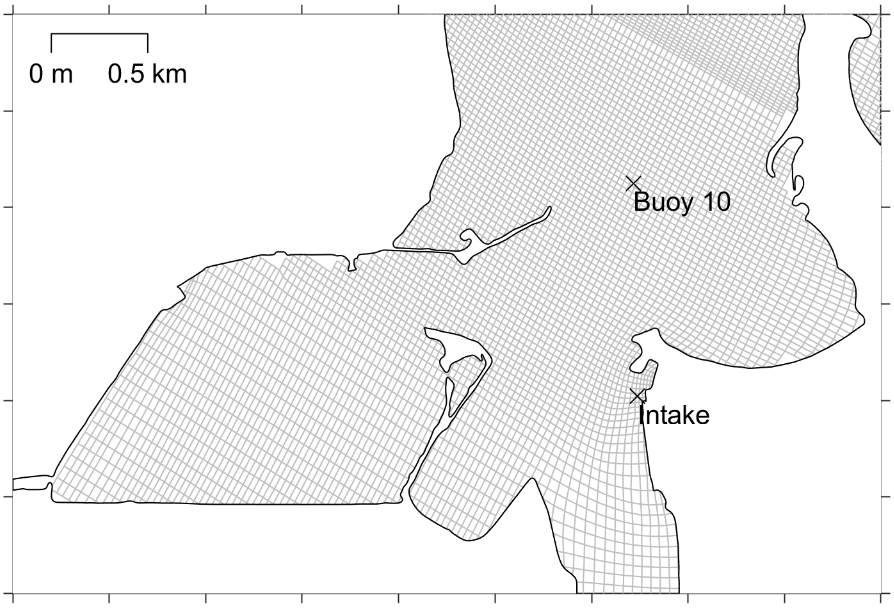

Figure 42. Fixed current meter location: Buoy 10

Comparison of the modelled and measured datasets are shown in Figure 43 for spring tides and Figure 44 for a neap condition. It should be remembered when examining the comparisons that:

- the layers in the model may not correspond exactly to the elevation of the instrument deployed in the field and none of the measurements would have been made for the exact tidal conditions, bathymetry and location being modelled. Hence a perfect calibration would not be expected.;
- the time period of the observations and model output is different. Comparison is between two data sets which have similar tidal ranges only.
- Field observations are represented by a poor temporal resolution of data points within the period of measurement. Hence variation within this period may have occurred which is not shown in the data.
- Freshwater regime during the collection period may be different from that specified in the model, which itself represents mean conditions.
- Time between the field observations and the present means that there could be differences in local bathymetry at and around the measured site compared to that modelled.

Comparisons were made at three layers within the water column: surface, middle and bed. There is generally good agreement between the phasing and magnitude in the datasets.

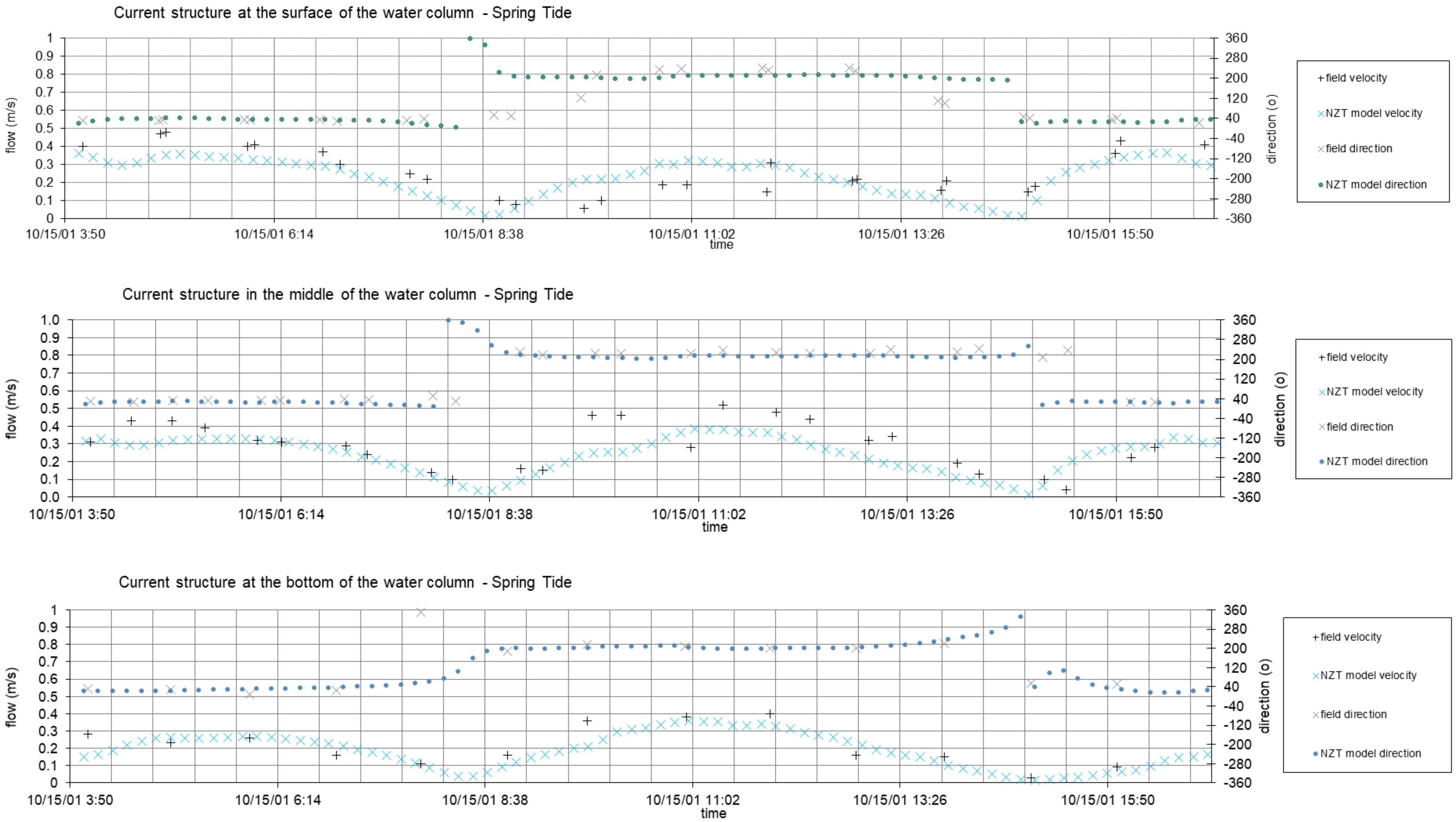

Figure 43. Measured and modelled flow speed and direction comparison – Spring tide

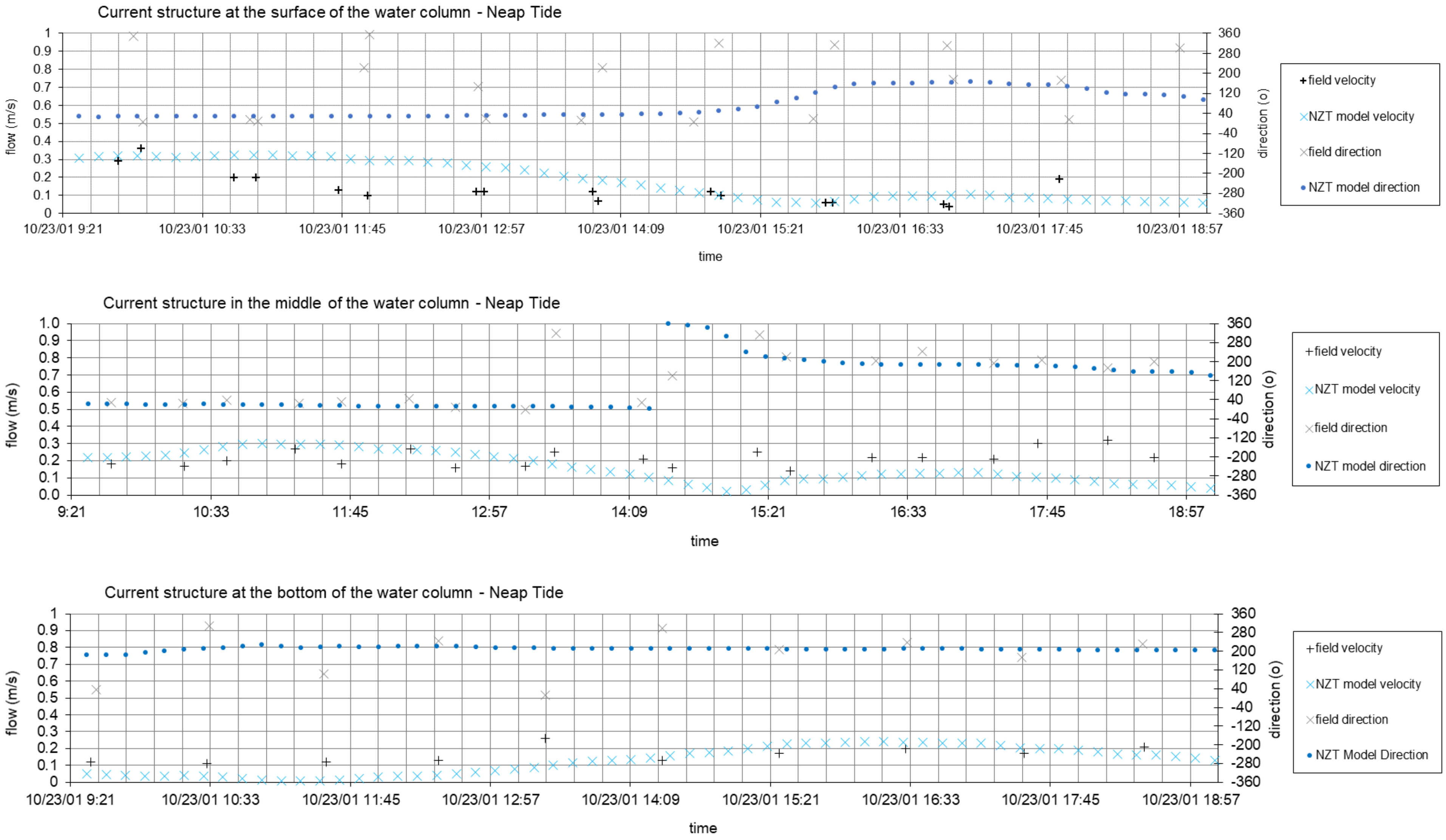

Figure 44. Measured and modelled flow speed and direction comparison – Neap tide

3.1.3 CTD data

AECOM have provided measurements of temperature and salinity from individual CTD (Conductivity, Temperature, Depth) casts deployed across the ADCP transects during the PD Teesport survey, conducted between 21/04/2005 to 30/04/2005.

All available CTD measured profiles have been plotted and compared against the model data available from the nearest model grid cell and coincident time. Sensitivity testing during the model build demonstrated that the salinity structure of the water column is sensitive to the starting salinity and to the discharge volume through the Tees Barrage. Three variations of the model have therefore been run for this data comparison to represent three alternative barrage discharges: Annual mean, summer and winter (as described in Table 4). The starting salinity of the model controls the resulting salinity of the bulk of the water column. The nature of the model setup (i.e. reasonably short duration with averaged discharge values across the barrage) means that the model will not reach a naturally stable point representative of a particular point in history: this would require a longer model duration and time varying discharges over a longer period, not felt necessary for the present study. The most appropriate starting value for the model salinity has been selected as 33.9 ppt based on values provided by AECOM from the Wood Draft Report (Wood, 2020) for seawater properties. This provides consistency throughout all modelled simulations (hydrodynamic and near-field thermal plume).

Figure 45 to Figure 48 present selected comparisons of CTD measurements and modelled profiles which are generally representative of the full set of profile comparisons.

It can be seen that the winter simulation (with higher freshwater flow discharges) creates the greatest variation in vertical structure, with the surface layer being significantly fresher for most states of the tide. This pattern is most consistent with the structure seen in the measured data. The salinity of the model tends to be fresher than the measurements for the bulk of the water column for all time periods and locations assessed, which tend to be closer to 35 ppt in most of the measured profiles. However, the measured salinity for this particular short period is more saline than other sources suggest for 'typical' conditions in the Tees Estuary, such as the Wood Draft Report (Wood, 2020), which documents 29.3 ppt for the Tees at Redcar Jetty and the Gares, and 32.8 ppt in the 'River Water'.

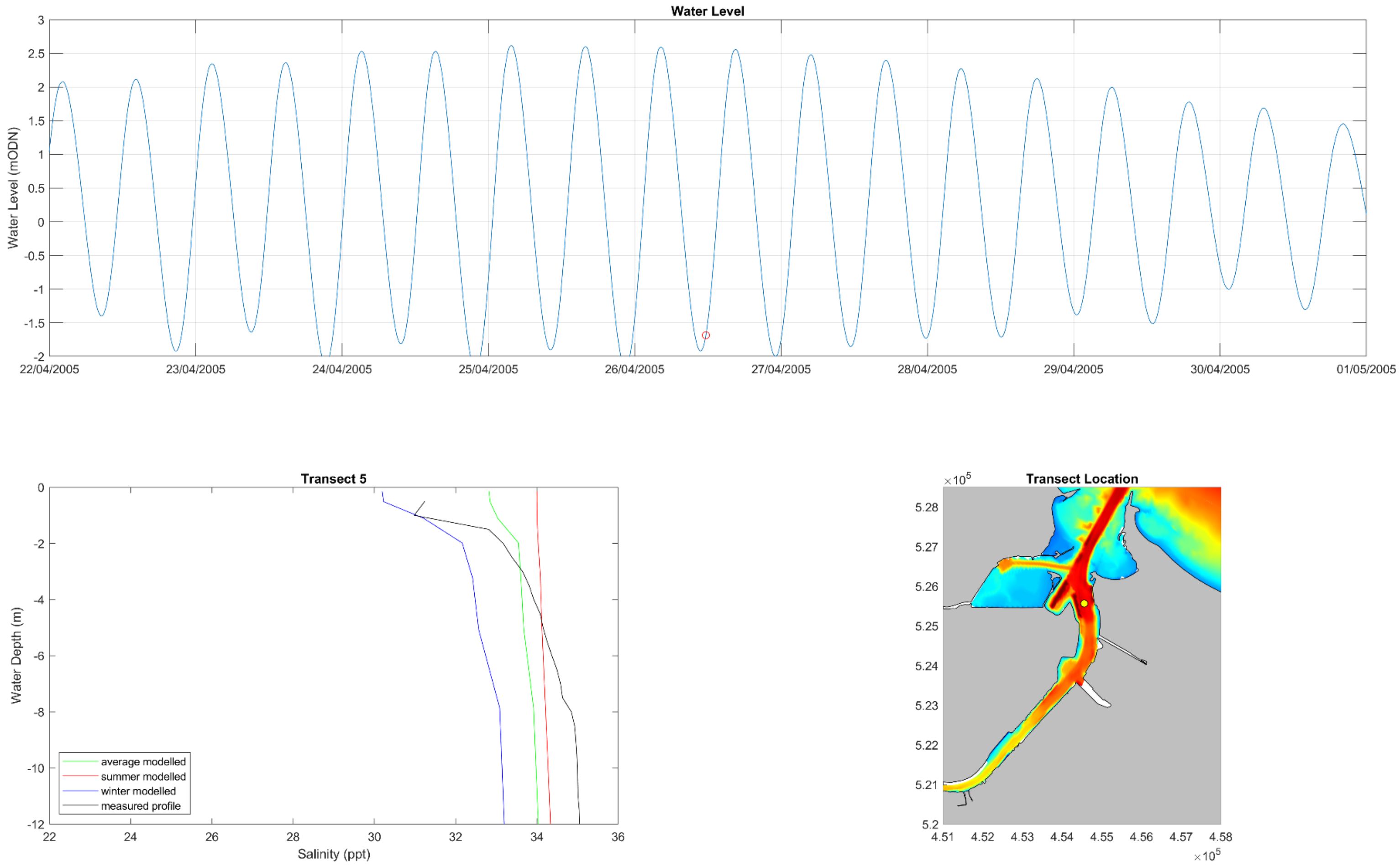

Figure 45. Comparison of measured and modelled salinity with depth: Transect 5

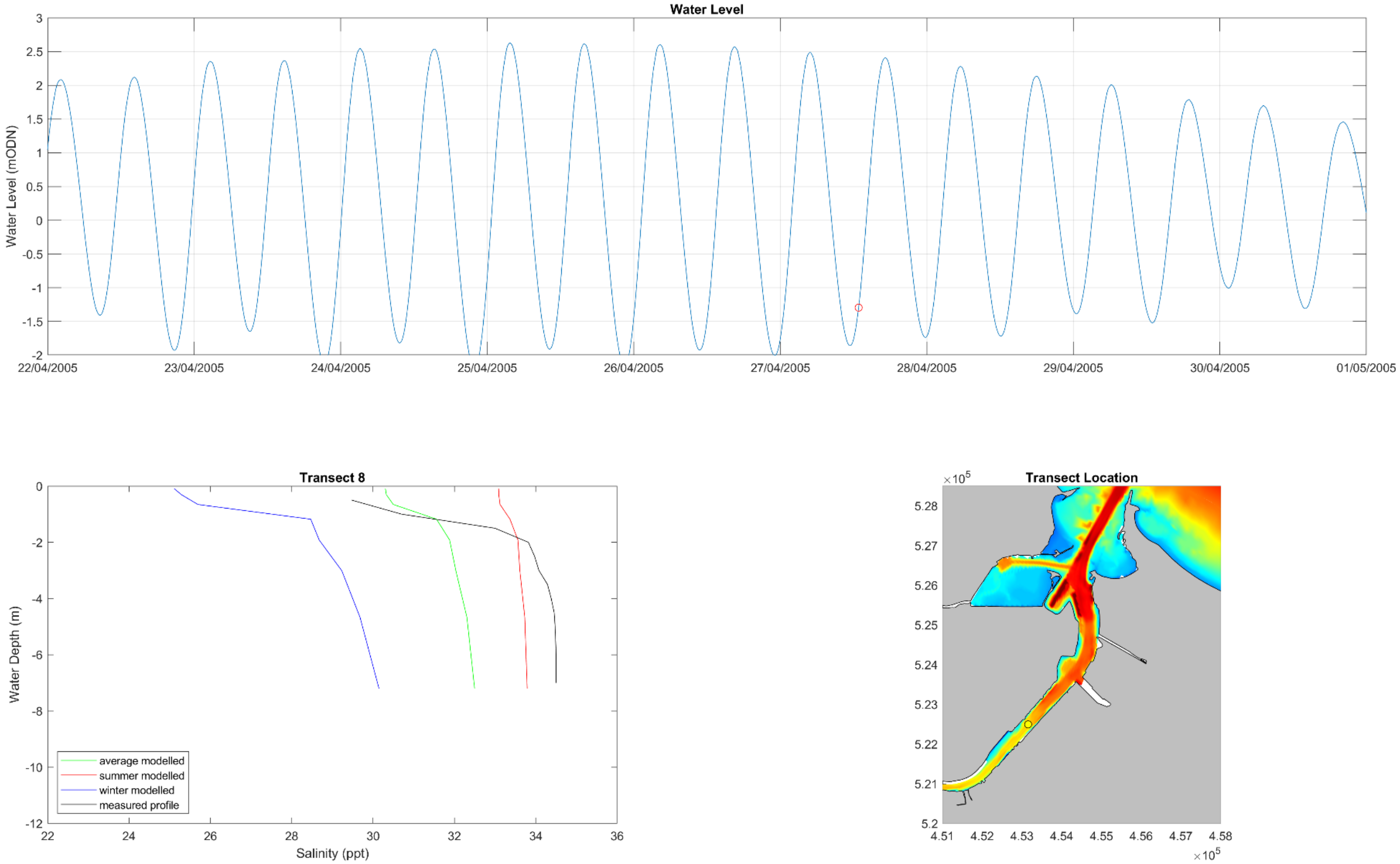

Figure 46. **Comparison of measured and modelled salinity with depth: Transect 8**

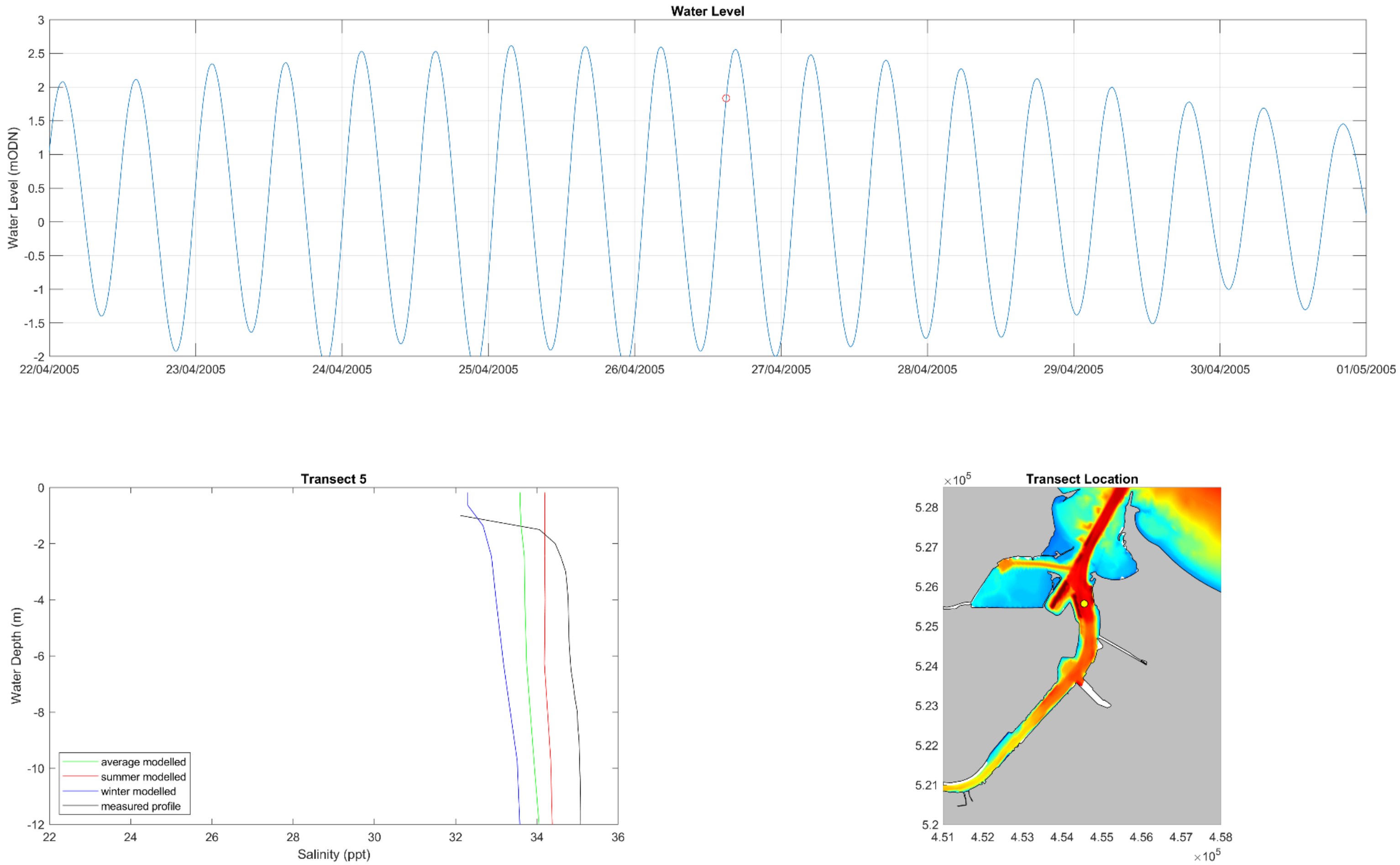

Figure 47. **Comparison of measured and modelled salinity with depth: Transect 5**

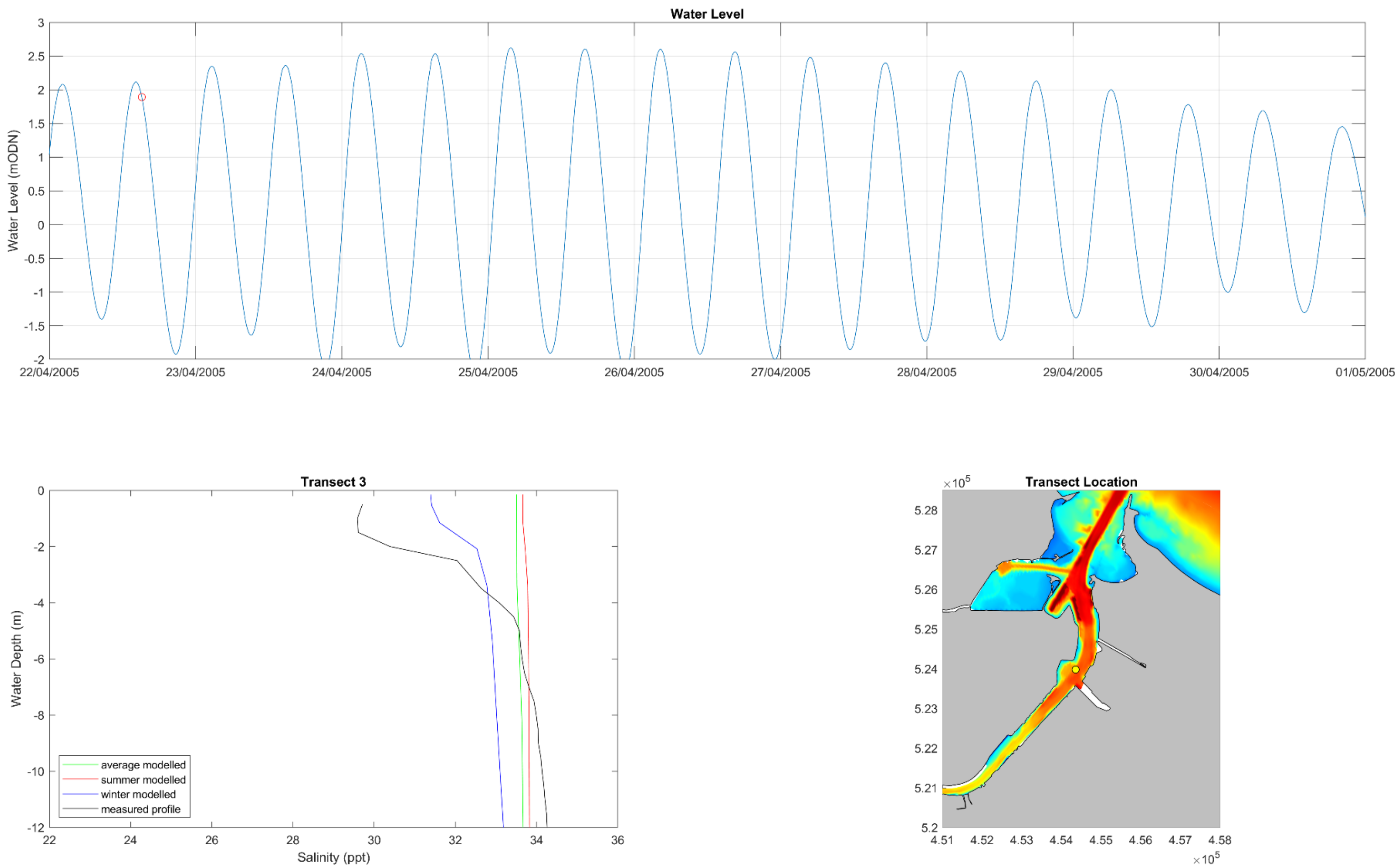

Figure 48. Comparison of measured and modelled salinity with depth: Transect 3

4 Baseline Flow Conditions

To illustrate the baseline flow conditions in the estuary selected area plots of model outputs are presented on the following pages. Flow vectors have been plotted from the baseline Delft3D model simulations for the surface (top 2%) of the water column in Section 4.1 and bottom 35% in Section 4.2, for an area covering the main estuary, including the intake site. Area plots are presented at hourly intervals relative to high water based on a central location in the estuary.

Comparisons show that the flow speeds in the surface layer are significantly higher than those in the bottom 35% of the water column. For a central location in the channel (shown by a yellow marker on Figure 49 to Figure 54) speeds in the surface layer peak at around 0.46 on the ebb tide and 0.32 m/s on the flood. In Layer 8 (bottom 35%) the speeds peak at 0.3 m/s on the ebb tide and 0.42 m/s on the flood.

Timeseries of current speeds near to the intake location are shown in Section 4.3.

4.1 Surface – Flow vector plots

Figures in this section present the flow vectors in the surface layer of the hydrodynamic model. This layer simulates the flow in the top 2% of the water column. For reference the water levels and flow speeds at a central location (indicated by the yellow marker) are shown beneath the vector plots to show the state of the tide and changes in flow speed for the vector plots presented on each page.

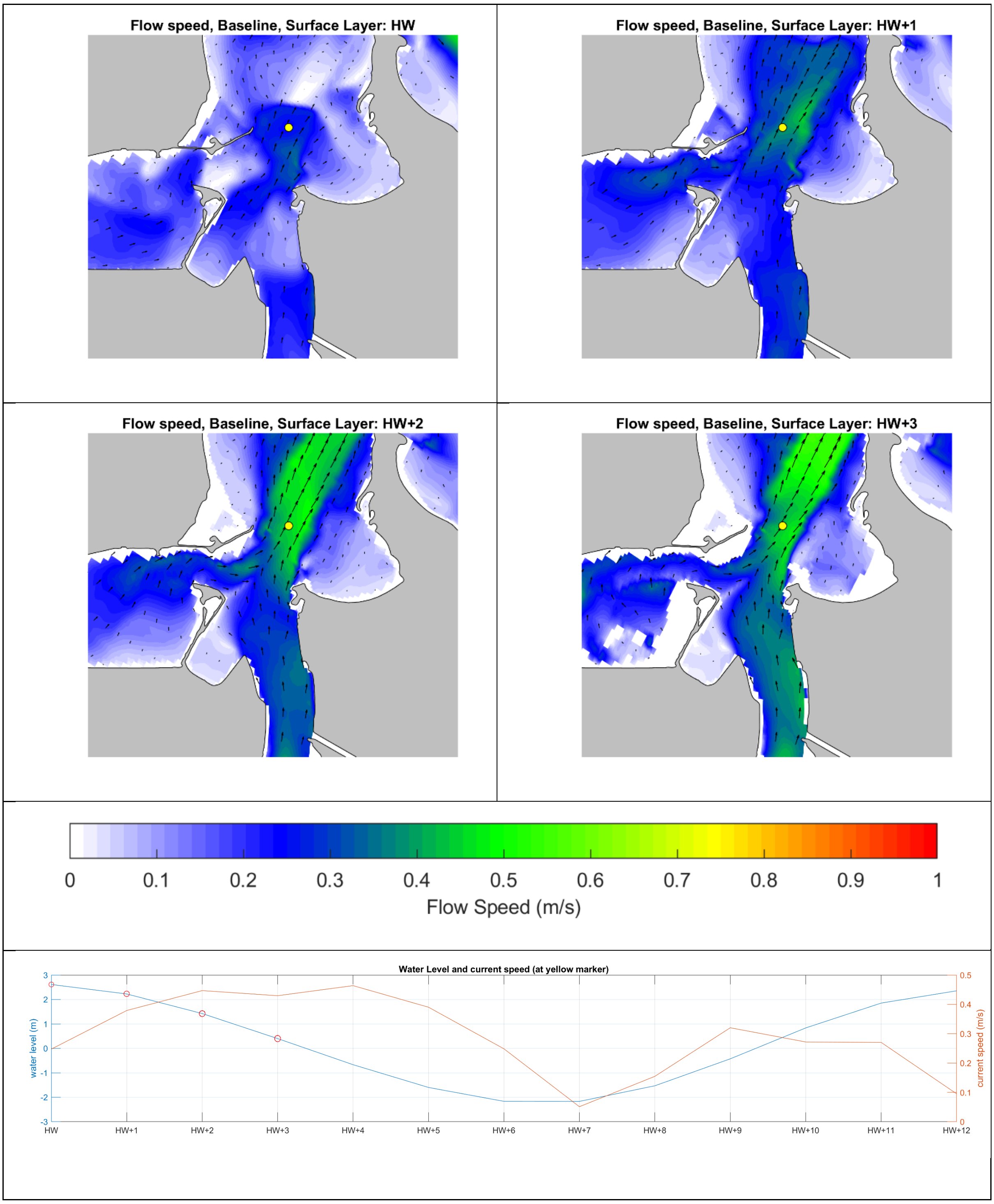

Figure 49. Flow speeds and vectors in the surface layer – Baseline condition: HW to HW +3

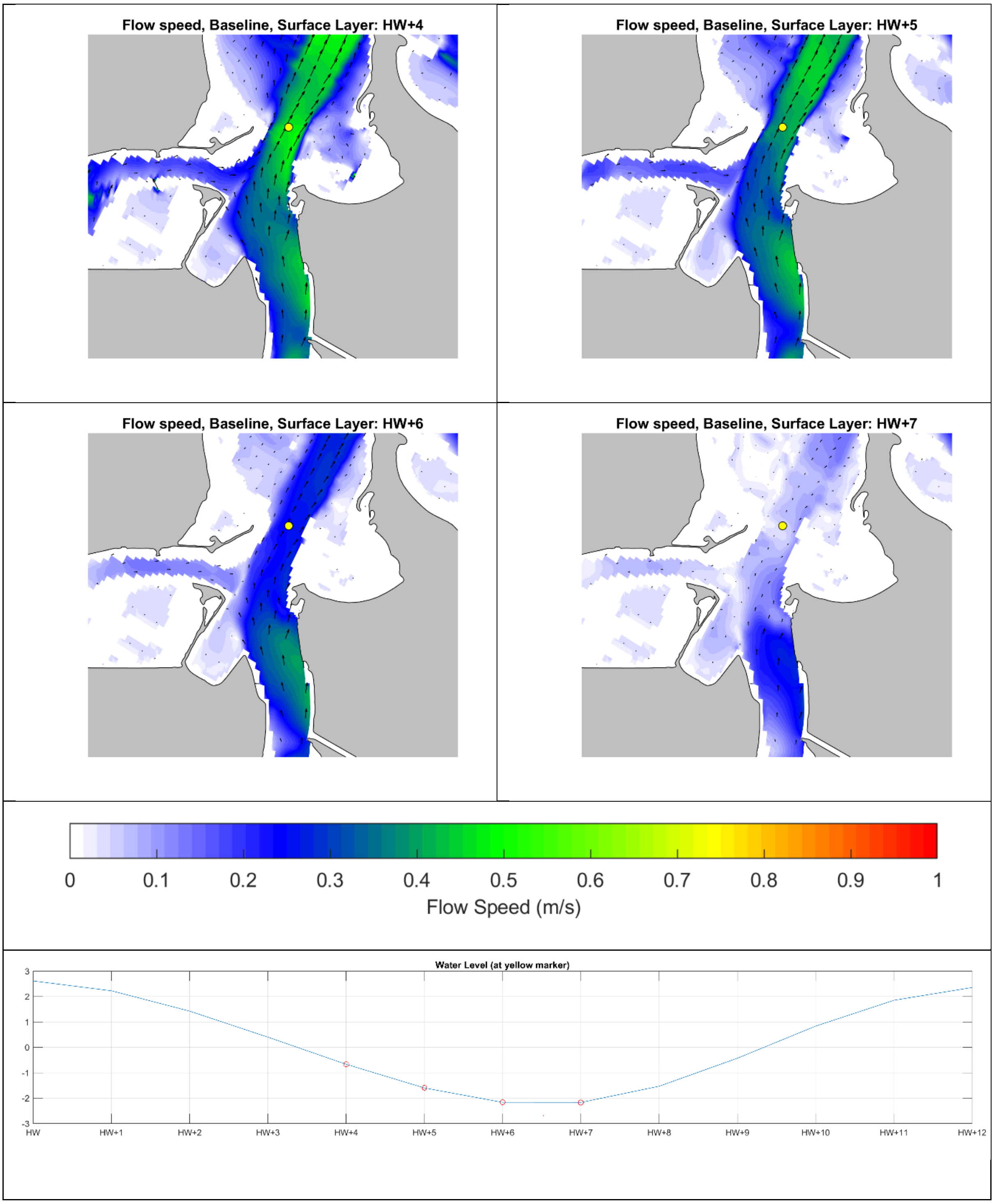

Figure 50. Flow speeds and vectors in the surface layer – Baseline condition: HW +4 to HW +7

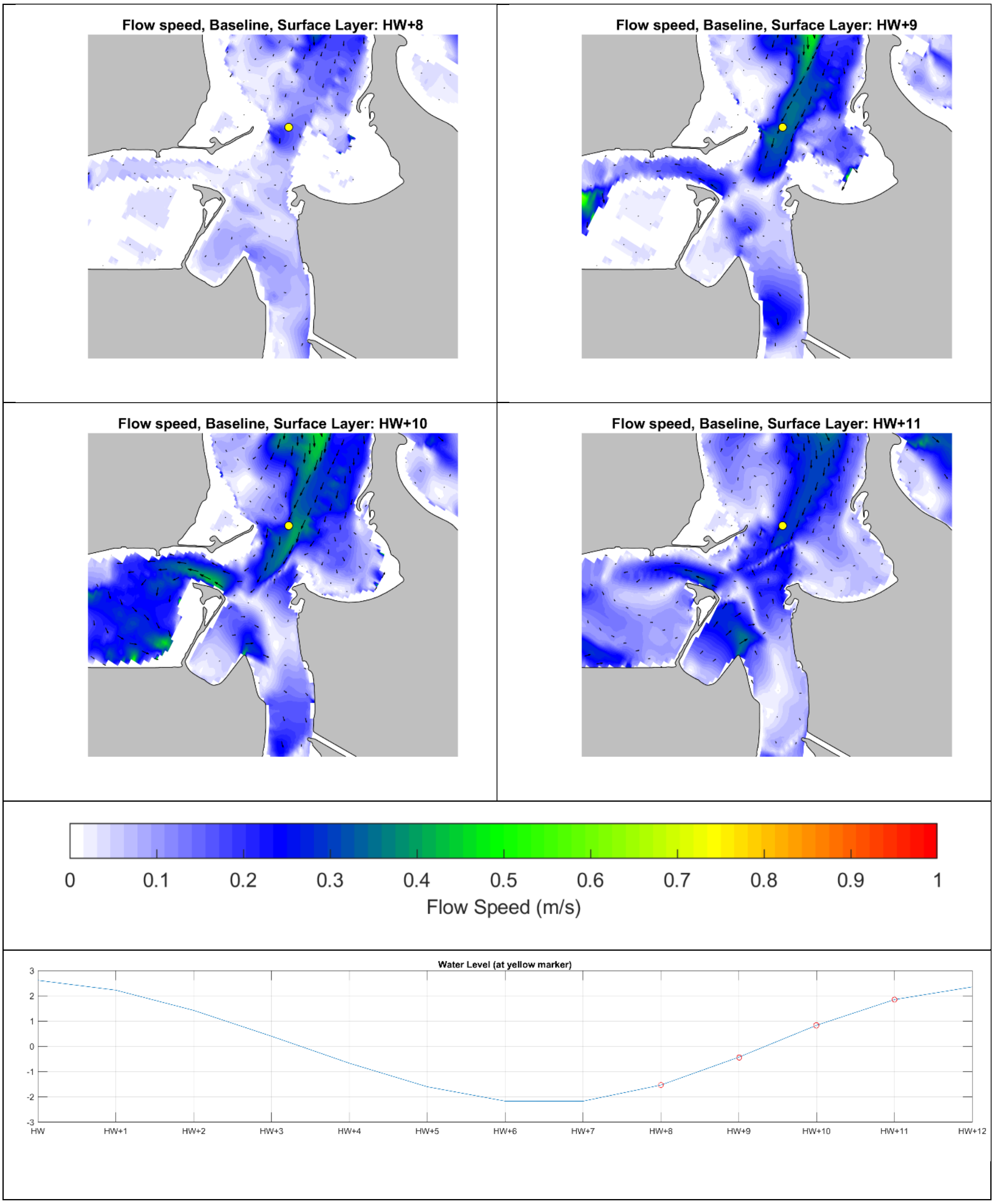

Figure 51. Flow speeds and vectors in the surface layer – Baseline condition: HW +8 to HW +11

4.2 Layer 8 – Flow vector plots

Figures in this section present the flow vectors in the Layer 8 of the hydrodynamic model. This layer simulates the flow in the bottom 35% of the water column. For reference the water levels and flow speeds at a central location (indicated by the yellow marker) are shown beneath the vector plots to show the state of the tide and changes in flow speed for the vector plots presented on each page.

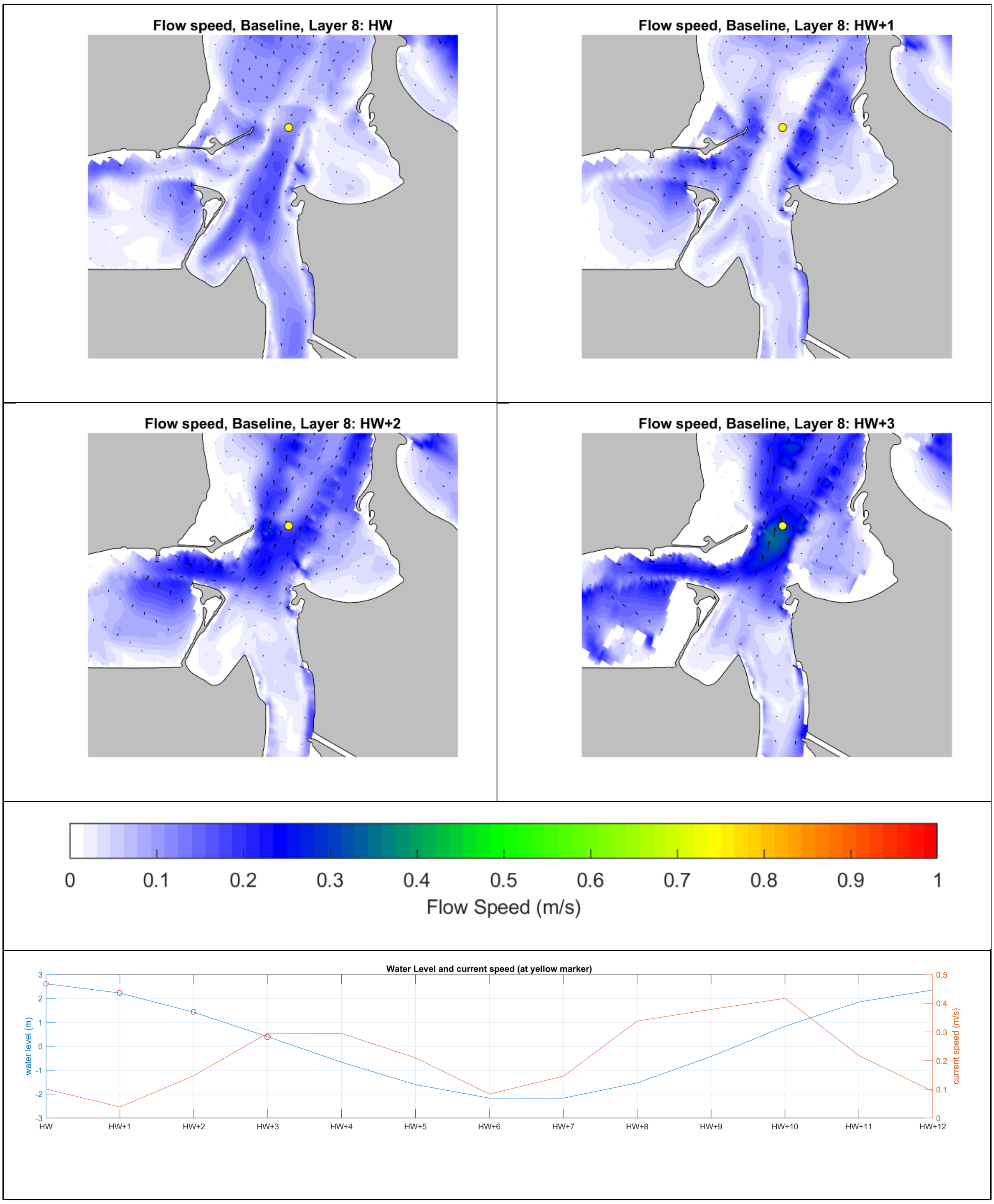

Figure 52. Flow speeds and vectors in Layer 8 – Baseline condition: HW to HW +3

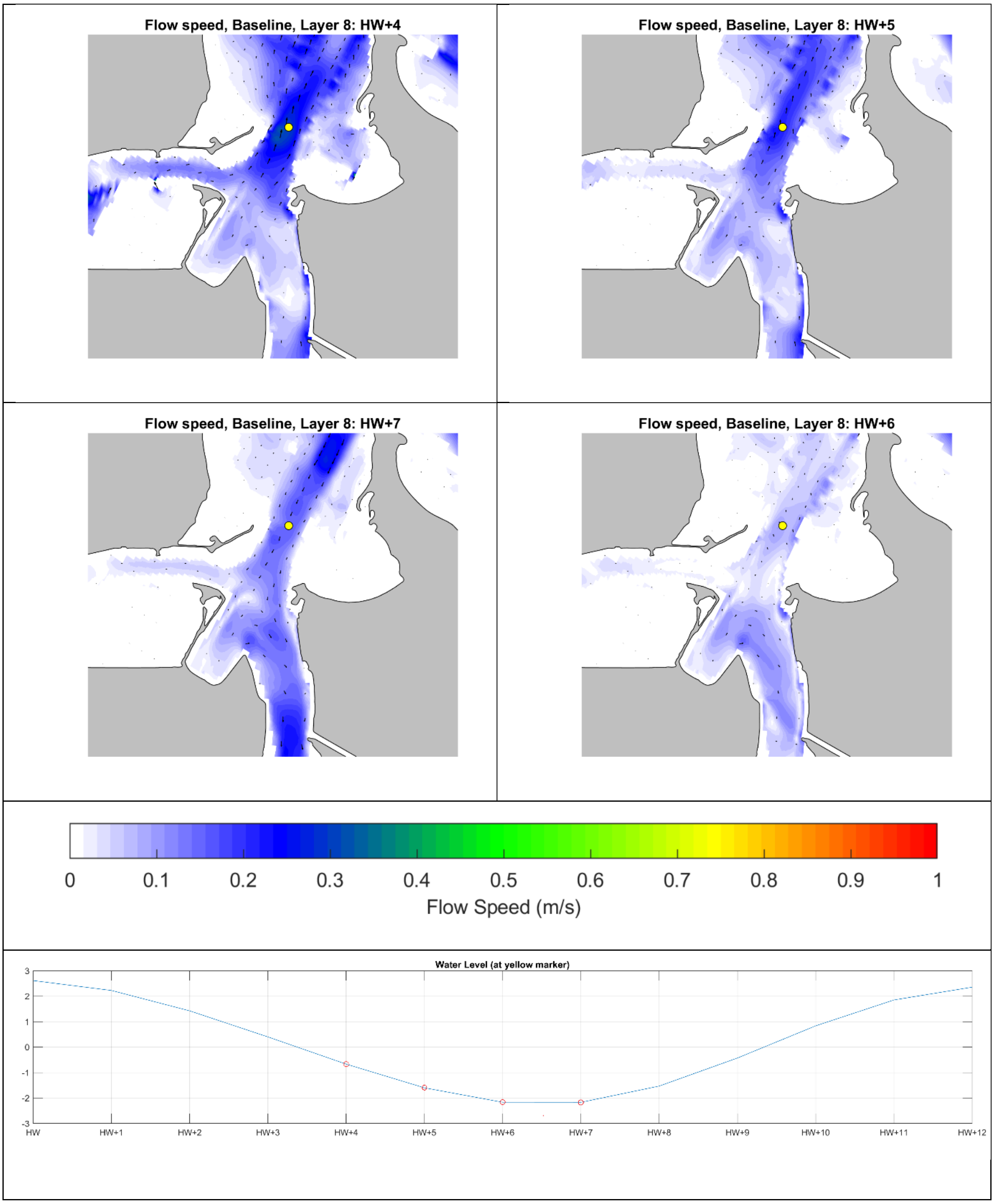

Figure 53. Flow speeds and vectors in the Layer 8 – Baseline condition: HW +4 to HW +7

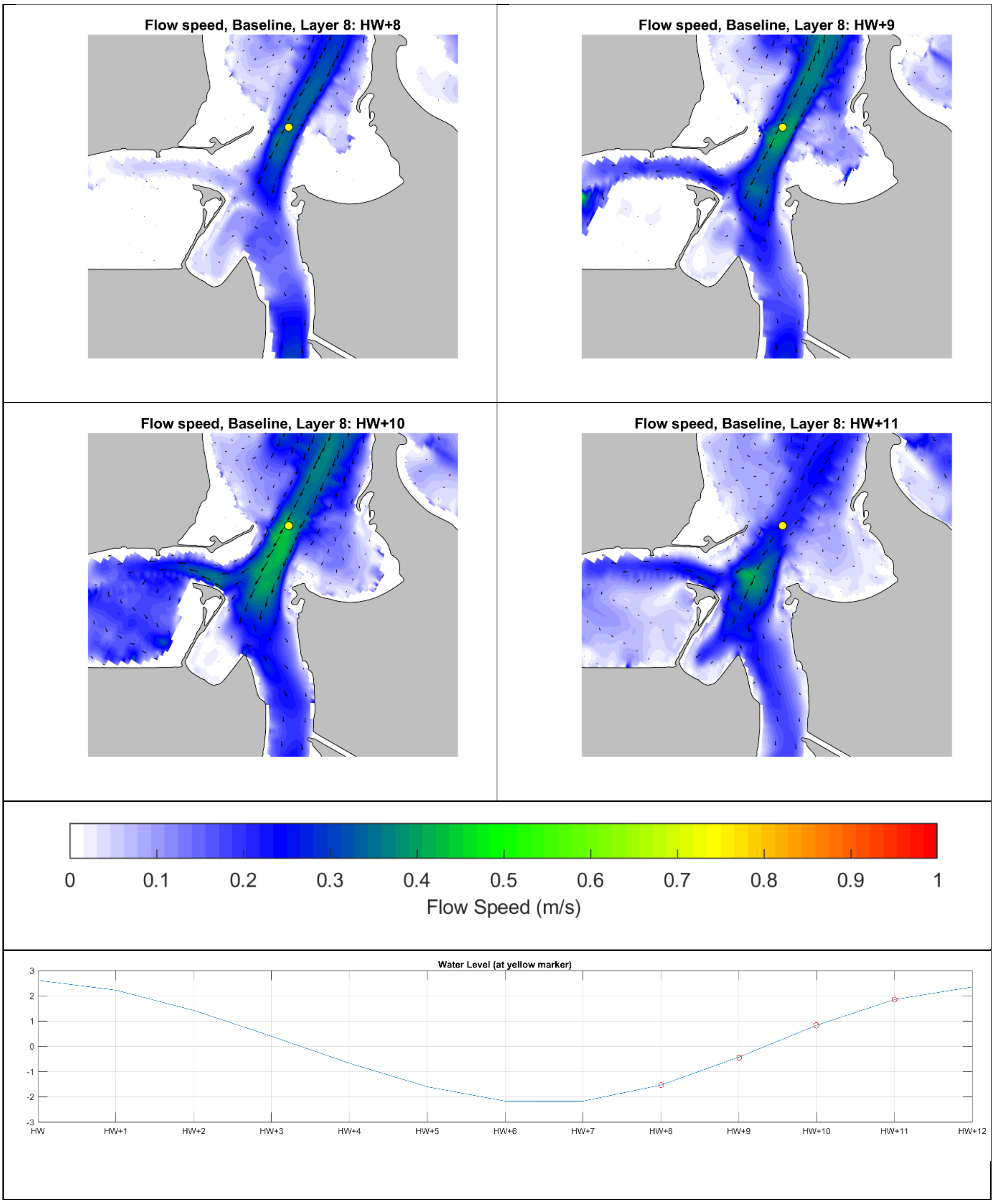

Figure 54. Flow speeds and vectors in the Layer 8 – Baseline condition: HW +8 to HW +11

4.3 Timeseries of flows

Timeseries of flow speeds and direction at the approximate intake location are provided in Figure 56 to Figure 59. The grid cell from which timeseries data are extracted is shown in Figure 55. It is worth noting that flow speeds in general are very low across this point. Flow speeds at the surface and in Layer 4 are very similar, then reducing significantly into Layer 8. Speeds at the surface reach approximately 0.3 m/s on a spring tide.

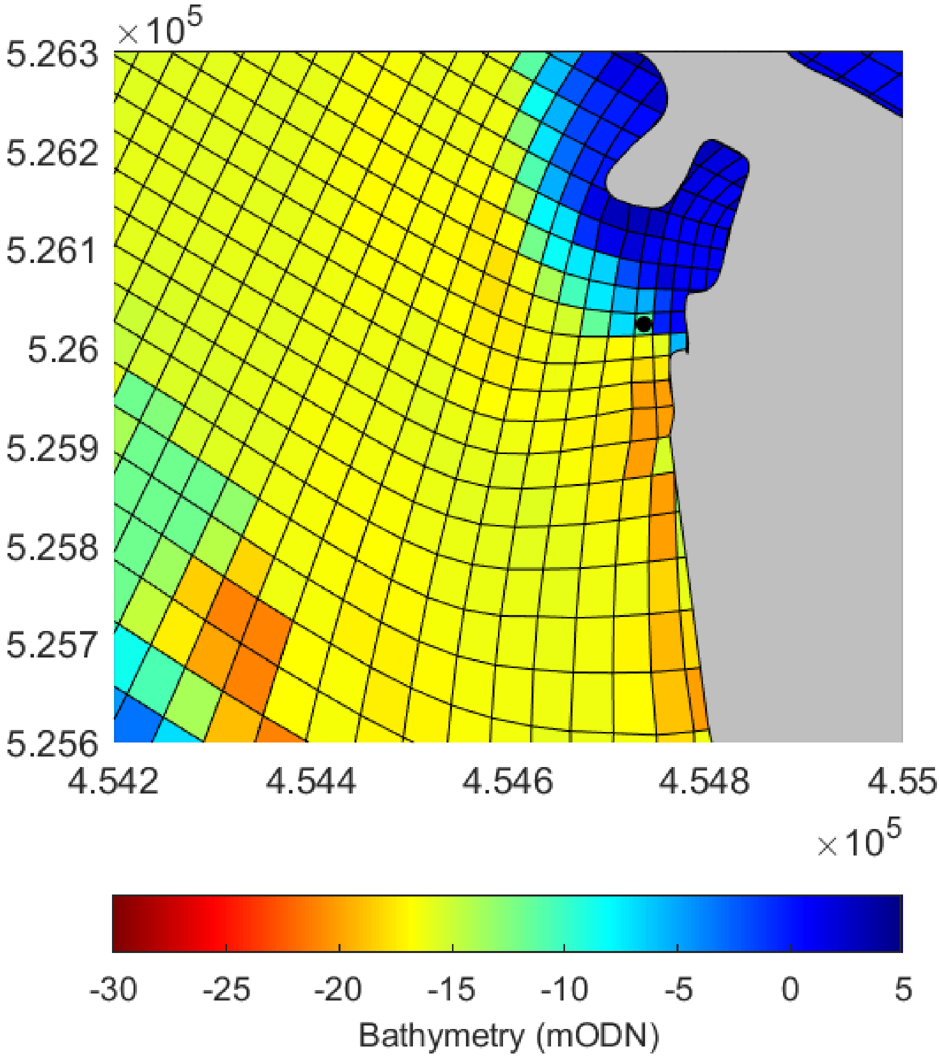

Figure 55. Location of time series extraction point for intake (indicated by the black dot)

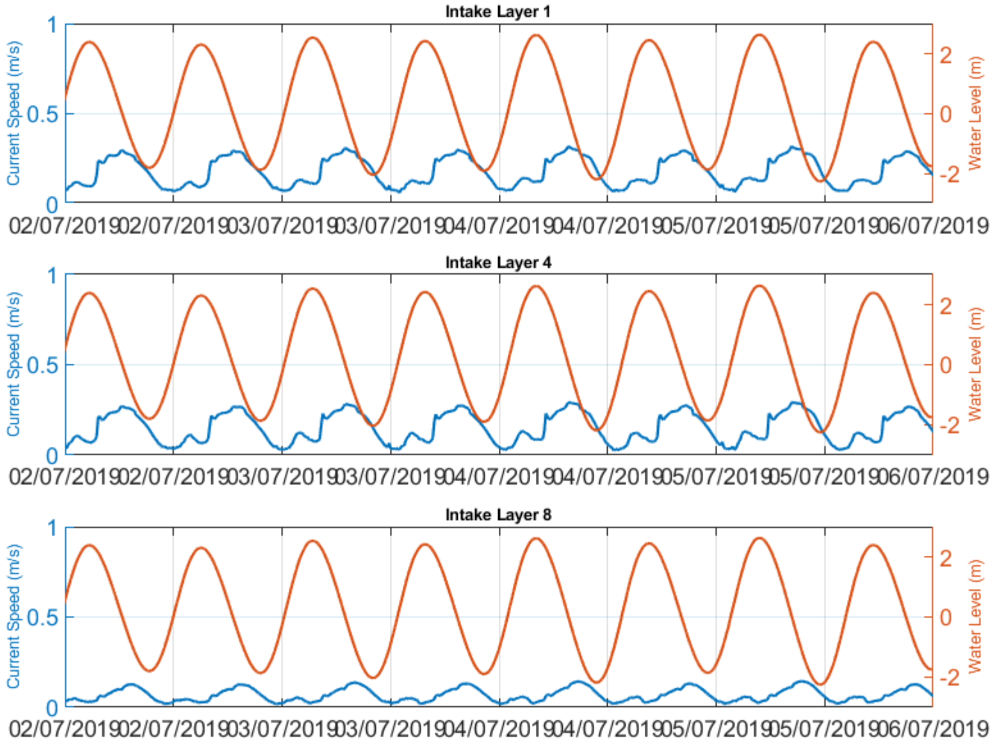

Figure 56. Baseline flow speeds at intake location (Spring Tide)

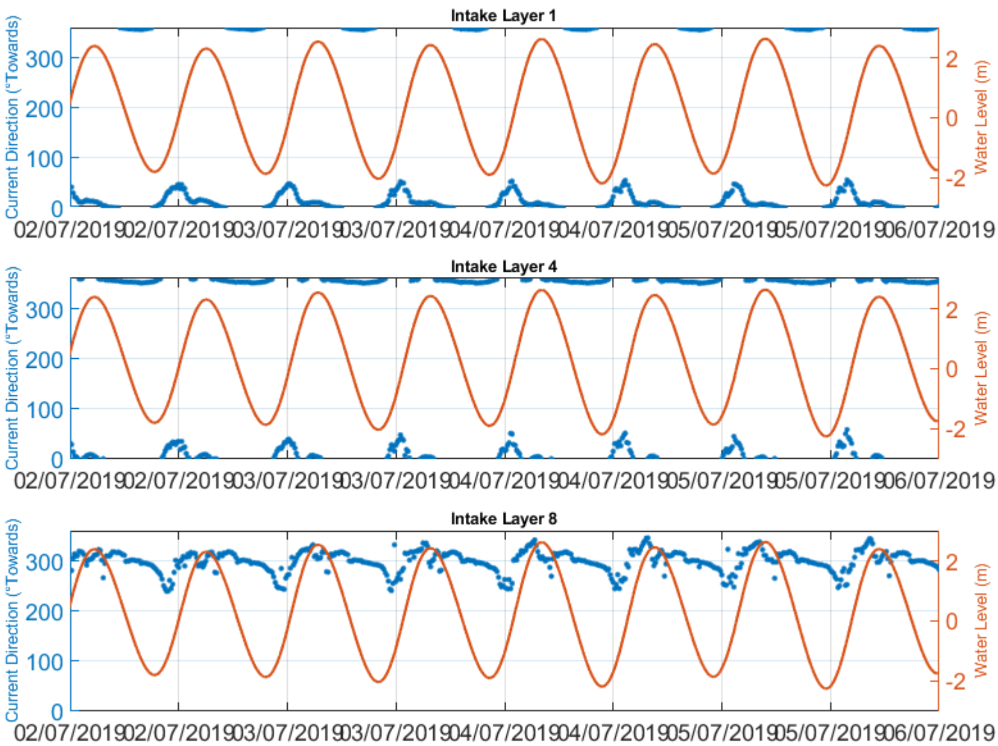

Figure 57. Baseline flow directions at intake location (Spring Tide)

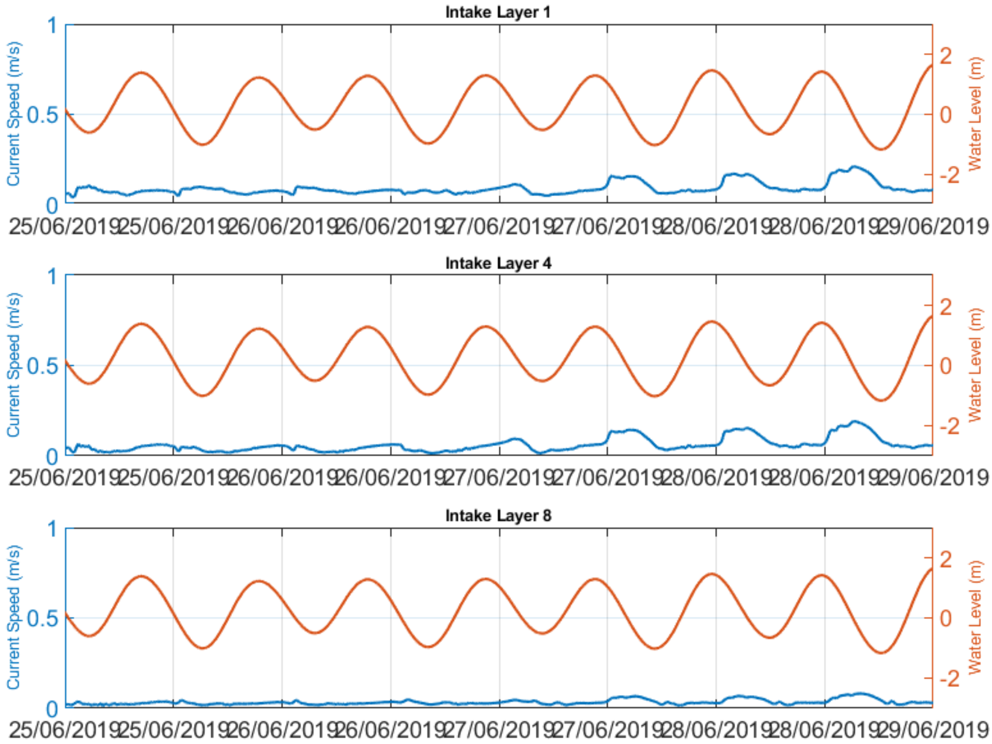

Figure 58. Baseline flow speeds at intake location (Neap Tide)

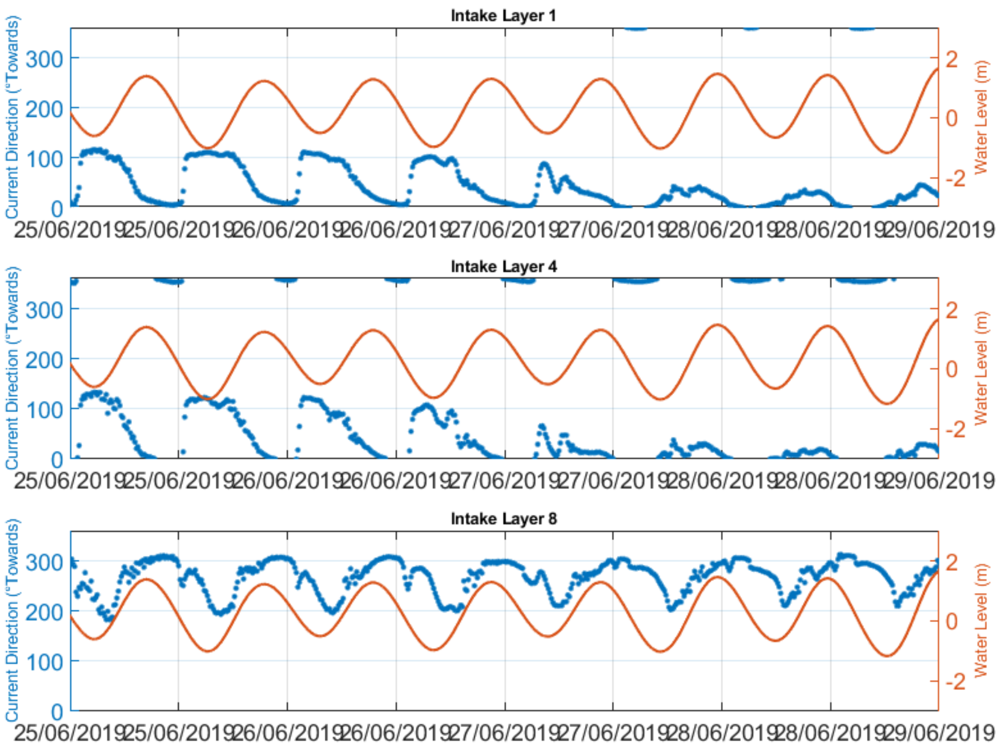

Figure 59. Baseline flow directions at intake location (Neap Tide)

4.4 Bed Shear Stress

Bed shear stress extracted from the model has been plotted at hourly intervals from high water to high water +11 hours. Vectors of the directional component are also shown by white arrows. For reference a time series of water level is shown (covering the period of the area plots). Time series of bed shear stress are shown for a central location (blue marker and blue line on the time series) and for the intake site (red marker and red line on time series)

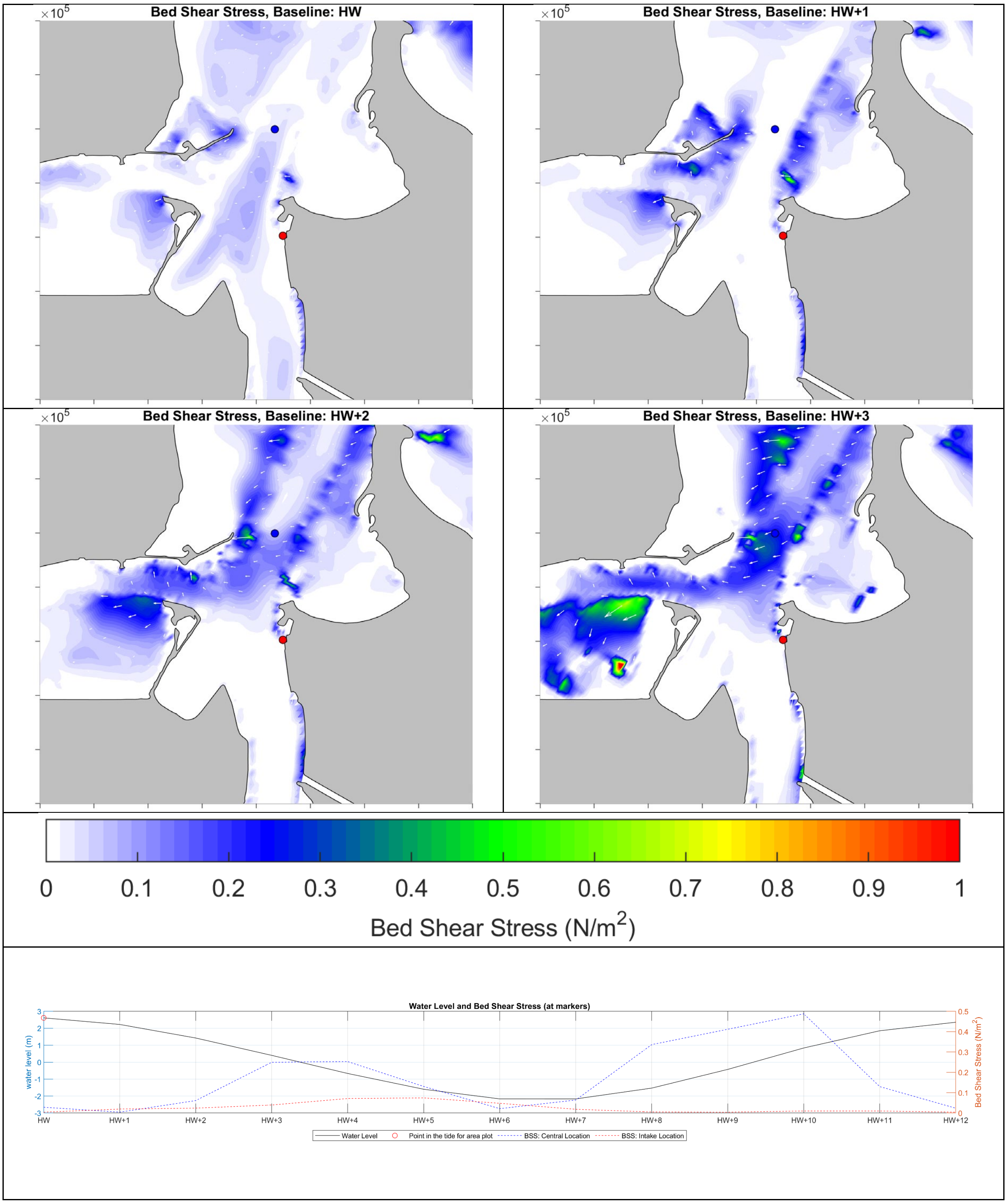

Figure 60. Bed Shear Stress – Baseline condition: HW to HW +3

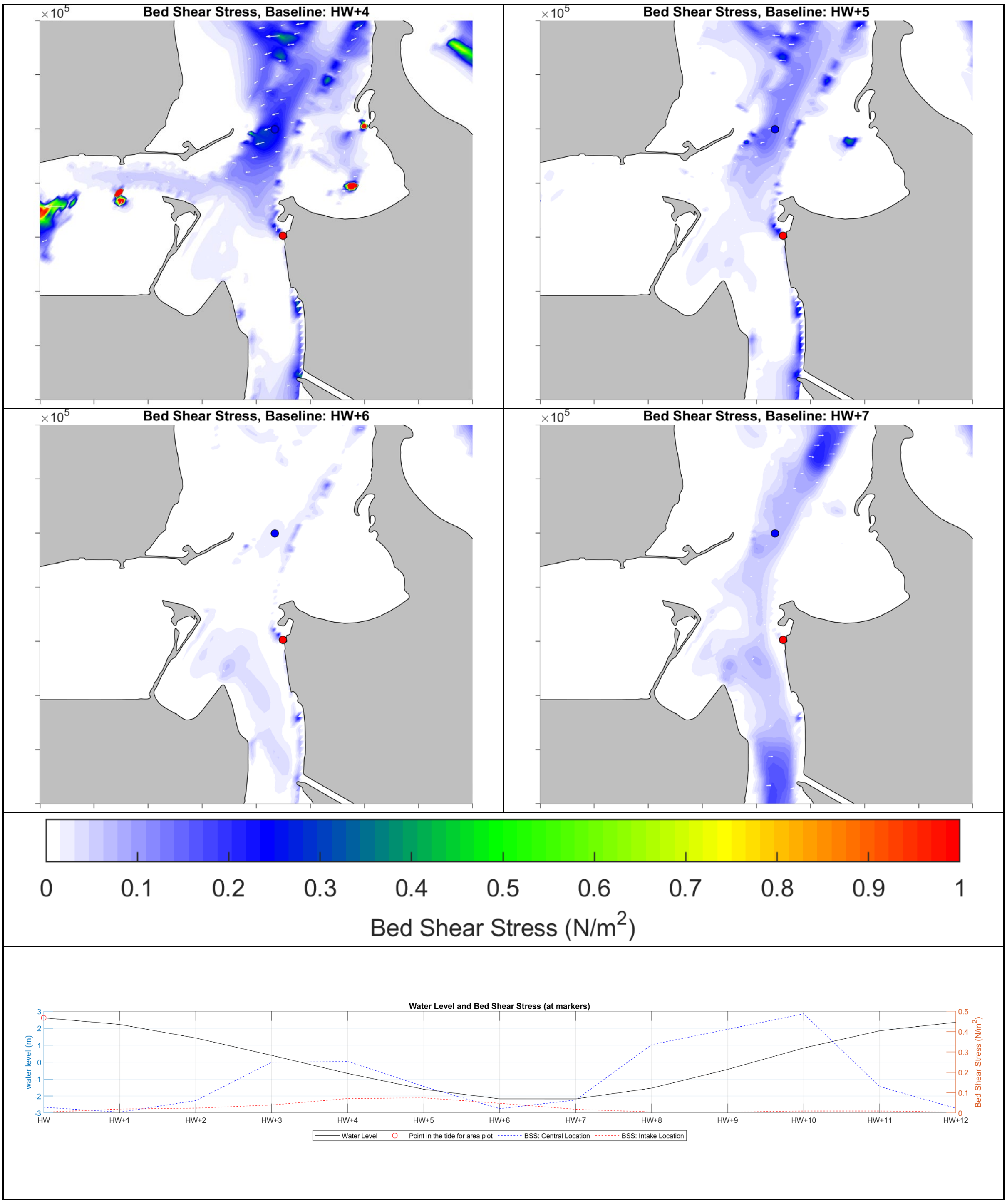

Figure 61. Bed Shear Stress – Baseline condition: HW +4 to HW +7

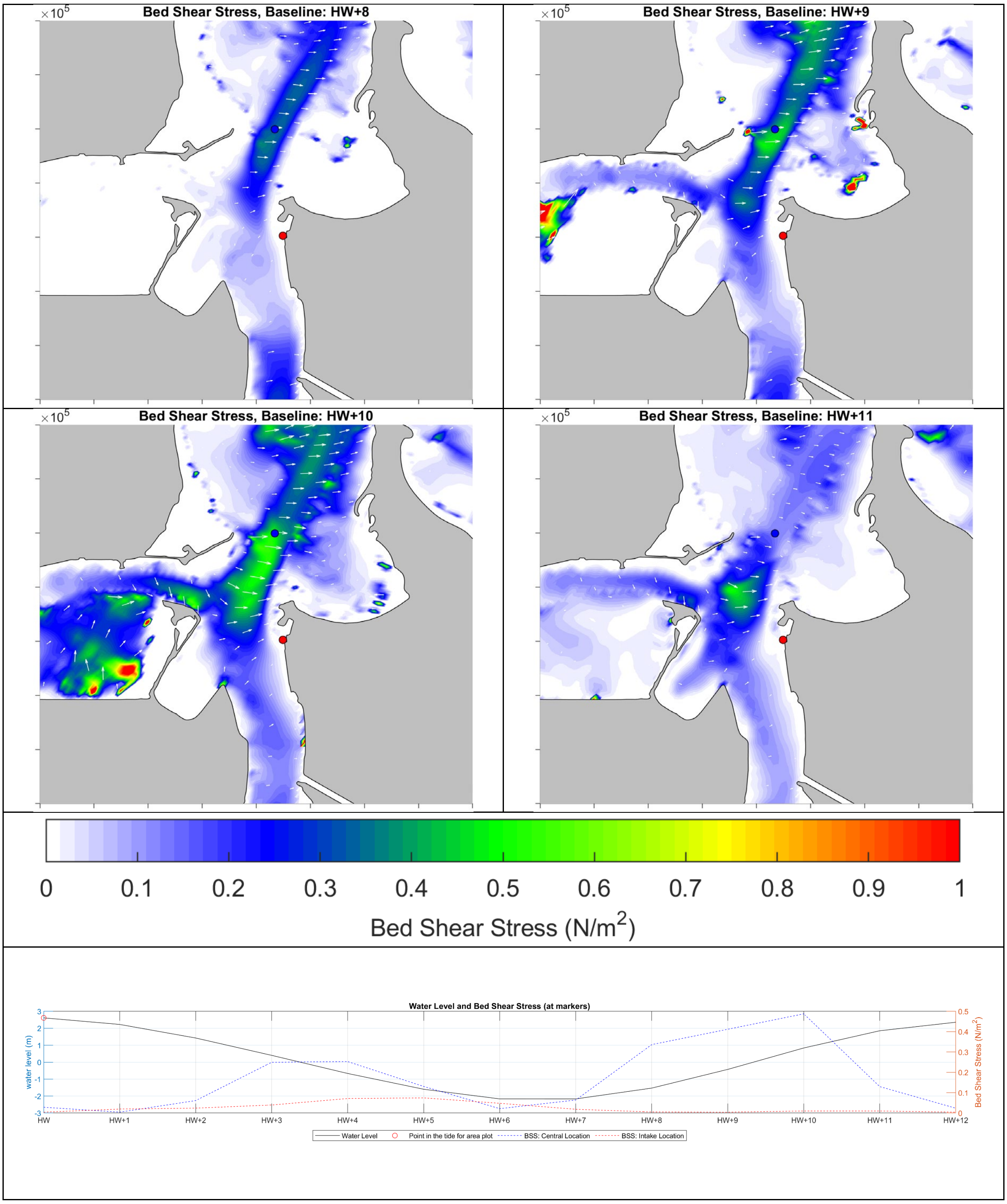

Figure 62. Bed Shear Stress – Baseline condition: HW +8 to HW +11

5 Delft3D Modelling – Scheme Impact

The following section presents the results of numerical modelling when the cofferdam structure is represented within the model domain. Details of the modelled structure are provided in Section 5.1, with the impact on the hydrodynamic regime presented in Section 5.2.

5.1 Representation of the cofferdam

AECOM have provided a schematic drawing to describe the position and scale of the proposed cofferdam structure during the period of construction works. This is shown in Figure 63 below. The structure extends approximately 15 m beyond the existing dock structure, which is represented by dry cells in the model.

Figure 63. Schematic layout of cofferdam

The cofferdam has been defined in the model by specifying 'thin dam' structures around the model cells representing the cofferdam, shown in Figure 64. The model mesh has been configured such that the dimensions of the cofferdam can be represented as closely as possible (see Section 2.1). The effect of this is to completely block the enclosed area in the model to flows, effectively creating an extended area of coastline. The Delft3D HD model was run for the 2019 annual average conditions to assess the impact of the cofferdam construction on the local flow regime. Comparison of the resulting model outputs are shown in Section 5.2.

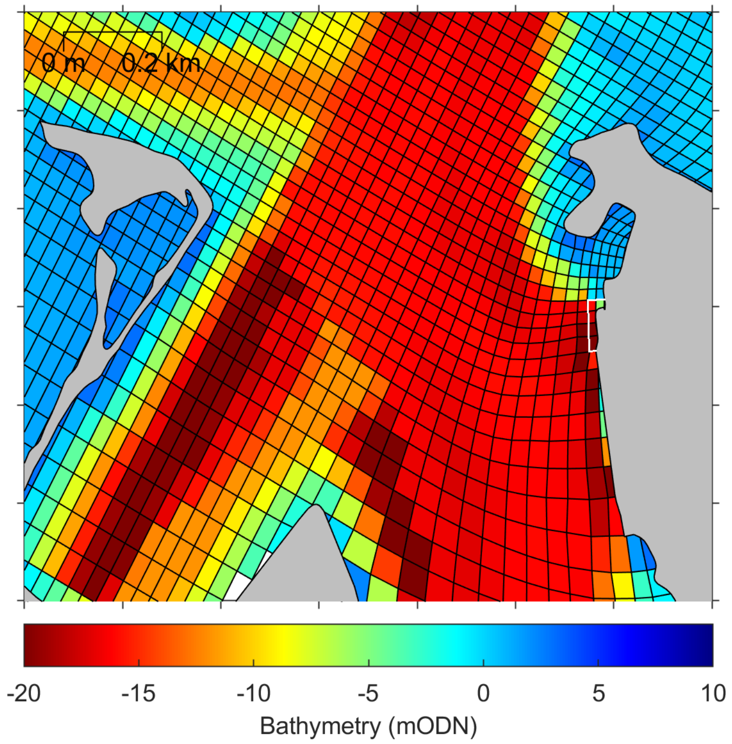

Figure 64. Location of thin dams in the Delft3D model

5.2 Scheme impact

This report section presents a comparison of flow conditions for the 2019 annual mean hydrodynamic conditions, without the cofferdam in place (baseline) and with the cofferdam defined in the model grid (scheme). The following plots are provided in this section:

- Area plots showing a comparison of baseline and scheme flow vectors in the surface layer (Figure 65 to Figure 67);
- Area plots showing flow speed differences at times of peak flood and ebb (Figure 68 and Figure 69; and
- Time series comparisons of flow speeds and directions around the cofferdam.

The modelled results indicate that the effect of the cofferdam on flow speeds is extremely localised (to within 150 m of the cofferdam edge, when considering flow speed changes greater than 0.05 m/s.

5.2.1 Flow vector comparison: surface layer

Figure 65 to Figure 67 show vector arrows of flow velocity for the baseline condition, shown by green arrows, overlaid by the scheme vectors, shown in black. A colourmap of flow speed is also plotted, which shows the BASELINE flow speed across the area. It should be noted that although the vector arrows on the plots appear quite large the flows across the cofferdam region are reasonably low (see the colourmap for reference). Vector scaling has been selected to maintain consistency between plots while still keeping the vectors visible at all stages of the tide. Vector plots are presented for HW to HW +11 in hourly intervals. All speeds are those extracted from the surface layer.

Variation in flow direction between the baseline and scheme scenarios is seen around the cofferdam, where the structure has the effect of redirecting flows where the blockage is applied. Variation in the flow speeds is harder to discern from these presentations, but is more clearly addressed in Section 5.2.2 and Section 5.2.3.

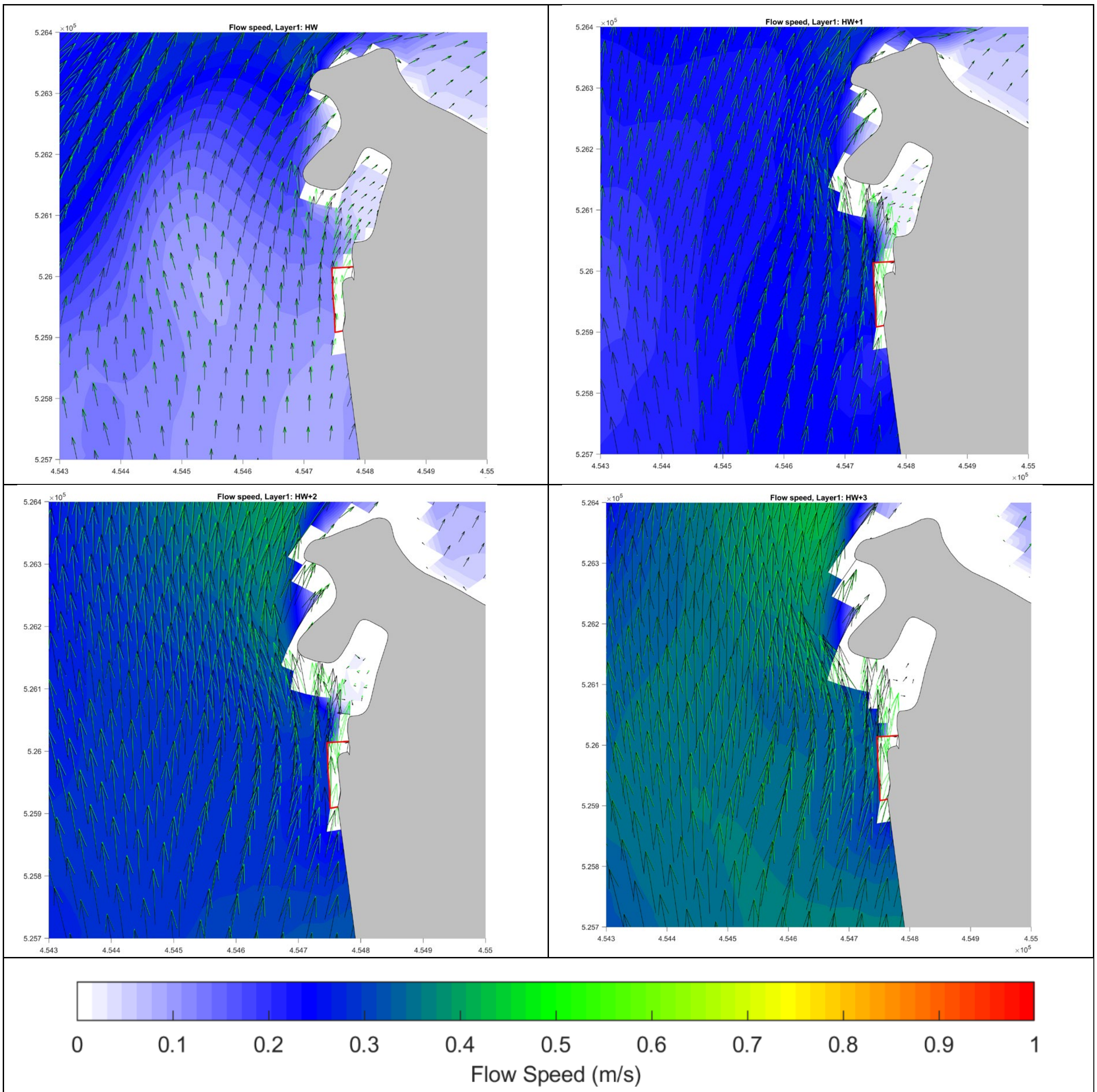

Colour contours of flow speed show the **baseline** *speeds. Baseline flow vectors are shown in green, scheme flow vectors are shown in* ***black***.

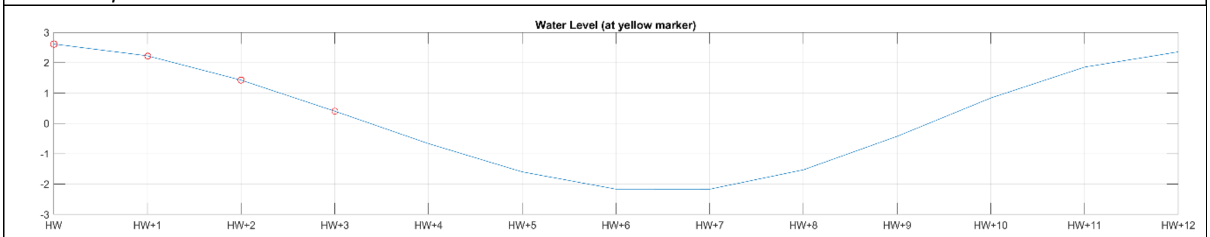

Figure 65. **Impact of cofferdam on flow vectors in the surface layer: Baseline (green) vs Scheme (black): HW to HW +3**

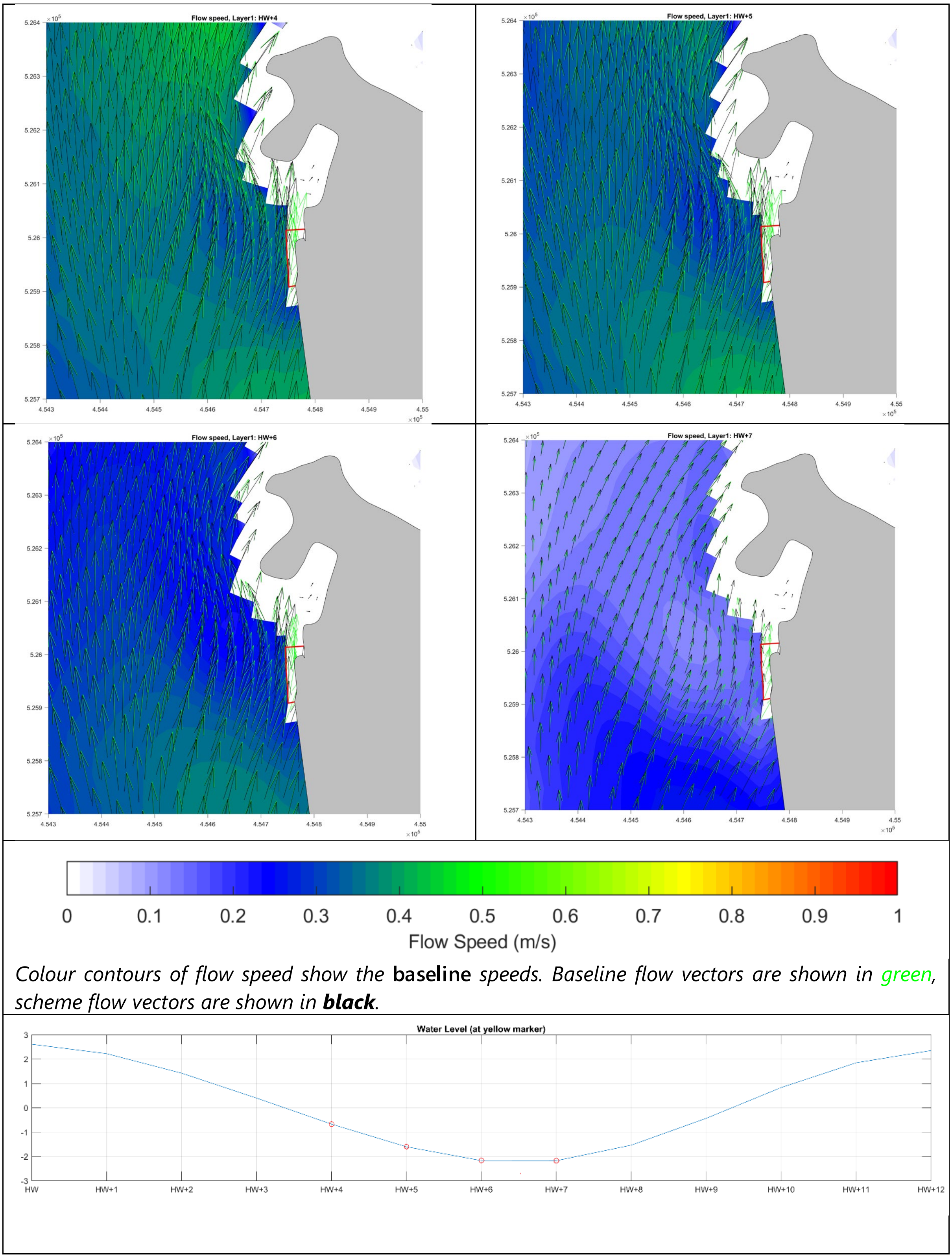

Figure 66. Impact of cofferdam on flow vectors in the surface layer: Baseline (green) vs Scheme (black): HW +4 to HW +7

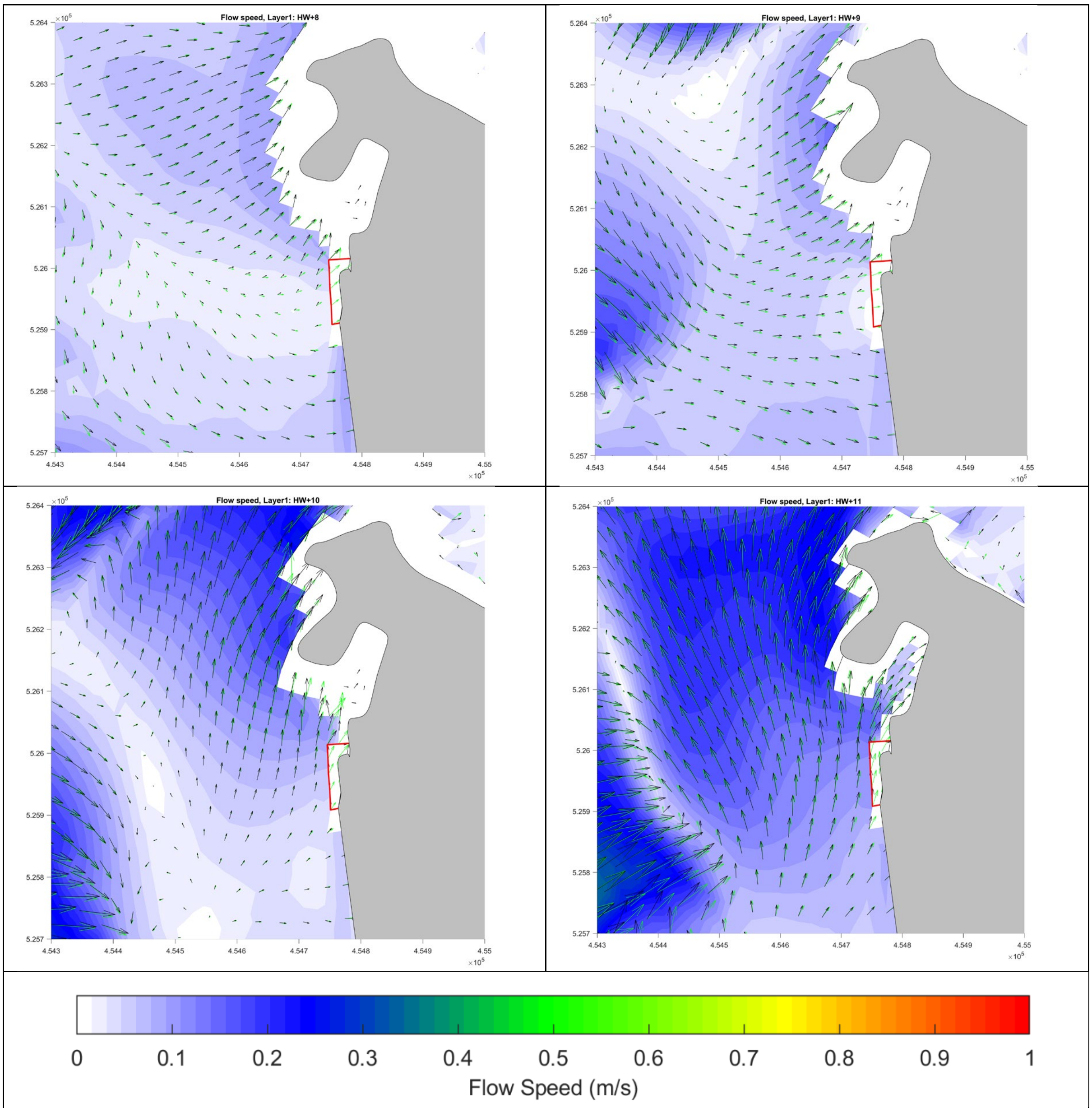

Colour contours of flow speed show the **baseline** *speeds. Baseline flow vectors are shown in green, scheme flow vectors are shown in* ***black****.*

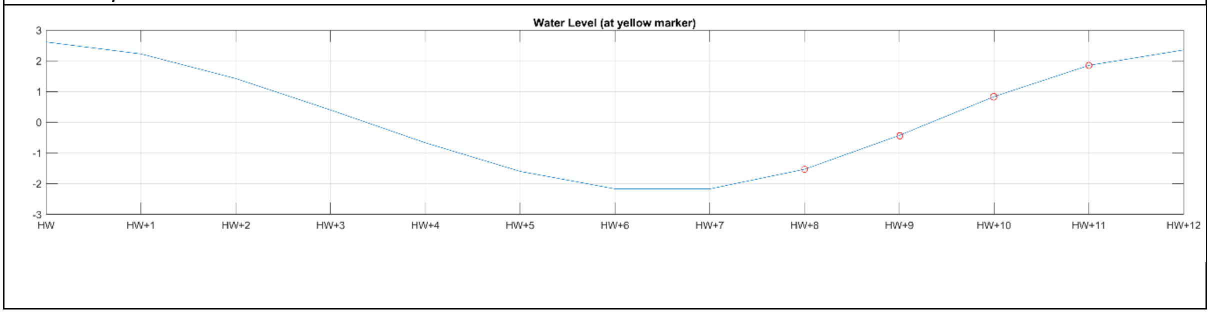

Figure 67. Impact of cofferdam on flow vectors in the surface layer: Baseline (green) vs Scheme (black): HW +8 to HW +11

5.2.2 Speed difference area plots

Figure 68 and Figure 69 show the difference in flow speed between the baseline and scheme model runs in the surface layer of the model. In general, the effects on flow speed are very small. On an ebb tide the flow speeds at the north and south side of the cofferdam structure decrease compared with the baseline condition, while the flow speeds to the west of the structure (moving in a northward direction) show an increase in speed compared to the baseline. The contour of 0.05 m/s flow increase extends approximately 150 m from the cofferdam edge.

On the flood tide the effect in the surface layer appears less with a small decrease in flow speeds observed around the cofferdam edge one the structure is included in the model.

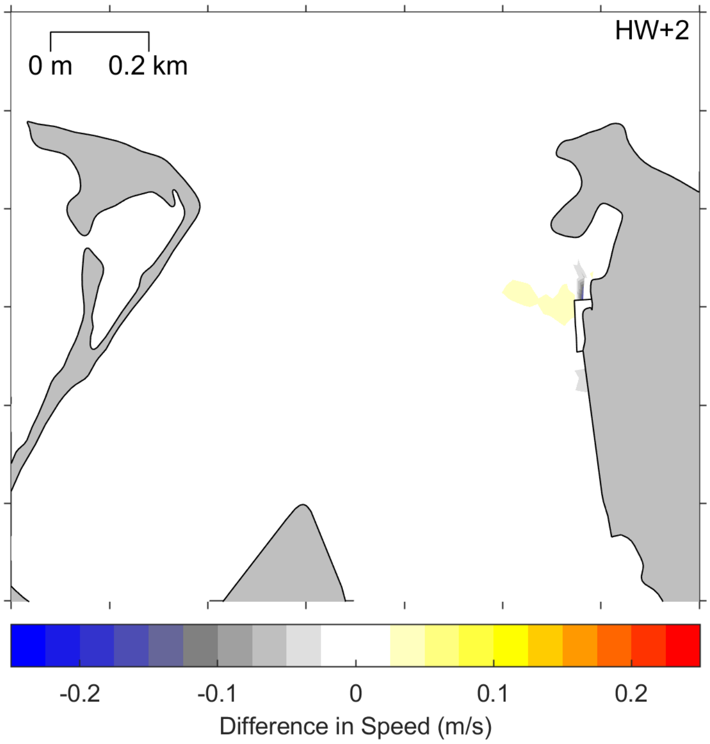

Figure 68. Impact of cofferdam on flow speeds in the surface layer during Ebb tide

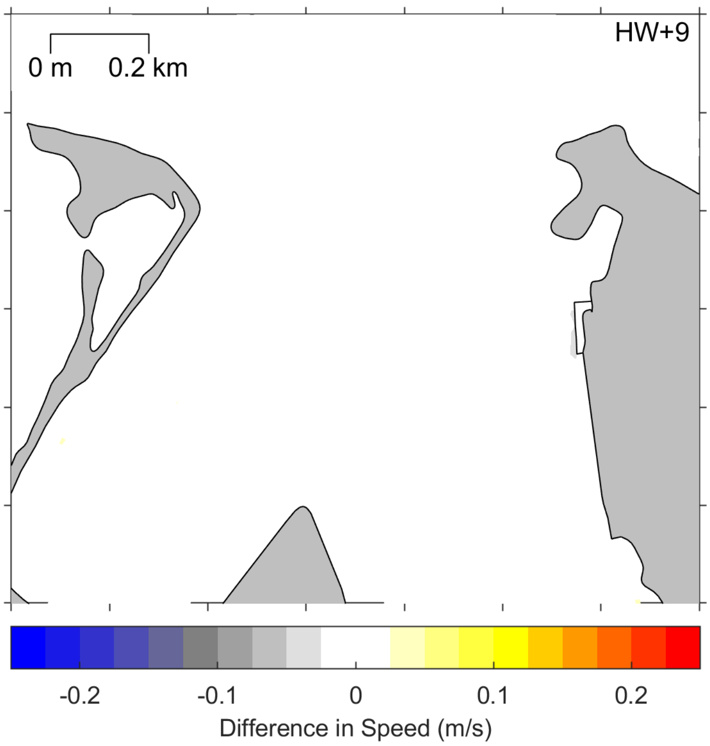

Figure 69. Impact of cofferdam on flow speeds in the surface layer during flood tide

5.2.3 Timeseries of scheme vs baseline flows

Figure 70 to Figure 72 on the following pages present time series of flow speeds for the scheme and baseline model runs at locations close to the cofferdam where the maximum impact on flow speeds occurs.

Time series have been plotted from data in the following modelled layers:

- The surface layer (top 2% of the water column);
- Layer 4: representing the vertical area between 10% and 17% of the total water depth (from the surface); and
- Layer 8 in the model (bottom 35% of the water column).

For each of the timeseries plots the location of the extracted data is shown by a black marker on the map plot on the same page.

Figure 70 and Figure 71 show the flow speeds at location just to the north of the proposed construction where the flow speeds reduce when the structure is in place. In these examples the impact on flow speeds is greatest at the surface where flow speeds are highest.

Figure 72 shows a location to the west of the cofferdam where the flow speeds increase around the structure in the surface and Layer 4. In the lower part of the water column (Layer 8) the effect varies across the ebb and flood, although speeds at this location are very low at these depths.

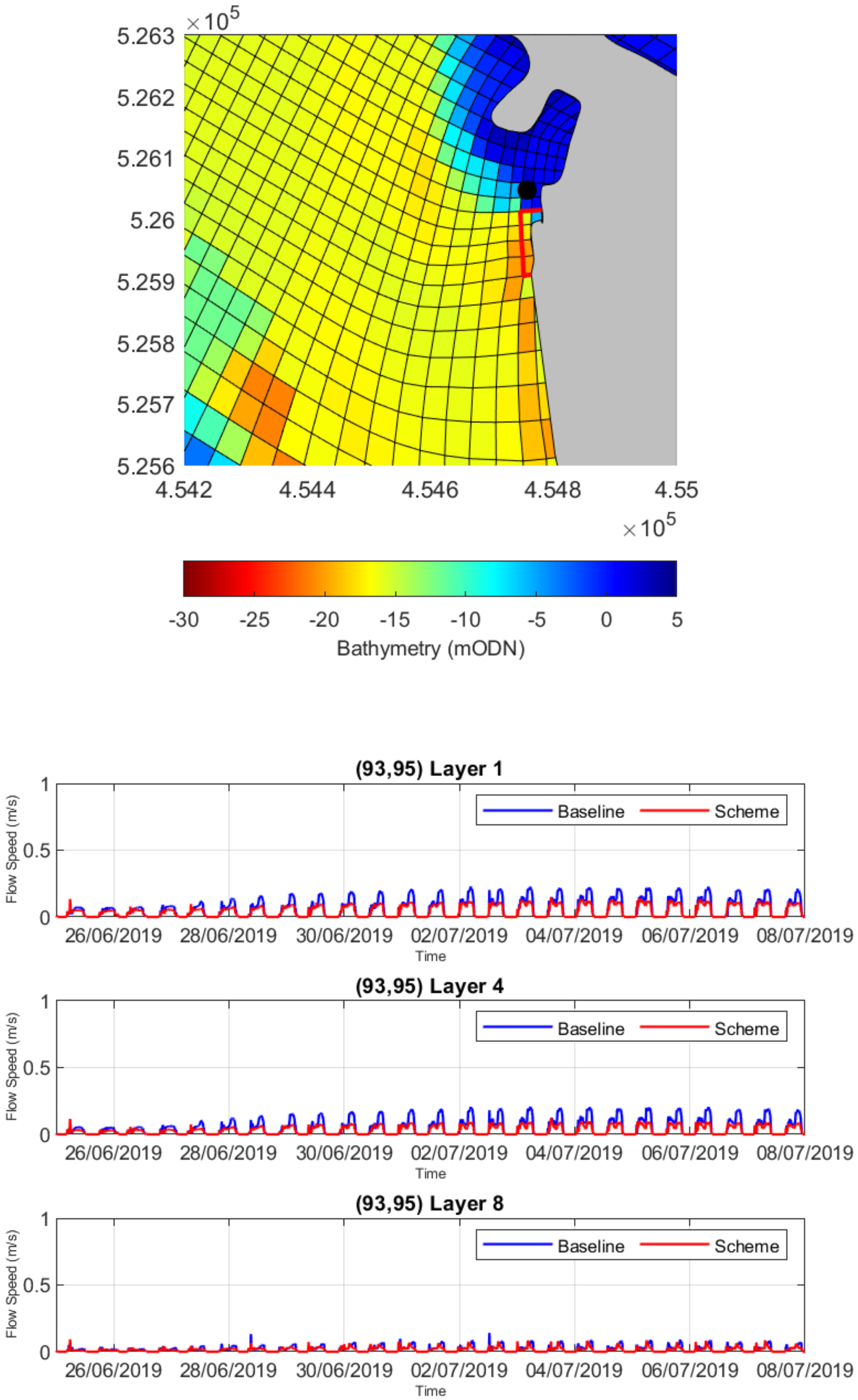

Figure 70. Impact of cofferdam on flow speeds north of construction

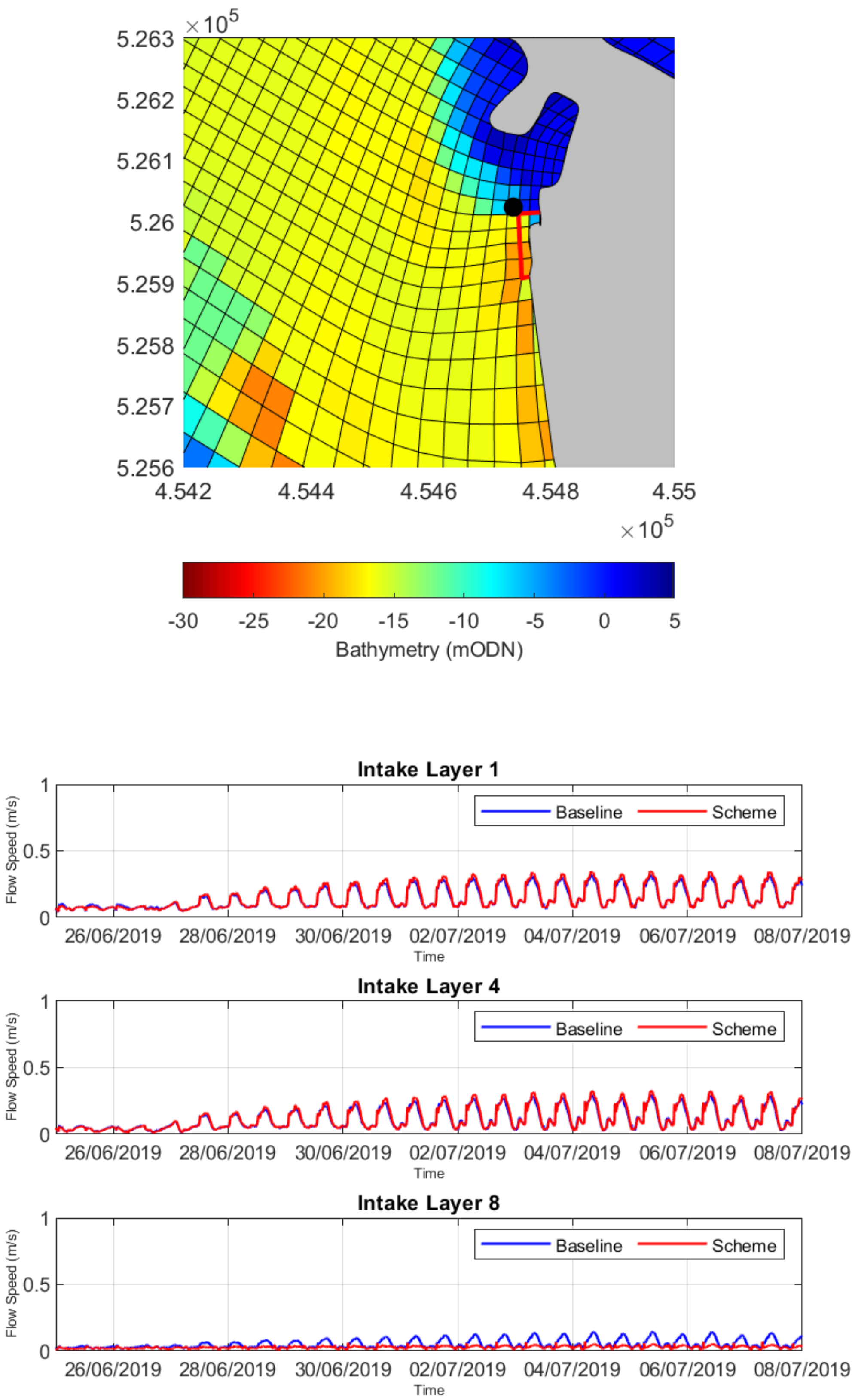

Figure 71. Impact of cofferdam on flow speeds at intake location

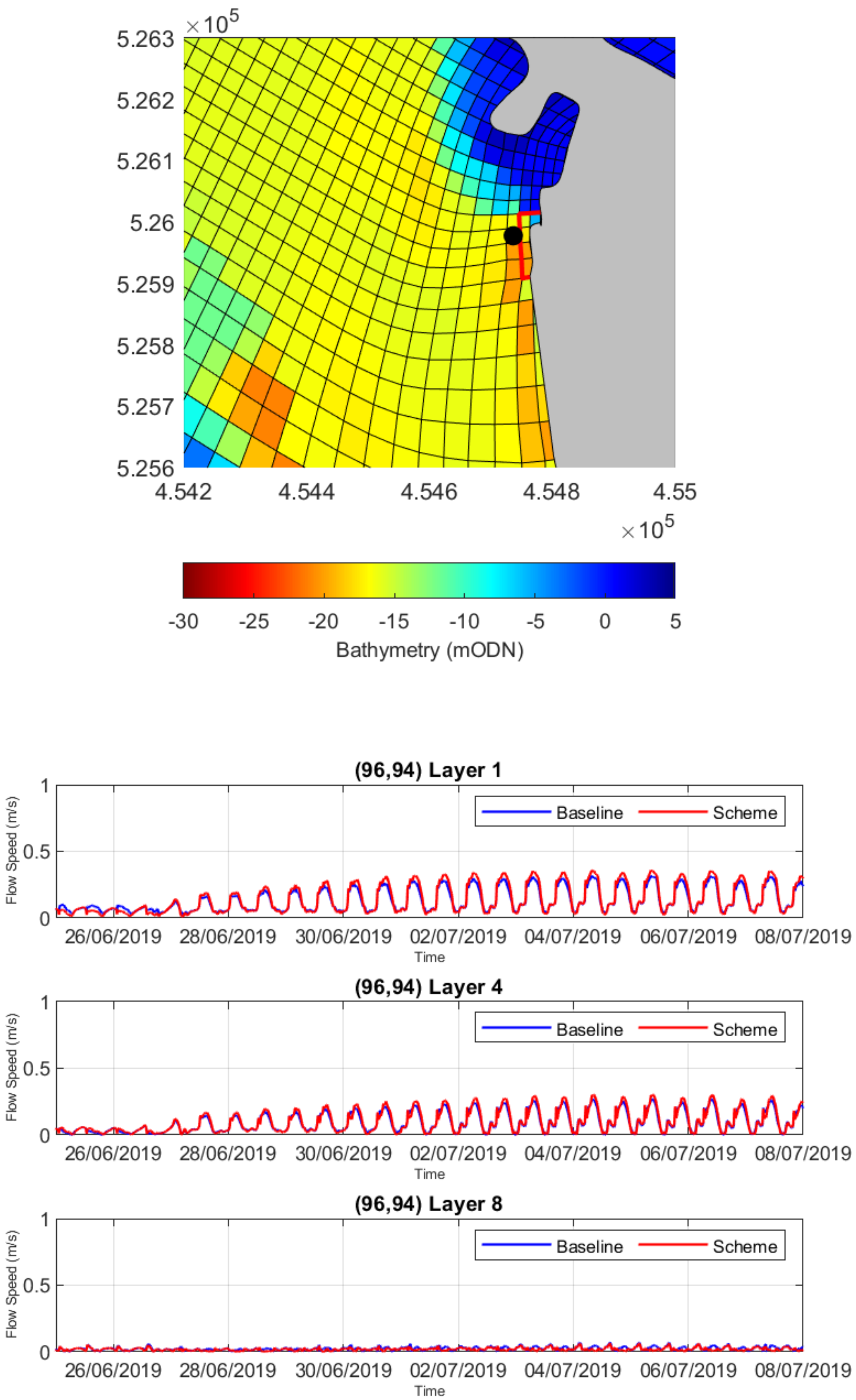

Figure 72. Impact of cofferdam on flow speeds west of construction

5.2.4 Change in Bed Shear Stress

Figure 73 and Figure 74 illustrate the impact of the scheme on the modelled bed shear stresses over a spring tide. Figure 73 shows the difference in bed shear stress at the time of most change. This also corresponds to the time of peak bed shear stress near the cofferdam in the baseline case (seen in Figure 60). Figure 74 shows a time series of the shear stresses at the intake location in the baseline (blue) and scheme (red) model runs.

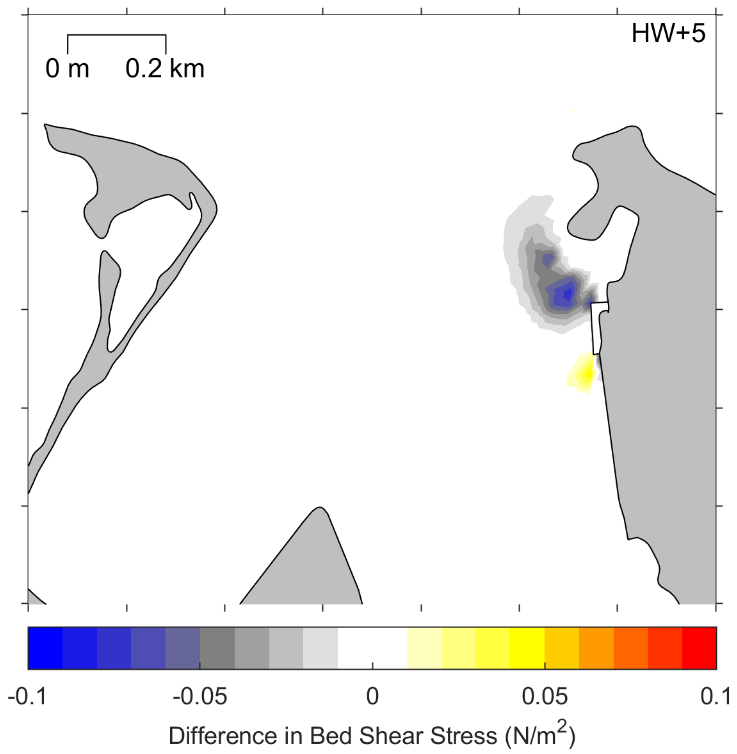

Figure 73. Difference in bed shear stress (scheme – baseline) at HW +5

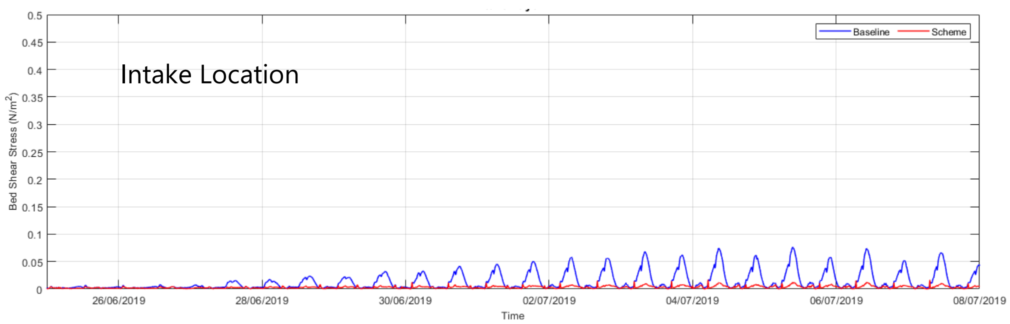

Figure 74. Bed shear stress at intake location: Bassline (blue) vs. scheme (red)

5.2.5 Sensitivity to model resolution

The cofferdam structure is represented in the model mesh by thin dams extending 4 model grid cells in the y direction and 2 in the x direction. The model has been configured to allow the correct blockage of the cofferdam structure in the model however some sensitivity testing is also required to ensure that the effect of the structure on local flows can be adequately represented by the selected model resolution.

In order to undertake this sensitivity testing a version of the model was created with a further refined grid, shown in Figure 75. The model grid has been refined by a factor of 3 in around the cofferdam area, resulting in a grid cell size of 6 m x 8.5 m. Two model runs were undertaken using the refined grid to simulate a baseline and a scheme condition. The model was run in 2D mode, which avoids the long computation time of a 3D model and provides an adequate assessment of sensitivity to grid resolution.

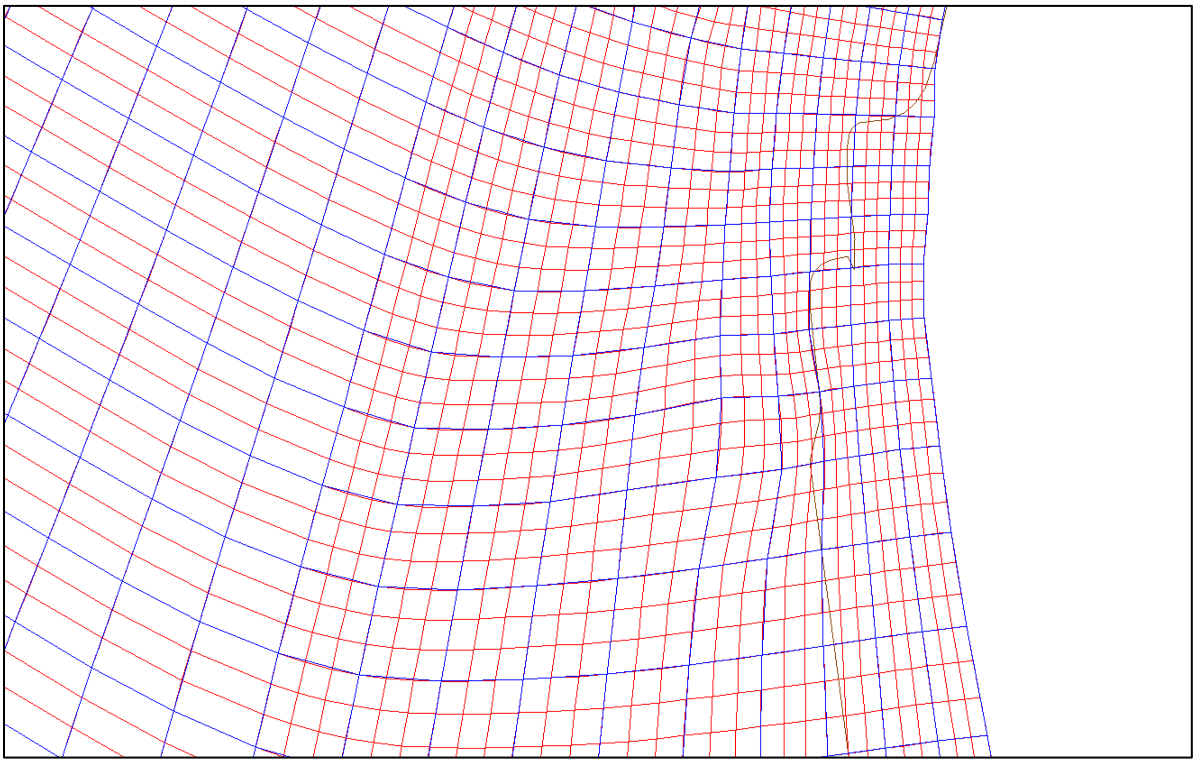

Existing model = blue, high resolution sensitivity test = red

Figure 75. Refined model grid around cofferdam

A comparison of speed differences between the high-resolution baseline and scheme runs showed less difference in flow speeds than the lower resolution runs (most likely a result of the depth averaging of flow speeds) and provides reassurance that the existing model mesh is providing an appropriate resolution of the hydrodynamic processes. The extent of change in the 2D higher resolution model is reduced compared with the lower horizontal resolution 3D simulation when considering the same magnitude of changes in flow speed. Figure 76 on the following page shows the difference in speeds resulting from the scheme implementation in the 2D model run at HW +2 (time of peak ebb). This is compared with the difference in the 3D model run in the mid depth layer (Figure 77). Note that the scales on these area plots have been adjusted compared with Section 5.2.2 in order to better compare the differences between the models.

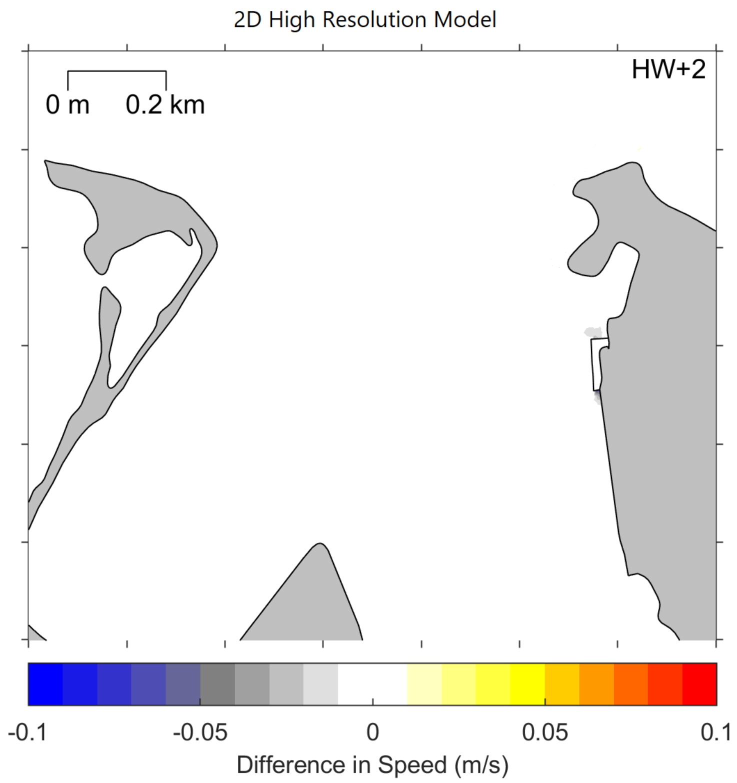

Figure 76. Difference in flow speed (scheme – baseline), 2D higher resolution model grid

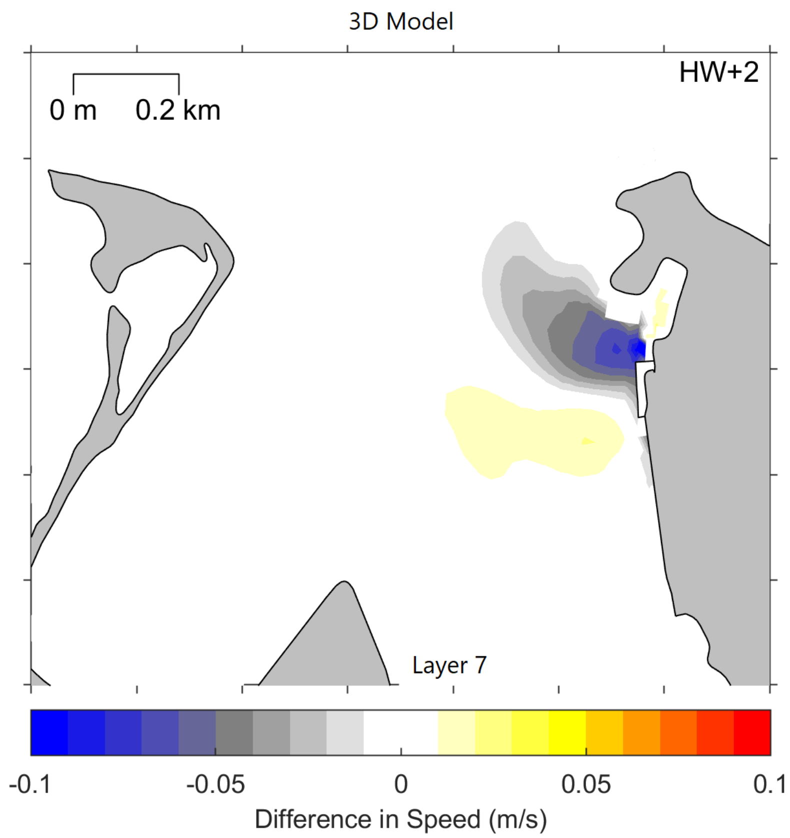

Figure 77. Difference in flow speed (scheme – baseline), 3D model, Layer 7 (42-65% of the water depth)

5.2.6 Consideration of localised dredge

It is possible that dredging would be required in advance of the cofferdam construction to deepen the channel depth around the cofferdam site. Details of is dredge are not known at this time but are likely to consist of a localised deepening which would not impact the main river channel. At this stage of the project no modelling of potential dredge depths is required. These could be undertaken at a later date if needed by altering the existing model bathymetry to proposed dredged depths.

We anticipate that the likely impact of increased water depths around the cofferdam would be to reduce the flow speeds around the structure. As a consequence, the impact of the cofferdam construction on the hydrodynamic regime is likely to also be reduced.

6 CORMIX Modelling

The CCUS project uses a hybrid cooling system which results in a thermally uplifted effluent being discharged from the generating station through the planned outfall location (Figure 78). An investigation of 'near-field' mixing processes is required to establish the scale of the mixing zone for the thermal discharge. Thermal plume modelling for this study has been undertaken using the CORMIX modelling software. The methods and results from this thermal plume modelling are presented in the following report sections.

The CORMIX modelling software, produced by MixZon Inc., has been designed for the prediction and analysis of aqueous toxic or conventional pollutant discharges into diverse water bodies, with the latter being addressed in this study. The user-interface requires singular values to represent specific controlling parameters of geometries (e.g. discharge port) and water body characteristics (e.g. densities). The model uses these parameters to create the predicted plume, which is represented as an instantaneous snap-shot in time of the dispersion and dilution of the two specified water bodies.

6.1 Outfall location

The location of the planned thermal outfall has been provided to ABPmer via a technical drawing specifying chainage values from fixed onshore landmarks. The orientation of the planned outfall pipe has been estimated by determining the existing outfall orientation to shore from Admiralty Charts and measuring the appropriate distance from shore along the same bearing. Using this approach, the estimated location for the outfall is: 54.64°N, 1.117°W. The water depth in the model at this location is 7.75 m (ODN). Hydrodynamic conditions for this location have been extracted from the Delft3D model, for depth averaged conditions at the time of a mean spring and mean neap range to input into the CORMIX thermal plume modelling, as described in the following sections.

Background image source: Google Earth 2020

Figure 78. Location of outfall

6.2 Model set-up

The CORMIX model set-up is composed of 3 main tabs that require the input of specific parameters to represent geometries and aqueous characteristics within the model. The three tabs are individually outlined below, with the used input parameters stated.

6.2.1 Effluent

The software allows specification of the key characterises of the effluent water body that will be discharged from the outfall into the marine environment. Consideration is given to the type of effluent i.e. non/ conservative in which growth and decay rates can be applied. Additionally; heated, saline and sediment discharges can be simulated.

For this study, the effluent was characterised as a heated, conservative (no growth/ decay processes) effluent, which required the following input parameters:

- Temperature Excess: 15°C;
- Flow rate: 1.37 m^3/s; and
- Density: 1,018/ 1,020 kg/m^3 (summer/ winter representations).

6.2.2 Ambient

To represent the ambient ocean conditions that the outfall will disperse into, hydrodynamic conditions at the proposed outfall location (457108.31 E, 527562.69 N (OSGB)) were extracted and analysed to determine key tidal characteristics; water levels (WL), current speed (CurSpd) and current direction (CurDir).

A mean spring tidal range (approximately 4.6 m) was isolated from the spring-neap cycle of the model output since a worse-case (spring tide) scenario will represent the greatest tidal excursion from the origin. Within this mean spring tide, the WL and CurDir that coincided with the peak CurSpd, for both the flood and ebb phases were obtained. Figure 79 highlights the tidal signal and its key characteristics, which have been isolated to represent the mean spring tide, with the value tabulated in Table 7. Additionally, seasonal wind speeds (m/s) were extracted from the analysis of Durham Tees Valley Airport measured data described in Section 2.3.5. Wind speeds of 4.08 and 5.32 m/s were selected to represent summer and winter, respectively.

To conclude this tab, the ambient density of the receiving water (1,026 kg/m^3) and bed roughness (default of 0.04) parameters were also applied. Furthermore, the enabling of the model environment to be classified as 'Unbounded' is possible, which indicates that there is only one 'bank' in the model (consistent with outfalls into the open sea). This is opposed to a riverine environment, which would be classed as 'Bounded', in which the distance between banks would be required.

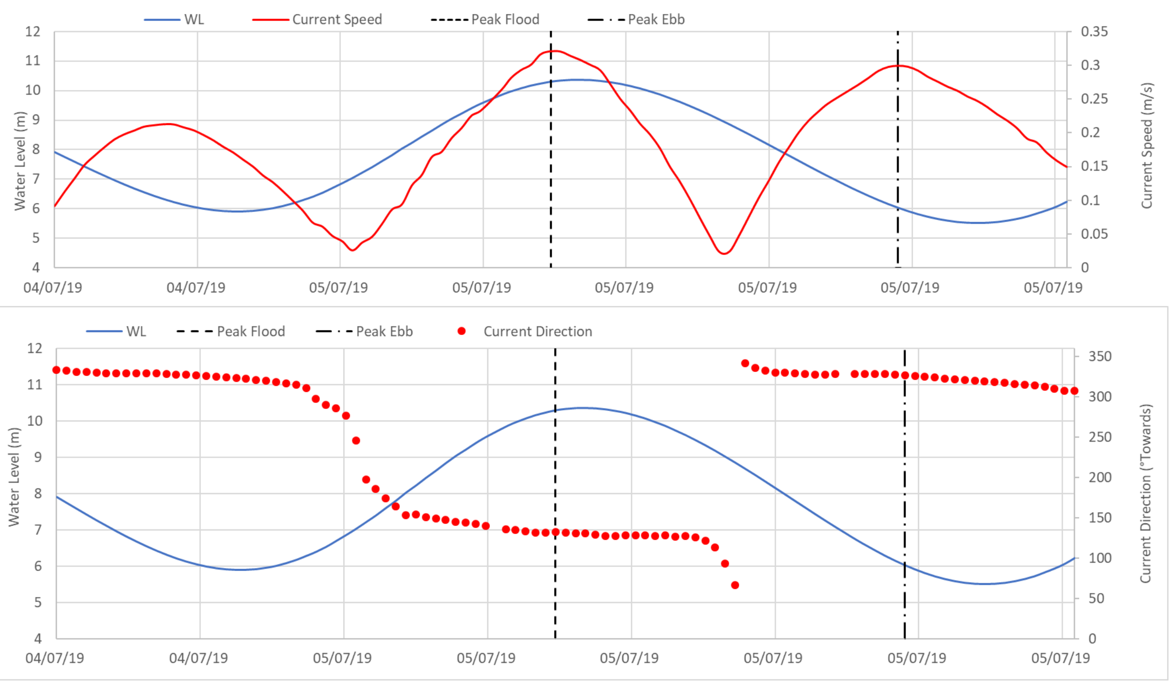

Figure 79. Tidal characteristics during a mean spring tide

Table 7. Tidal characteristics for a mean spring tide.

Tidal Charicteristic	Peak Flood	Peak Ebb
Water Level (m)	10.3	6.0
Current Speed (m/s)	0.32	0.30
Current Direction (°N)	132	327

6.2.3 Discharge

For this study, the discharge has been represented as standard 'simple port' that is 860 m from the nearest bank, with a 90° (vertical) projection. The Current Direction (CurDir) is considered by determining the direction of the nearest bank – right or left, based on flood or ebb flow direction. The software assumes the user is looking downstream of the flow to determine this. By using the flood and ebb CurDir (132° and 327° as in Table 1), under ebb conditions the nearest bank is defined on the left and on the right under flood phases.

The specific port geometries are also specified within this tab which include:

- Port diameter: 0.8 m; and
- Port height above bed: 1 m.

7 Results

7.1 Sensitivity tests

Following a range of sensitivity tests, it was concluded that the spring tidal range under summer conditions offered the largest plume extent, which included the following seasonal parameters;

- Effluent density of 1,018 kg/m^3; and
- A mean wind speed of 4.08 m/s.

This model setup has been used as a 'baseline' scenario to use as a comparison for a range of sensitivity tests. The tests completed to reach this conclusion are outlined below. A summary of the sensitivity tests presented in this report section are provided in Table 8.

Table 8. CORMIX Run Summary

Run no	Description
01	Spring flood tide (summer season) baseline case, this includes: ▪ Seasonal wind speeds ▪ 0.8 m pipe diameter ▪ Pipe orientation vertical
02	Spring flood tide (winter season)
03	Spring flood tide (summer season) no winds applied
04	Spring flood tide (winter season) no winds applied
05	Spring flood tide (summer season) 0.6 m pipe diameter
06	Spring flood tide (summer season) 1 m pipe diameter
10	Spring ebb tide (summer season)
16	Spring flood tide (summer season) 15 m/s wind speed
17	Spring flood tide (summer season) horizontal pipe orientation, directed offshore

7.1.1 Spring flood - Seasonal variation

Shown in Figure 80 is the spring flood tide, demonstrating the seasonal variation (summer/ winter). The winter variation is distinguished by applying different wind speeds (4.08 and 5.23 m/s) and effluent densities (1,018 and 1,020 kg/m³) in separate runs. The seasonal variation is negligible with the summer plume extending very slightly further than the winter, highlighted at around 150 m and the red (summer) 2 and 3°C flags extending slightly further from the origin than the blue (winter).

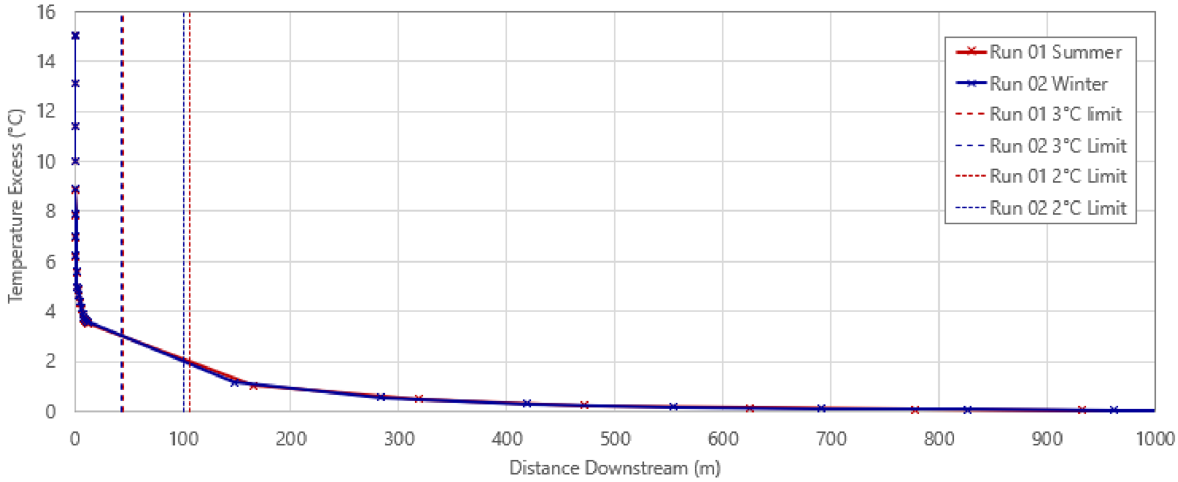

Figure 80. Spring flood seasonal variation

7.1.2 Summer season – Tidal variation

In Figure 81 the summer season has the ebb and flood phases compared against each other (variable for flood and ebb conditions as in Table 7) and shows the ebb plume (Run 10) to better maintain its excess temperature, especially within the first 100 m, which is also shown by the 2 and 3°C flags (blue) extending further than that of the flood (red). However, outside of the near-field region, around 300 m, the two runs converge.

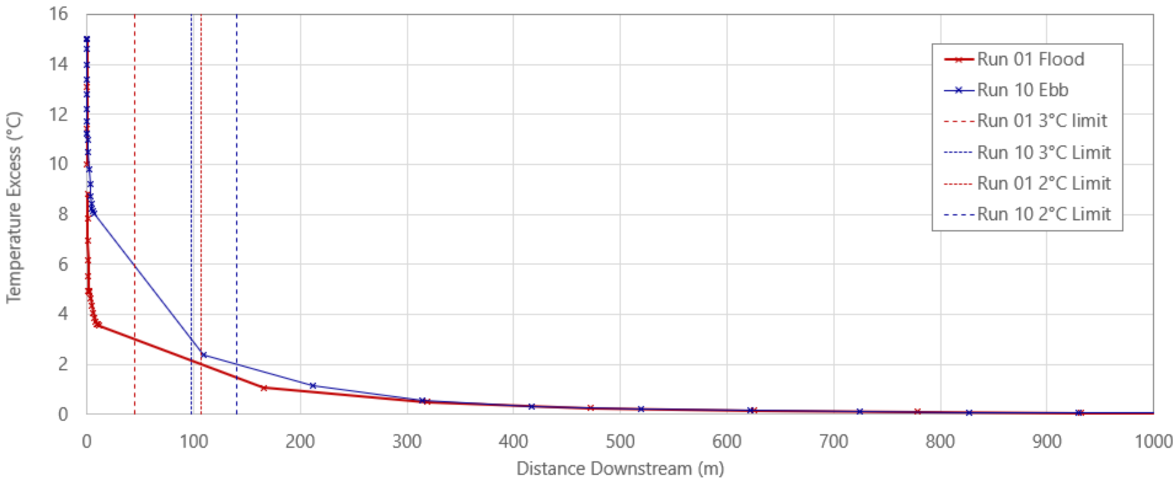

Figure 81. Summer scenario, flood and ebb sensitivity

7.1.3 Spring flood – Wind sensitivity

Shown in Figure 82 is the plume sensitivity to winds. The summer wind value of 4.08 m/s is a light wind and doesn't appear to have any influence on the plume when comparing runs 01 and 03. When a significantly stronger wind of 15 m/s is applied (Run 16), the plume is slightly affected causing the excess temperature to drop slightly quicker around the 100 m mark, also shown by the difference in the 2 and 3°C flags. However, it's to be noted that this wind speed of 15 m/s is approximately triple the speed of the faster mean winter wind speed of 5.32 m/s, and is considered here for sensitivity testing purposes only.

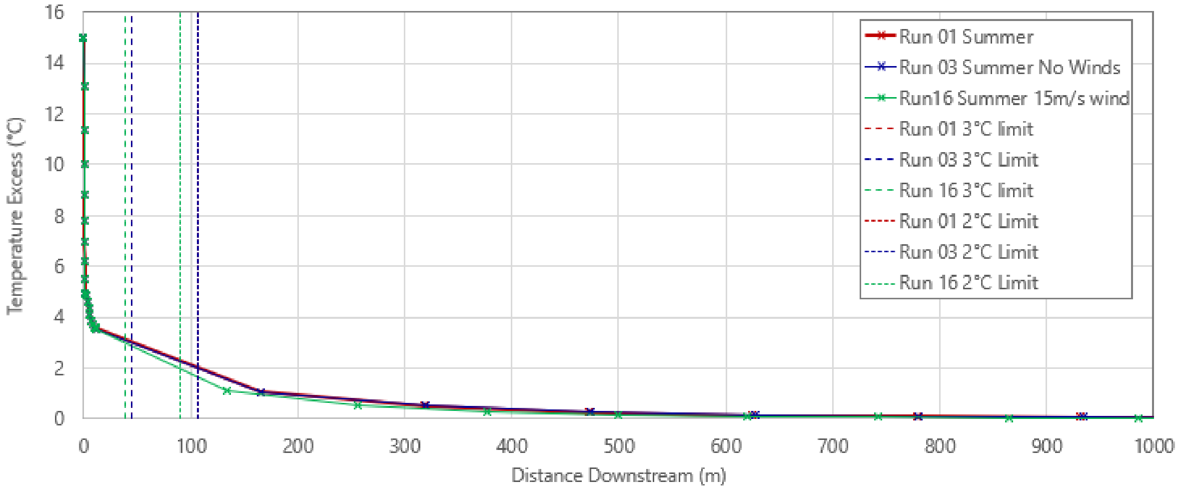

Figure 82. Spring flood wind sensitivity

7.1.4 Spring flood – Pipe diameter

Figure 83 shows the tests addressing the plume sensitivity to the discharge port diameter. The baseline run (Run 01 Summer) has a diameter of 0.8 m, with ±0.2 m applied in sensitivity runs; Run05 (0.6 m) and Run06 (1.0 m). The larger port diameter (Run 06) shows the excess temperature dilutes notably faster than the two smaller diameters in the near-field region, after which, at around 160 m all the runs converge.

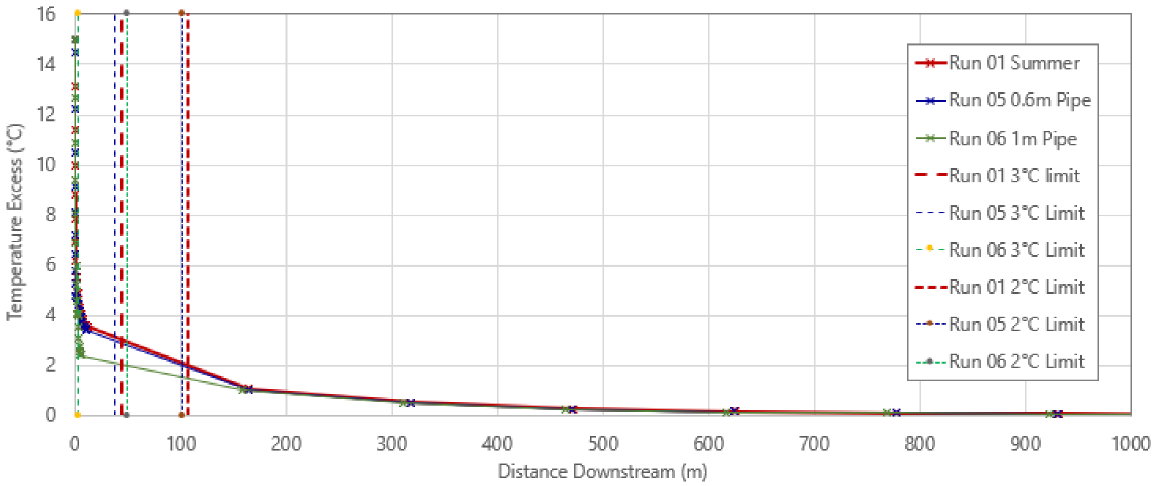

Figure 83. Spring flood, pipe diameter sensitivity

7.1.5 Spring flood – Pipe projection

Figure 84 shows the plume sensitivity to projection of the outfall port. Run 01 has a vertical projection off the seabed, contrasted by Run 17 having an offshore-aligned, horizontal projection, which shows dispersion of the excess temperature far more efficiently, with the 2°C being exceed at around 15 m, compared to approximately 105 m for the vertical projection in Run 01.

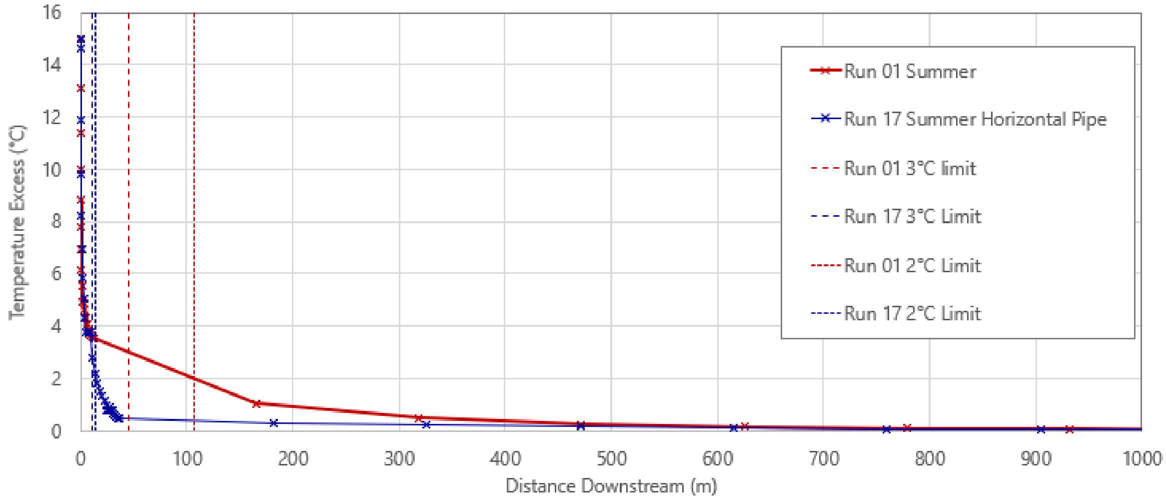

Figure 84. Spring flood, outfall projection sensitivity

7.2 Temperature excess isolines

The spring tidal range under summer conditions has also been utilised to demonstrate the plume extent for both the peak flood and ebb flow conditions (tidal characteristics as in Table 7). The plume shown in Figure 85 represents the extents of the excess temperatures isolines from +5°C to +0.1°C and have been overlaid on a map view to indicate the plume extent in relation to the site. A zoomed extent is also shown in Figure 86. Additionally, each isoline extent from the outfall is tabulated for both flood and ebb conditions in Table 9.

Table 9. Excess temperature isoline extents from the outfall under peak ebb and flood for a mean spring tide

Excess Temperature Isoline (°C)	Peak Flood (Run 01)		Peak Ebb (Run 10)	
	Isoline Extent from Outfall (m)	Area of Excess Temperature (m^2)	Isoline Extent from Outfall (m)	Area of Excess Temperature (m^2)
5.0	1.6	32	61.3	2
4.0	6.6	49	79.4	3
3.0	44.7	71	97.6	21
2.0	106.5	1,673	140.0	76
1.0	179.3	7,500	235.4	1,455
0.1	754.2	81,256	718.1	74,578

Figure 85. CORMIX excess temperature isolines (°C) under mean spring, peak flood (SE) and ebb (NW) tidal states

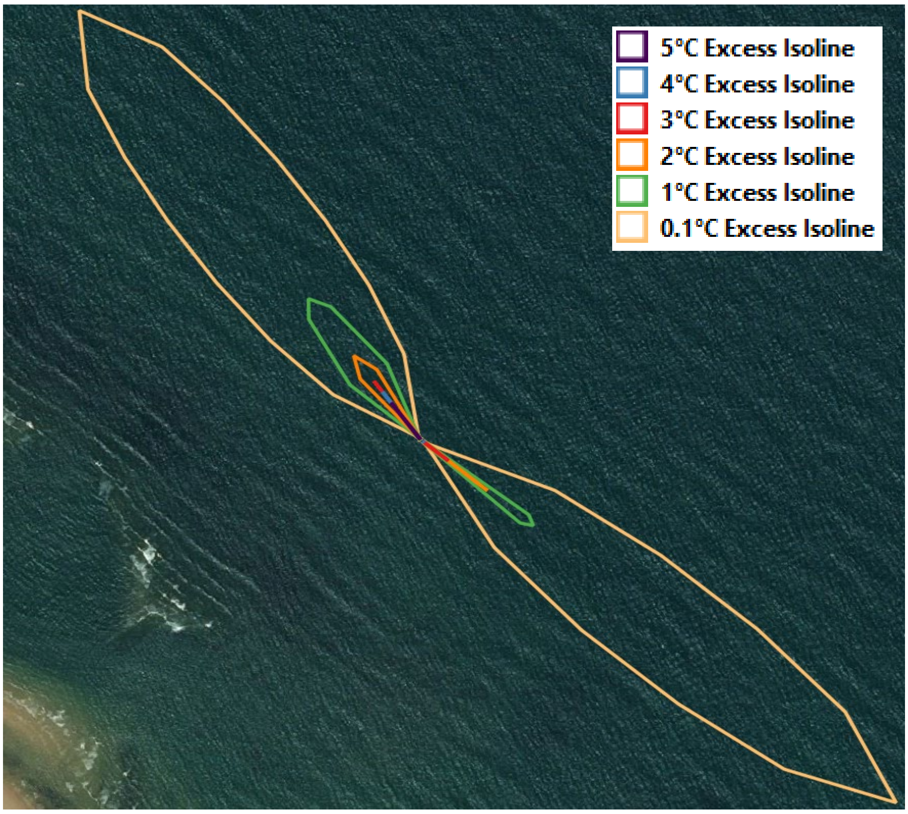

Figure 86. Zoomed extent of the CORMIX excess temperature isolines (°C) under mean spring, peak flood (SE) and ebb (NW) tidal states

8 Conclusion

Hydrodynamic modelling has been undertaken using the Delft3D flow modelling software to create a representative baseline condition of the Tees Estuary which produces a good comparison of flow, water level and vertical water column structure in the estuary in comparison with available measurements. Implementing the proposed cofferdam within the model run suggests that the impacts on flow speeds around the construction site will be very limited and restricted to within approximately 150 m of the structure when considering flow speed differences of >0.05 m/s. Changes in flow will be felt mostly in the faster flowing surface and mid water layers and less so nearer to the bed where flow speeds are lower. Flow directions will alter as flows are redirected around the new structure, extending further from the coastline than the original infrastructure. The proposed cofferdam structure is only temporary whilst enabling works are completed. Once finished, the cofferdam will be removed, and the orientation of the coastline will revert to the existing (baseline) condition.

Near-field thermal plume modelling has been undertaken using the CORMIX modelling software to trace the likely extent of thermal discharge at the proposed outfall location. Under spring conditions, the likely extent of a thermal plume (of the properties modelled) would be very localised: a 3°C temperature excess only extends approximately 45 m from the discharge point on the flood and 98 m on the ebb. Considering a 2°C temperature excess the ebb extent of the plume increases to 140 m, and then 235 m to the 1°C excel temperature contour, which still represent a very limited excursion from the original discharge point.

To examine the wider plume dispersion a 0.1°C temperature excess contour was exported from CORMIX. This shows that a 0.1°C temperature excess is estimated to extend around 750 m from the origin on a spring flood tide, and 720 m on an ebb. At lower speeds (e.g. near slack water), reduced mixing could allow the plume to stay buoyant for longer, however the excursion from the plume would be limited by the speeds and mixing with subsequent dispersion occurring as speeds increase through the tidal cycle. Sensitivity testing showed only small influence on plume extent due to wind and seasonal variations, while the outfall orientation (horizontal or vertical) has a relatively larger impact on the dispersion of the plume.

9 References

ABPmer. (2003). Tees Entrance Channel Study, Part II: Numerical Modelling of Deepening of Seaton Channel. ABP Marine Environmental Research Ltd, Report No. 991.

GOV.UK: https://environment.data.gov.uk/DefraDataDownload/?Mode=survey

JBA. (2011). Tidal Tees Integrated Flood Risk Modelling Study. JBA Consulting, September 2011.

NFRA: https://nrfa.ceh.ac.uk/data/search

UKHO (2020) Admiralty Tide Tables, United Kingdom and Ireland, NP201B, Volume 1B. UK Hydrographic Office 2020.

Wood (2020). Gas Power – Cooling System Analysis Report 13430-01-8110-RP-3001 REV F1 **DRAFT** report. Selected data shared by AECOM, access to full report not provided to ABPmer.

10 Acronyms/Abbreviations

2D	Two Dimension(al)
3D	Three Dimension(al)
ADCP	Acoustic Doppler Current Profiler
AECOM	AECOM Ltd
CCUS	Carbon Capture, Utilisation and Storage
CD	Chart Datum
CTD	Conductivity-Temperature-Depth
CurDir	Current Direction
CurSpd	Current Speed
DHI	Danish Hydraulic Institute
Dir	Direction
HD	Hydrodynamic
HW	High Water
ITT	Invitation to Tender
JBA	JBA Consulting
LAT	Lowest Astronomical Tide
LiDAR	Light Detection and Ranging
NRFA	National River Flow Archive
ODN	Ordnance Datum Newlyn
OSGB	Ordnance Survey Great Britain
Q	Quartile
RoRo	Roll-on/Roll-Off
THPA	Tees and Hartlepool Port Authority
UKHO	United Kingdom Hydrographic Office
WL	Water Levels
WS	Wind Speed

Cardinal points/directions are used unless otherwise stated.

SI units are used unless otherwise stated.

Contact Us

ABPmer

Quayside Suite,
Medina Chambers
Town Quay, Southampton
SO14 2AQ

T +44 (0) 23 8071 1840
F +44 (0) 23 8071 1841
E enquiries@abpmer.co.uk

www.abpmer.co.uk